Manuscript Details

Manuscript number	ALGAL_2016_43
Title	Higher packing of thylakoid complexes ensures a preserved Photosystem II activity in mixotrophic Neochloris oleoabundans
Article type	Full Length Article

Abstract

A better understanding of the microalgal basic biology is still required to improve the feasibility of algal bio-products. The photosynthetic capability is one of the parameters that need further progress in research. A superior PSII activity was previously described in the green alga Neochloris oleoabundans. In this study, N. oleoabundans was grown in a glucose-supplied culture medium, in order to provide new information on the organisation and interaction of thylakoid protein complexes under mixotrophy. Fluorescence measurements suggested a strong association of light harvesting complex II (LHCII) to PSII in mixotrophic samples, confirmed by the lack of LHCII phosphorylation under growth light and the presence of PSI-PSII-LHCII megacomplexes in Blue-Native gel profile. The chloroplast ultrastructure was accordingly characterised by a higher degree of thylakoid appression compared to autotrophic microalgae. This also affected the capability of mixotrophic microalgae to avoid photodamage when exposed to high-light conditions. On the whole, it emerged that the presence of glucose affected the photosynthetic performance of mixotrophic samples, apparently limiting the dynamicity of thylakoid protein complexes. As a consequence, PSII is preserved against degradation and the PSI:PSII is lowered upon mixotrophic growth. Apparent increase in PSII photochemical activity was attributed to a down-regulated chlororespiratory electron recycling.

Keywords	Neochloris oleoabundans, mixotrophy, Photosystem II, thylakoid protein complexes, photosynthetic performance, BN-PAGE
Taxonomy	Chloroplast, Light-Harvesting Complex, Photosystem Ii, Thylakoid Membrane, Algal Biology, Algae Cultivation
Manuscript category	Algal Biotechnology

Corresponding Author	Simonetta Pancaldi
Order of Authors	Martina Giovanardi, Mariachiara Poggioli, Lorenzo Ferroni, Maija Lespinasse, Costanza Baldisserotto, Eva-Mari Aro, Simonetta Pancaldi

Suggested reviewers	Roberta Croce, Patricia Leonardi, Barbato Roberto, Joan Salvado

Submission Files Included in this PDF

File Name [File Type]

Letter to Editor.docx [Cover Letter]

Declaration of Author contribution-revised.docx [Author Agreement]

Answer to Reviewers' comments.docx [Response to Reviewers]

Giovanardi et al MS-Marked.docx [Response to Reviewers]

Giovanardi et al MS-Clean.docx [Manuscript File]

Fig. 1.pptx [Figure]

Fig. 2.tif [Figure]

Fig. 3.tif [Figure]

Fig. 4.tif [Figure]

Fig. 5 - Marked.tif [Figure]

Fig. 6.tif [Figure]

Fig. 7.pptx [Figure]

Fig. 8.tif [Figure]

Fig. 9.tif [Figure]

Fig.10.tif [Figure]

Highlights.docx [Highlights]

Acknowledgments-revised.docx [Supporting File]

Supplementary material - mod.docx [Supporting File]

To view all the submission files, including those not included in the PDF, click on the manuscript title on your EVISE Homepage, then click 'Download zip file'.

UNIVERSITÀ DEGLI STUDI DI FERRARA
DIPARTIMENTO DI SCIENZE DELLA VITA E BIOTECNOLOGIE
Sezione di Botanica Applicata, C.so Ercole I d'Este 32, 44121 Ferrara

Dear Prof. Olivares,

We are very grateful that our MS n° ALGAL_2016_43 was positively evaluated by the Reviewers, who we thank very much for their comments and suggestions.

We have considered carefully the Reviewers' suggestion in order to improve our MS and let it suitable for publication on Algal Research. Following the Instructions for Authors, we have provided two version of the MS: a marked MS whit changes highlighted in yellow, and a clean version of the revised MS. Tables are embedded in the text, whereas Figures are attached separately. Fig.5, which has been modified, is now included as "Fig. 5 – Marked".

According to Reviewer 1, we have included new analyses that could be helpful to make some point of the MS clearer than previous submission. As Maija Lespinasse, working at the Molecular Plant Biology Laboratory of the University of Turku, contributed to perform these analyses, we ask for the possibility to add her name to the list of Author. Please find attached the written confirmations from all the Authors that they agree with her addition to the Authorship list, including the acceptance of Maija Lespinasse herself. We hope that you agree with this rearrangement of the Autorship list.

Hoping that your MS can be now eligible for publication on Algal Research, I convey you my very best regards.

Prof. Simonetta Pancaldi

UNIVERSITÀ DEGLI STUDI DI FERRARA
DIPARTIMENTO DI SCIENZE DELLA VITA E BIOTECNOLOGIE
Sezione di Botanica Applicata, C.so Ercole I d'Este 32, 44121 Ferrara

Ferrara, the 6th of February, 2017

Dear Prof. Pancaldi,

I am writing to you about the rearrangement of the Authorship list of the MS n° ALGAL_2016_43 entitled "Higher packing of thylakoid complexes ensures a preserved Photosystem II activity in mixotrophic *Neochloris oleoabundans*" whose revised version is going to be resubmitted to Algal Research.

With this letter, I declare my agreement with the addition of Maija Lespinasse among the Authors of the MS.

Sincerely,

Dr. Martina Giovanardi

UNIVERSITÀ DEGLI STUDI DI FERRARA
DIPARTIMENTO DI SCIENZE DELLA VITA E BIOTECNOLOGIE
Sezione di Botanica Applicata, C.so Ercole I d'Este 32, 44121 Ferrara

Ferrara, the 6th of February, 2017

Dear Prof. Pancaldi,

I am writing to you about the rearrangement of the Authorship list of the MS n° ALGAL_2016_43 entitled "Higher packing of thylakoid complexes ensures a preserved Photosystem II activity in mixotrophic *Neochloris oleoabundans*" whose revised version is going to be resubmitted to Algal Research.

With this letter, I declare my agreement with the addition of Maija Lespinasse among the Authors of the MS.

Sincerely,

Dr. Mariachiara Poggioli

UNIVERSITÀ DEGLI STUDI DI FERRARA
DIPARTIMENTO DI SCIENZE DELLA VITA E BIOTECNOLOGIE
Sezione di Botanica Applicata, C.so Ercole I d'Este 32, 44121 Ferrara

Ferrara, the 6th of February, 2017

Dear Prof. Pancaldi,

I am writing to you about the rearrangement of the Authorship list of the MS n° ALGAL_2016_43 entitled "Higher packing of thylakoid complexes ensures a preserved Photosystem II activity in mixotrophic *Neochloris oleoabundans*" whose revised version is going to be resubmitted to Algal Research.

With this letter, I declare my agreement with the addition of Maija Lespinasse among the Authors of the MS.

Sincerely,

Dr. Lorenzo Ferroni

Turun yliopisto
University of Turku

Turku, the 8th of February, 2017

Dear Prof. Pancaldi,

I am writing to you about the rearrangement of the Authorship list of the MS n° ALGAL_2016_43 entitled "Higher packing of thylakoid complexes ensures a preserved Photosystem II activity in mixotrophic Neochloris oleoabundans" whose revised version is going to be resubmitted to Algal Research.

With this letter, I declare my agreement with the addition of Maija Lespinasse among the Authors of the MS.

Sincerely,

MOLECULAR PLANT BIOLOGY
DEPARTMENT OF BIOCHEMISTRY
UNIVERSITY OF TURKU
FI-20014 TURKU
FINLAND

Prof. Eva Mari Aro

Matemaattis-luonnontieteellinen tiedekunta
Faculty of Mathematics and Natural Sciences

FI-20014 Turun yliopisto, Finland • www.utu.fi

Puhelin/Telephone +358 2 333 6576
Faksi/Fax +358 29 450 5040

utu.fi /sci

Turku, the 8th of February, 2017

Dear Prof. Pancaldi,

I am writing to you about the rearrangement of the Authorship list of the MS n° ALGAL_2016_43 entitled "Higher packing of thylakoid complexes ensures a preserved Photosystem II activity in mixotrophic Neochloris oleoabundans" whose revised version is going to be resubmitted to Algal Research.

With this letter, I declare my agreement with the addition of my name among the Authors of the MS.

Sincerely,

MOLECULAR PLANT BIOLOGY
DEPARTMENT OF BIOCHEMISTRY
UNIVERSITY OF TURKU
FI-20014 TURKU
FINLAND

MSc. Maija Lespinasse

UNIVERSITÀ DEGLI STUDI DI FERRARA
DIPARTIMENTO DI SCIENZE DELLA VITA E BIOTECNOLOGIE
Sezione di Botanica Applicata, C.so Ercole I d'Este 32, 44121 Ferrara

Ferrara, the 6th of February, 2017

Dear Prof. Pancaldi,

I am writing to you about the rearrangement of the Authorship list of the MS n° ALGAL_2016_43 entitled "Higher packing of thylakoid complexes ensures a preserved Photosystem II activity in mixotrophic *Neochloris oleoabundans*" whose revised version is going to be resubmitted to Algal Research.

With this letter, I declare my agreement with the addition of Maija Lespinasse among the Authors of the MS.

Sincerely,

Dr. Costanza Baldisserotto

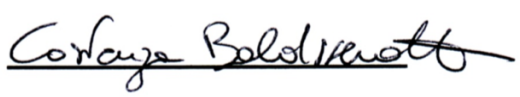

Author contribution

MG, LF, EMA and SP participated in the conception and design of the study; MG, MP, LF, ML, CB collected data and performed analyses; MG, LF and SP drafted the article; LF, EMA and SP assisted the results interpretation and critical reviewed the manuscript; all Authors read and approved the final manuscript.

List of changes and answers to Reviewers' comments

We are grateful to Reviewers for their positive evaluation of our MS and for their highly appreciate opinions and suggestions. The answers to their comments can be found below.

Reviewer 1

We agree with Reviewer 1 that the detection of PsaB in autotrophic samples was already saturated at 50%. Despite we had obviously performed several times the Western Blot, which gave consistent results and showed a good linear range of autotrophic samples, we unfortunately were not able to obtain an image with a resolution as high as the one reported in Fig. 5. To make the result clearer, as requested by the Reviewer, we decided to add to Fig. 5 also the 77K fluorescence emission spectra of autotrophic and mixotrophic cells (Fig. 5B). As it can be observed, when spectra were normalized on their maximum emission peak, i.e. the region corresponding to the emission of PSII, autotrophic cells showed a higher emission in the region of PSI as compared to mixotrophic samples, confirming, then, the immunoblot results (see also page 7, lines 147-153 and page 15-16 lines 335-346). Additionally, we also included as a Supplementary Figure the Immunoblot detection of PsaA subunit of PSI (page 15 line 330 and Supplementary Material). In Supplementary Figure S2, the linear range of both autotrophic and mixotrophic samples can be appreciated, and the lower abundance of PsaA in cells grown with glucose can be further confirmed. To prove that samples were homogeneously loaded on gel, and thus to confirm the efficiency of the electroblotting, Ponceau-stained nitrocellulose membrane was also included in the Figure. We hope that the improvements of the MS will satisfy the requirements of the Reviewer.

Reviewer 2

The choice of cultivating *Neochloris oleoabundans* in the presence of 2.5 gL^{-1} of glucose derives from previous investigation in which the microalga was grown adding to the culture medium different glucose concentrations ranging from 0 to 30 gL^{-1}, with the aim of stimulating growth and induce lipid accumulation inside cells. The results of this study have been already published (Giovanardi et al., 2014, Protoplasma 251, 115-125) and demonstrated that the concentration of 2.5 gL^{-1} of glucose was the optimal, allowing to obtain maximum cell densities and lipid accumulation. Indeed, at glucose concentrations higher than 2.5 gL^{-1}, the growth rates appeared slightly, but progressively, decreasing, as well as 2.5 gL^{-1} was sufficient to yield the maximum lipid content inside cells. Moreover, glucose was completely utilized during the experiment, whereas at higher concentrations an excess of

substrate was observed. Subsequently, biomass composition of autotrophic and mixotrophic cells, in terms of total proteins and fatty acid profile, was also evaluated, as reported in Baldisserotto et al. 2016, Algal Research 16, 255-265.

About what was limiting cell growth in the stationary phase, it has been often reported that nitrogen is one the most relevant macronutrient in the cultivation media, and its starvation induces limiting cell growth and lipid accumulation (Baldisserotto et al., 2012, Phycologia 51, 700-710 and references whitin). As reported in Baldisserotto et al. (2016), the source of nitrate was already completely consumed at the 6^{th} day of growth in mixotrophic cells, which soon after entered the stationary phase. Conversely, nitrate concentration in the cultivation medium of autotrophic cells gradually decreased throughout the experiment, but was not totally consumed, in line with the progressive slowing down of control cells, that reached the stationary phase later than mixotrophic samples.

We agree with the Reviewer that all this information might be very important for biotechnological application and commercial viability of the process. As data were already published in previous works, we did not go in depth on the matter in this MS. However, we have better specified how we selected the glucose concentration of 2.5 gL^{-1} to be used in the following experiments in the "Material and Methods" section of the MS (page 5, lines 107-110).

Minor observations:

1) "FV was not defined clearly in the abbreviation section": OK, we added its definition in the abbreviation section;
2) "lisate on sentence 149 should be spelled lysate": OK, we corrected lisate in lysate (now line 158);
3) "Perhaps stating the context of the broader vision for the referenced grants could help": OK, we added some information about some referenced grants and the grant recipient.

Higher packing of thylakoid complexes ensures a preserved Photosystem II activity in mixotrophic *Neochloris oleoabundans*

Martina Giovanardi[1], Mariachiara Poggioli[1], Lorenzo Ferroni[1], Maija Lespinasse[2], Costanza Baldisserotto[1], Eva-Mari Aro[2], Simonetta Pancaldi[1*]

[1]University of Ferrara, Department of Life Science and Biotechnology, C.so Ercole I d'Este 32, 44121 Ferrara, Italy.

[2] University of Turku, Molecular Plant Biology, Department of Biochemistry, FI-20014, Turku, Finland.

*Corresponding Author. E-mail address: simonetta.pancaldi@unife.it (S. Pancaldi)

Abbreviations:

2D: second dimension; ATPase: ATP synthase; BN-PAGE: Blue-Native polyacrylamide gel electrophoresis; BSA: bovin serum albumin; Chl: chlorophyll; Cyt: cytochrome; DCMU: 3-(3,4-dichlorophenyl)-1,1-dimethylurea; F_0: basal fluorescence level excited by a very low measuring light after dark incubation; F_M: maximum fluorescence level obtained by a saturating light pulse after dark incubation; F_M': maximum fluorescence level during a light-adapted state; F_t: basal fluorescence level during a light-adapted state; F_V: variable fluorescence level obtained by the difference of F_M and F_0; F_V/F_M: maximum photochemical quantum yield of Photosystem II; LHC: Light-harvesting pigment-protein complexes; PAM: pulse amplitude modulation; PQ: plastoquinone; PQH_2: plastohydroquinone; PSI: Photosystem I; PSII: Photosystem II; Q_A: quinone A; Q_B: quinone B; SDS-PAGE: Sodium Dodecyl Sulphate polyacrylamide gel electrophoresis; TEM: transmission electron microscopy.

Abstract

A better understanding of the microalgal basic biology is still required to improve the feasibility of algal bio-products. The photosynthetic capability is one of the parameters that need further progress in research. A superior PSII activity was previously described in the green alga *Neochloris oleoabundan*s. In this study, *N. oleoabundans* was grown in a glucose-supplied culture medium, in order to provide new information on the organisation and interaction of thylakoid protein complexes under mixotrophy. Fluorescence measurements suggested a strong association of light harvesting complex II (LHCII) to PSII in mixotrophic samples, confirmed by the lack of LHCII phosphorylation under growth light and the presence of PSI-PSII-LHCII megacomplexes in Blue-Native gel profile. The chloroplast ultrastructure was accordingly characterised by a higher degree of thylakoid appression compared to autotrophic microalgae. This also affected the capability of mixotrophic microalgae to avoid photodamage when exposed to high-light conditions. On the whole, it emerged that the presence of glucose affected the photosynthetic performance of mixotrophic samples, apparently limiting the dynamicity of thylakoid protein complexes. As a consequence, PSII is preserved against degradation and the PSI:PSII is lowered upon mixotrophic growth. Apparent increase in PSII photochemical activity was attributed to a down-regulated chlororespiratory electron recycling.

Key words: *Neochloris oleoabundans*, mixotrophy, Photosystem II, thylakoid protein complexes, photosynthetic performance, Blue-Native PAGE, fluorescence measurements.

47 # Introduction

48 Photosynthesis supports almost all life on Earth and involves several light-dependent reactions,
49 which start with the absorption of light energy for the synthesis of NADPH and ATP (Geider and
50 MacIntyre, 2002), used during the Calvin-Benson cycle for CO_2 fixation (Falkowski and Raven,
51 2007). Important features of the light reactions of photosynthesis are: collection of photons by
52 light-harvesting antennae, migration of excitation energy to the reaction centers, electron transfer
53 from H_2O to $NADP^+$, and ATP generation (Geider and MacIntyre, 2002). Light-harvesting
54 pigment-protein complexes (LHC) deliver the absorbed light energy to the reaction centers of
55 Photosystem II (PSII) and Photosystem I (PSI) (Minagawa and Takahashi, 2004). The major LHC
56 of PSII, LHCII, is also essential for maintaining thylakoid membranes stacked and promoting
57 distribution of absorbed light energy between photosystems (Tikkanen *et al.*, 2008; Nevo *et al.*,
58 2012). PSII transfers electrons from water to plastoquinone (PQ) using light energy as a driving
59 force (Chow *et al.*, 1990; Minagawa and Takahashi, 2004; Daniellson *et al.*, 2006). The electrons
60 from plastohydroquinone reach PSI via Cytochrome (Cyt) b_6f complex and plastocyanin. PSI is
61 involved in a light-dependent electron transport to ferredoxin and to $NADP^+$ (Chow *et al.*, 1990).
62 ATP synthase (ATPase) is the highly-conserved complex that catalyses ATP synthesis using the
63 trans-membrane proton gradient created during the electron flow (Nelson and Ben-Shem, 2004).

64 Important for understanding the molecular basis of the photosynthetic process is a detailed
65 knowledge of the structure of its components (Barber, 2002; Dekker and Boekema, 2005; Nelson
66 and Yocum, 2006). All protein complexes are composed of several protein subunits coordinating
67 a large number of cofactors, which show a tendency to form higher-order associations, the so-
68 called supercomplexes (Dekker and Boekema, 2005; Caffarri, 2009; Minagawa, 2009; Croce and
69 van Amerongen, 2011; Suorsa *et al.*, 2015). The dynamic organisation of the pigment-protein
70 complexes in the thylakoid membrane plays important roles in maintaining an optimal
71 photosynthetic efficiency under several conditions, including different light regimes, temperature

and nutrient supply (Chow et al., 1990; Anderson *et al.*, 1995). In green microalgae, whose cell volume is mainly occupied by the chloroplast, the photosynthetic efficiency is an indicator of their wellness conditions (White *et al.*, 2011). This is an important factor to be taken into account, considering the importance of green microalgae for biotechnological purposes (Chisti, 2007; Borowitzka, 2013). In this scenario, mixotrophic microalgae have been largely investigated for their capability to highly increase their biomass content, benefitting from the exogenous organic carbon source assimilation together with light harvesting and CO_2 fixation for growth (Lee, 2001; Xu *et al.*, 2006; Scott *et al.*, 2010; Stephens *et al.*, 2010). However, there are few works concerning the interaction between photosynthetic complexes in thylakoid membranes during the assimilation of organic carbon by microalgae; in general, a specific reduction in PSII photochemistry was observed (Valverde *et al.*, 2005; Oesterhelt *et al.*, 2007; Liu *et al.*, 2009). Very differently, mixotrophy promoted a very high PSII maximum quantum efficiency in the Chlorophyta *Neochloris oleoabundans* (Baldisserotto *et al.*, 2014; Giovanardi *et al.*, 2014). In this work, the effects of glucose supplied in the culture media of *N. oleoabundans* were assessed in order to provide new information on the photosynthetic metabolism and to understand the interaction of the different pigment-protein complexes during the organic carbon source assimilation. Immunodetection of different subunits of thylakoid multi-protein complexes was employed to identify differences in their relative abundance between autotrophic and mixotrophic samples, whereas Blue-Native polyacrylamide gel electrophoresis (BN-PAGE) was employed to obtain information on native interactions of photosynthetic protein complexes in thylakoids (Hippler *et al.*, 2001; Rokka *et al.*, 2005). In parallel, chlorophyll (Chl) fluorescence measurements were performed *in vivo* on freshly-collected samples to identify differences in photosynthetic electron transport in autotrophic and mixotrophic cells.

97 # Materials and methods

98 ## Algal strain and culture condition

99 The Chlorophyta *Neochloris oleoabundans* UTEX 1185 (syn. *Ettlia oleoabundans*,
100 *Sphaeropleales, Neochloridaceae*) was obtained from the Culture collection of the University of
101 Texas (UTEX, USA; www.utex.org). Cells were grown and maintained in axenic liquid BM
102 medium (Baldisserotto *et al.*, 2012) in a growth chamber (24 ± 1 °C temperature, 80 $\mu mol_{photons}$
103 m^{-2} s^{-1} PAR and 16:8 h of light-darkness photoperiod), without shaking and external CO_2 supply.
104 For experiments, cells were inoculated at least in triplicate at a density of 0.6 ± 0.1 x 10^6 cells mL^{-1}
105 in BM medium containing 0 (autotrophic cells) or 2.5 gL^{-1} of glucose and grown in 500 mL
106 Erlenmeyer flasks (300 mL of total volume) in the growth chamber described above, with
107 continuous shaking at 80 rpm. The glucose concentration of 2.5 gL^{-1} was selected in previous
108 experiments in which the microalga was grown in the presence of increasing concentrations of
109 glucose from 0 to 30 gL^{-1}, comparing among them growth rates, cell morphology, glucose
110 consumption and lipid accumulation inside cells, as reported in Giovanardi et al. (2014). Growth
111 was estimated measuring the optical density at 750 nm with a Pharmacia Biotech Ultrospec®2000
112 UV–vis spectrophotometer (1 nm bandwidth; Amersham Biosciences, Piscataway, NJ, USA) and
113 counting cells with a Thoma's haemocytometer under the light microscope (Zeiss, Axiophot, Jena,
114 DE), on 1 mL of culture samples at days 0, 2, 3, 4, 7, 9, 11.

115 ## Fluorescence measurements

116 *Modulated chlorophyll fluorescence: slow kinetics.*

117 *In vivo* Chl*a* fluorescence was determined from liquid cultures at the late exponential phase of
118 growth, i.e. at the 6th day from the inoculum, harvested by centrifugation to contain 15 µg mL^{-1}
119 Chl. Chlorophyll quantification was performed according to Wellburn (1994). Cell suspensions

were pre-incubated in darkness for 10 min and samples were subsequently exposed to actinic blue light. The following program was triggered: 90 $\mu mol_{photons}\ m^{-2}s^{-1}$, 11 min; dark, 11 min; 1000 $\mu mol_{photons}\ m^{-2}s^{-1}$, 15 min; dark, 5 min. Light saturating pulses (0.6 s) were given every 40 s. Initial fluorescence F_0 and maximum fluorescence F_M after dark incubation were used to calculate the maximum quantum yield of PSII (F_V/F_M ratio), according to Lichtenthaler *et al.* (2005). Time course of Chl fluorescence parameters F_M', i.e. the maximum fluorescence in the light-adapted state measured applying the pulse, and F_t, i.e. the steady-state fluorescence yield, were determined with a DUAL-PAM-100 (Walz, Germany).

The effects of far red light on PSII fluorescence were determined using an ODC OS1-FL portable fluorimeter (ADC Bioscientific Ltd, Hoddesdon, Hertfordshire, UK) on cell pellets prepared as described in Ferroni *et al.* (2011). Measurements were performed on 10 min dark-adapted samples. Cells were excited with far red light (740 nm) for 10 min. After that, recovery was followed for 10 min in darkness. During the experiment, light saturating pulses were given every minute during the far red light exposure and at times 1, 2, 5 and 10 min during dark relaxation. The F_M'/F_M ratio was calculated and used to determine variations of PSII fluorescence.

Fast chlorophyll fluorescence.

Q_A^- reoxidation kinetics was determined by flash-induced Chl fluorescence relaxation kinetics. The single turnover flash-induced increase in Chl*a* fluorescence yield and its subsequent relaxation in darkness (FF-relaxation) were measured with a double-modulation fluorimeter (Photon System Instruments, Brno, Czech Republic). For analyses, 1 mL of samples containing 8 $\mu g\ mL^{-1}$ Chl was incubated in darkness for 10 min and then Q_A^- reoxidation kinetics was recorded, after a single-saturating flash (10 μs) provided by red LED, in the 150 μs - 100 s time range. Analyses were carried out either in the presence or absence of 5 μM 3-(3,4-dichlorophenyl)-1,1-dimethylurea (DCMU) (Allahverdiyeva *et al.*, 2007). For easier comparison, the fluorescence relaxation curves

were averaged and normalised to the same amplitude. The relative Q_A^- concentration was estimated according to the model of Joliot (Joliot and Joliot, 1964). Multicomponent deconvolution of the relaxation curves was performed according to Vass and colleagues (1999).

77K fluorescence emission spectra

Fluorescence emission spectra measured *in vivo* from samples containing 8 µg mL^{-1} Chl were recorded at 77 K using a diode array spectrophotometer (S2000; Ocean Optics, Dunedin, FL, USA) equipped with a reflectance probe as described in Keranen et al. (1999). The spectra were obtained by excitation with light at 440 nm, defined using LS500S and LS700S filters (Corion, Holliston, MA, USA) placed in front of a slide projector, whereas the emission between 600 and 800 nm was recorded. For each biological replicate, at least 3 measurements were recorded.

Thylakoid isolation

Thylakoid membranes were isolated according to Järvi *et al.* (2011), with modifications. For extraction, 300 mL of cultures in late-exponential phase of growth were harvested by centrifugation at 600 *g* for 10 min. Pellets were transferred to an ice-cold mortar containing sand quartz. The extraction was performed grinding cells with liquid N_2, then the ~~lisate~~ lysate was resuspended in a grinding buffer (330 mM sorbitol, 50 mM Tricine-NaOH pH 7.5, 2 mM Na_2EDTA, 1 mM $MgCl_2$, 5 mM ascorbate, 0.05% bovine serum albumin, 10 mM NaF) and transferred to 15 mL tubes. Samples were centrifuged at 300 *g* for 5 min at 4°C and then at 700 *g* for 5 min at 4°C, to remove sand quartz and cell debries. Pellets were discarded and the thylakoids present in the supernatant were collected by centrifugation at 7000 *g* for 10 min at 4°C. The supernatant was discarded and thylakoids were resuspended in 1 mL of shock buffer (5 mM sorbitol, 50 mM Tricine-NaOH pH 7.5, 2 mM Na_2EDTA, 5 mM $MgCl_2$, 10 mM NaF) and centrifuged at 7000 *g* for 10 min at 4°C. After that, the supernatant was removed and around 100 µL of storage buffer (100 mM sorbitol, 50 mM Tricine1-NaOH pH 7.5, 2 mM Na_2EDTA, 5 mM

168 $MgCl_2$, 10 mM NaF) were added to the pellet. Thylakoid samples were rapidly frozen in liquid
169 nitrogen and stored at -80°C until further analyses. Manipulation was always performed on ice and
170 in very dim safe light. Quantification of Chl and proteins in thylakoid samples was performed
171 according to Porra *et al.* (1989) and Lowry (1951), respectively. Before extraction, autotrophic
172 and mixotrophic cultures were incubated in darkness for 1 h or maintained in growth light (80
173 $\mu mol_{photons}\ m^{-2}\ s^{-1}$) inside the growth chamber.

174 **SDS-PAGE and immunoblotting**

175 Thylakoid proteins were separated by SDS-PAGE according to Laemmli (1970) on a 15%
176 acrylamide resolving gel containing 6 M urea. After electrophoresis, proteins were visualised by
177 Coomassie staining overnight, followed by destaining for 5 h, or blotted onto a polyvinylidene
178 difluoride membrane (Millipore, Watford, Hertforshire, U.K.). Western blotting was performed
179 with standard techniques using protein-specific antibodies. For the detection of D1-DE loop of D1
180 protein, PsaB subunit of PSI and ATP-β subunit of ATPase, the antibodies were obtained from
181 Agrisera (www.agrisera.com), whereas for the detection of the entire LHCII complex the antibody
182 was kindly provided by L. Zhang. Before immunodetection, membranes were blocked with 5%
183 milk (www.bio-rad.com) in TBS buffer (Tris-HCl 10 mM pH 7.4 and NaCl 1.5 M). For the
184 detection of phosphoproteins, a polyclonal anti-phosphothreonin antibody was used (Zymed,
185 www-invitrogen.com) and membranes were blocked with 1% BSA in TBS buffer. Horseradish
186 peroxidase-linked secondary antibody in conjunction with chemiluminescent agent (GE heathcare,
187 www.gehealthcare.com) was used for protein detection. Protein band intensity was quantified with
188 Image J freeware (National Institutes of Health, Bethesda, MD, USA).

189 **BN-PAGE and second dimension (2D) electrophoresis**

190 BN-PAGE was performed according to Järvi *et al.* (2011) with minor modifications. Thylakoids
191 (8 µg Chl) were solubilised on ice for 15 min with dodecyl β-D-maltoside (Sigma) at a final

concentration of 1.5% (w/v), followed by centrifugation at 18000 *g* at 4°C for 15 min. Electrophoresis was performed with a Hoefer Mighty Small system (Amersham Biosciences) at 0°C for 3.5 h by gradually increasing the voltage from 75 to 200 V. For comparison, thylakoids from *Arabidopsis thaliana* were included in the analyses. Quantification of band volume was performed with Image J software. After BN-PAGE, the lanes were cut out and incubated in 10% SDS Laemmli buffer (Laemmli, 1970) containing 5% (v/v) β-mercaptoethanol for 1.5 h, followed by separation of the protein subunits of the complexes in the 2D with SDS-PAGE (12% polyacrylamide and 6 M urea). After electrophoresis, proteins were visualised by silver or SYPRO Ruby staining, according to the manufacturer's instructions (www.invitrogen.com). The intensity of every spot in SYPRO- stained gels was determined with ProFinder 2D, version 2005 (Nonlinear Dynamics).

Transmission electron microscopy (TEM)

For transmission electron microscopy, autotrophic and mixotrophic cells were harvested after 6 days of growth and prepared as previously reported (Baldisserotto *et al.*, 2007; Baldisserotto *et al.*, 2016).

Statistical analyses

For each analysis, at least three biological replicates for each sample were set up. Elaboration of data was carried out with Origin Pro 2015 software (OriginLab, Northampton, MA, USA). To compare autotrophic and mixotrophic samples, Student's *t* test was used. For statistical comparison of data obtained by SYPRO Ruby staining, one-way analysis of variance (ANOVA) was used.

Results

Growth kinetics of autotrophic and mixotrophic *N. oleoabundans* cells

Cell density of autotrophic and mixotrophic cultures during the experiment is reported in Supplementary Figure S1. As expected, cell densities were comparable with those observed in previous works (Giovanardi *et al.*, 2014; Baldisserotto *et al.,* 2016). Autotrophic and mixotrophic cells grew with no differences during the first 2 days, after that a significant cell density enhancement was observed in cells grown in presence of glucose starting from the 3rd day (p<0.01 at day 3, p<0.001 at the following times). At the 7th day, both autotrophic and mixotrophic samples entered the stationary phase. Between day 2 and 7, an increase in PSII maximum quantum yield F_V/F_M occurred in mixotrophic cells. Analyses were subsequently performed on cells sampled at the 6th day of growth, period in which mixotrophic cells, still having high F_V/F_M values, also showed the maximum cell density value before entering the stationary phase of growth.

In vivo fluorimetric analyses of autotrophic and mixotrophic *N. oleoabundans*

*Slow kinetics of Chl*a *fluorescence*

In order to clarify the effects of glucose on the dynamics of photosynthetic electron transfer in *N. oleoabundans*, Pulse Amplitude Modulated (PAM) fluorescence trace was monitored in freshly-collected samples of autotrophic and mixotrophic cultures, measuring the time-course of Chl fluorescence parameters F_M' and F_t. Samples were pre-incubated in darkness for 10 min for determination of the initial F_0 and F_M values before triggering the measuring routine. A 90 $\mu mol_{photons}\ m^{-2}s^{-1}$ irradiance was meant to reproduce a growth light condition, while a 1000 $\mu mol_{photons}\ m^{-2}s^{-1}$ represented a condition of high light stress. In Fig. 1 representative Chl*a* fluorescence kinetics are shown for autotrophic (Fig. 1A) and mixotrophic (Fig. 1B) cells. On the whole: i) no differences in the minimal level of fluorescence F_0 were observed before turning on the actinic light; ii) during the 90 $\mu mol_{photons}\ m^{-2}s^{-1}$ - darkness sequence of the triggered program,

F_M' increased over the initial F_M in autotrophic cells (Fig. 1A). On the other hand, the F_M' increase effect in the light was not always observed in mixotrophic samples and, when it occurred, the fluorescence increase was not as marked as in cells grown in the absence of glucose (Fig. 1B). In the light of these results, maximum quantum yield of PSII was re-calculated for both samples considering the real maximum F_M value, i.e. F_M' at the end of 90 $\mu mol_{photons}\ m^{-2}s^{-1}$ irradiance, hereafter named F_{Mtrue}. The obtained F_V/F_{Mtrue} ratio revealed no differences between autotrophic and mixotrophic cells in the maximum photochemistry quantum yield (Table 1). Same result was obtained calculating the F_tLL/F_{Mtrue} ratio, where F_tLL was the basal fluorescence at the end of the 90 $\mu mol_{photons}\ m^{-2}s^{-1}$ exposure period (Table 1); iii) when cells were exposed to 1000 $\mu mol_{photons}\ m^{-2}s^{-1}$, an initial rise in the basal fluorescence F_t was observed in autotrophic cells, followed by a strong decrease. These two phases were less evident in mixotrophic samples because of a less marked fluorescence rise as compared to autotrophic cells at the beginning of the high-light exposure period. Interestingly, the calculated F_tHL/F_{Mtrue} ratio, where F_tHL was the basal fluorescence at the end of the 1000 $\mu mol_{photons}\ m^{-2}s^{-1}$ exposure period, was significantly lower in autotrophic (-41%, $p<0.01$) than in mixotrophic cells (Table 1), suggesting a more reduced state of plastoquinone in mixotrophic cells after a prolonged exposure to high-light conditions; iv) when cells were finally exposed to darkness, maximum fluorescence F_M' gradually increased with no differences between samples.

	Autotrophic *N. oleoabundans*	Mixotrophic *N. oleoabundans*
F_V/F_{Mtrue}	0.708 ± 0.018	0.704 ± 0.044
F_tLL/F_{Mtrue}	0.409 ± 0.076	0.374 ± 0.042
F_tHL/F_{Mtrue}	0.303 ± 0.046	0.510 ± 0.125**

Table 1. PSII fluorescence ratios in autotrophic and mixotrophic *N. oleoabundans*. Values were obtained from Chl*a* fluorescence kinetics traces reported in Fig. 1. Values are means of n≥3 ± standard deviation. **: $p < 0.01$ according with Student's *t* test.

Effect of far red exposure on PSII photochemistry

In order to investigate the reason for the increase in F_M' beyond F_M during the exposure of autotrophic cells to growth light conditions, dark-adapted samples were exposed to far red light (740 nm), which selectively excites PSI and promotes the association of LHCII to PSII. Chl*a* fluorescence, recorded as F_M' and normalised on the initial fluorescence F_M, gradually and significantly increased in autotrophic samples to a maximum value of 1.78 after 9 min of far red exposure ($p<0.05$ at times 1, 5-9 min; $p<0.01$ from the 10th min) (Fig. 2). Conversely, in mixotrophic samples Chl*a* fluorescence increased during the first 3 min, but subsequently stabilized at values of about 1.3 during far red exposure, indicating that LHCII relocation to PSII

in mixotrophic cells was less inducible by far red treatment. During the subsequent dark relaxation, Chl*a* fluorescence rapidly decreased in both samples, even though the autotrophic cells maintained values higher (around 1.1) than initial fluorescence value, whereas mixotrophic samples showed values around 0.9 (p<0.01).

Effects of mixotrophy on reoxidation kinetics of Q_A

The effects of mixotrophy on the activity of both quinone components of the quinone-iron acceptor complex, Q_A and Q_B, can be studied by measuring flash-induced changes in the yield of Chl fluorescence (Vass *et al.*, 2002). The reduction of Q_A upon flash excitation results in a prompt increase in Chl fluorescence yield, which is followed by a dark decay in the range of 100 μs – 100 s, a time range allowing the reoxidation of Q_A through various pathways (Vass *et al.*, 2002). The fluorescence relaxation is dominated by a fast component (few-hundred μs), arising from Q_A^- to Q_B electron transfer in the RCII that had an oxidised or semi-reduced PQ molecule in the Q_B pocket at the time of flashing. The middle phase (few ms) arises from Q_A^- reoxidation in centers in which Q_B site in darkness is empty and PQ has to be bound from the pool. Finally, the slow phase of flash-induced fluorescence relaxation curve (few s) shows the recombination of the S2 state of the water oxidising complex with Q_B^- via the $Q_A^-Q_B \leftrightarrow Q_AQ_B^-$ equilibrium (Vass *et al.*, 1999; Vass *et al.*, 2002; Allahverdiyeva *et al.*, 2005). Analyses of the kinetics of the flash-induced fluorescence relaxation showed no differences between autotrophic and mixotrophic samples, suggesting that the presence of glucose in the cultivation medium did not affect the forward electron transfer through the PQ pool (Fig. 3; Table 2). The kinetics was dominated by the fast phase of decay (around 560 μs; 85%), followed by a middle phase of around 10 ms time of decay with 7.7% amplitude and a slow phase of around 2 s with 7% amplitude. Despite mixotrophic samples showed a tendency to accelerated time of decay during the middle phase (around 30% less), the results were not statistically significant compared to autotrophic samples (p=0.42). In the presence of DCMU, which blocks the reoxidation of Q_A^- by forward electron transfer, the fluorescence

303 relaxation indicates the status of the PSII donor side as revealed by recombination of Q_A^- with
304 donor side components. In a functional PSII complex, the recombination partner of Q_A^- is the S2
305 state of the water oxidising complex (Allahverdiyeva *et al.*, 2005). As is shown in Fig. 3 (insert),
306 Q_A^- reoxidation kinetics in the presence of DCMU appeared slowed-down in mixotrophic samples.
307 This might reflect a defect in the assembly of the oxygen evolving complex (Allahverdiyeva *et al.*,
308 2013).

309

Sample	Total Amp (%)	Fast phase T/Amp (ms/%)	Middle phase T/Amp (ms/%)	Slow phase T/Amp (s/%)
A	100	0.568 ± 0.081 / 85.825 ± 2.597	13.500 ± 4.759 / 7.694 ± 1.300	2.066 ± 0.665 / 6.480 ± 1.369
M	100	0.553 ± 0.116 / 84.835 ± 4.471	9.414 ± 1.960 / 7.891 ± 2.187	1.806 ± 0.577 / 7.275 ± 2.335

310

311 Table 2. Characteristics of flash-induced Chl fluorescence relaxation in autotrophic (A) and mixotrophic
312 (M) *N. oleoabundans* cells. Values are time of decay (T) and relative amplitudes (Amp) in percent of total
313 variable fluorescence obtained after the fired flash. Values are means of $n \geq 3$ ± standard deviation.

314

315

316

317

Chl-protein complexes in thylakoid membranes of autotrophic and mixotrophic *N. oleoabundans* exposed to different light

Chl and protein quantification

Quantification of Chl and protein amounts in thylakoids of autotrophic and mixotrophic *N. oleoabundans* are reported in Table 3. Total Chl quantified in thylakoids was compared with the protein amount, to obtain Chl/protein ratios. Interestingly, in the mixotrophic cultures, Chl/protein was halved as compared to autotrophic samples, because of a halved concentration of pigments upon an unchanged amount of proteins. This result was clearly visible also observing Coomassie-stained SDS-PAGE (Fig. 4). About the Chl*a*/Chl*b* molar ratio, instead, higher values were calculated in mixotrophic samples than in the autotrophic, suggesting a different distribution in the proportion of Chl*a* and Chl*b* between samples (Table 3). Some of the key proteins which belong to major thylakoid complexes were detected and quantified by immunoblot analyses (Fig. 5A). Interestingly, lower amounts of PsaA (Supplementary Figure S2) and PsaB were detected in mixotrophic samples (-42.4% as compared to autotrophic cells). A slight decrease in the amount of ATP-β and LHCII protein was also observed with the addition of glucose upon growth, but it was not significant. Conversely, D1 protein was detected in higher amounts in 2.5 gL^{-1} of glucose-grown cells (+47% as compared to autotrophic samples).

To support the belief that autotrophic and mixotrophic cells had a different PSI:PSII stoichiometry, 77K spectra were recorded *in vivo* from aliquots of samples containing 8 µg mL^{-1} Chl, frozen and maintained in liquid N_2 before analyses (Fig. 5B). As clearly visible in mixotrophic samples, the peak at around 684 nm was attributed to PSII, while the peak at 714 nm was attributed to PSI-LHCI (Ferroni et al., 2011). Moreover, a broad shoulder between 692 and 703 nm was observed. Emission around 700 nm can be attributed to LHCII aggregates (Horton et al., 1991). When mixotrophic were compared to autotrophic samples, spectra, normalized at the PSII emission

342 region, appeared very different (Fig. 5B). In fact, peaks were slightly shifted in control, at 683 nm
343 for PSII and 713 nm for PSI-LHCI. Moreover, the shoulder at 692-703 nm was not observed
344 between PSII and PSI emission regions. It is possible that this emission was not evident because
345 of the higher emission from PSI-LHCI in autotrophic samples, confirming, then, the decrease in
346 the PSI amount over PSII in mixotrophic *vs* autotrophic cells observed by immunoblot reactions.

347

348

Sample	Chlorophylls ($\mu g\ \mu L^{-1}$)	Proteins ($\mu g\ \mu L^{-1}$)	Chl/proteins	Chl*a*/Chl*b*
A	3.38 ± 0.19	24.30 ± 1.53	0.139 ± 0.014	3.47 ± 0.10
M	1.65 ± 0.23 ***	25.77 ± 1.79	0.064 ± 0.011 **	4.09 ± 0.03***

349

350 Table 3. Chl amounts, protein amounts and corresponding ratios in thylakoids extracted from *N.*
351 *oleoabundans* grown with 0 (*A*) and 2.5 gL^{-1} (*M*) of glucose. n≥3 ± standard deviation. **: $p < 0.01$; ***:
352 $p < 0.001$, according with Student's *t* test.

353

354 *Organisation of thylakoid complexes*

355 In order to obtain the separation of the thylakoid membrane complexes from autotrophic and
356 mixotrophic *N. oleoabundans*, a BN-PAGE system was optimised. In a first analysis, the pattern
357 of protein complexes in autotrophic *N. oleoabundans* was compared to that of *A. thaliana*.

(Supplementary Figure S3), whose BN-PAGE profile was structured as previously described (Aro *et al.*, 2005; Caffarri, 2009; Croce and van Amerongen, 2011). In the BN-PAGE of autotrophic *N. oleoabundans*, only some protein complexes corresponded to those separated in *A. thaliana*. Autotrophic *N. oleoabundans* lacked the LHCII assembly complex. Moreover, LHCII monomers were extremely abundant as compared to LHCII trimers. The following bands with higher molecular mass were identified: band I, apparently corresponding to PSII monomer; region II, which comprised all the smearing profile between band I and the following more intense band; band III and band IV, which had a mass similar to C_2S supercomplexes of *A. thaliana*.

In a subsequent step, membrane protein complexes from autotrophic and mixotrophic *N. oleoabundans* were solubilized with dodecyl β-D-maltoside and separated by BN-PAGE with the same procedure (Fig. 6). Before thylakoid extraction, autotrophic and mixotrophic cells were exposed in parallel to darkness (dark autotrophic-*DA* and mixotrophic-*DM* samples) or maintained in growth light for 1 h (light autotrophic-*LA* and mixotrophic-*LM* samples), in order to detect differences in the protein-complexes organisation of photosynthetic membranes between samples and after a dark-light transition. BN-PAGE of the thylakoid protein complexes demonstrated a less abundant band of LHCII trimers in mixotrophic samples compared to the autotrophic ones (Fig. 6), but the light-dark differences were not evident in BN-PAGE in the first dimension.

Subsequently, each stripe from the BN-PAGE was analysed by SDS-PAGE in the 2D, enabling the separation of different protein complexes into constituting subunits (Fig. 7). In 2D silver-stained gel of dark and light autotrophic cells (Fig. 7A), the first conspicuous band from right to left was identified as the LHCII monomers. The subsequent band corresponded to LHCII trimers. Two different series of LHCII protein spots were resolved, indicating the co-existence of two types of LHCII trimers with slightly different molecular mass. The more evident BN-PAGE band above LHCII trimers, the above-mentioned complex I, comprised a small amount of Psa A/B subunits co-migrating with all the subunits of PSII monomer. Just below band I, a very faint band, indicated

as I', was shown to contain PSII monomer subunits, except CP47. Interestingly, different spots corresponding to Psa A/B subunits characterized the series of complexes having increasing molecular mass in the so-called region II. Band III, fainter than band I, comprised Psa A/B subunits of PSI co-migrating with CP43, CP47, D1 and D2 subunits of dimeric PSII. In this complex, small amounts of LHCII were also observed. Based on the comparison with *A. thaliana* profile (Supplementary Figure S3), band III was interpreted as the result of the co-migration of two independent complexes, PSII-LHCII (C_2S) and PSI-LHCII (state-transition-like complex). Finally, in band IV Psa A/B subunits of PSI were observed associated to noticeable amounts of LHCI and LHCII complexes, but only negligible amount of PSII. Interestingly, despite silver-stained gels are not precisely quantitative, two aspects were noteworthy in autotrophic samples: 1) the amount of LHC associated with PSI in band IV decreased during the dark-light transition of the microalga, suggesting a stronger affinity of the subunits which compose this complex in darkness; 2) PSI subunits of thylakoids extracted from samples maintained in growth light were more evenly distributed from lower to higher molecular mass complexes as compared to thylakoids extracted from cells incubated in the dark. About the 2D BN/SDS-PAGE silver-stained image of mixotrophic samples (Fig. 7B), no major differences were observed in the general thylakoid protein pattern by comparison with autotrophic samples, except for the presence of a region above band IV, indicated as "megacomplexes", which was resolved in the 2D gel in subunits belonging to PSII and PSI. In dark-acclimated mixotrophic samples, only Psa A/B subunits were clearly detectable in the band, whereas in light-acclimated mixotrophic samples CP47, CP43, D2, D1 and LHC proteins were also resolved. As compared to the autotrophic samples, in the mixotrophic cells: 1) PSI was mainly concentrated in band IV independent of the dark/light incubation; 2) band IV was shown to also contain PSII, i.e. presumably a C_2S LHCII-PSII supercomplex with higher molecular mass than the C_2S PSII complex in band III; 3) PSI and PSII tended to associate into stable large megacomplexes with LHCII, especially in light conditions.

Quantification of spot density of thylakoid proteins was performed staining the 2D BN/SDS-PAGE gels with SYPRO® Ruby dye. Psa A/B and CP43 were used to quantify the relative amounts of PSI and PSII, respectively. LHC proteins generated too intense signal to give reliable results in a gel-stained protein quantification. PSI and PSII distribution in thylakoid complexes was compared between light and dark autotrophic and mixotrophic samples (Fig. 8). When PSII distribution was examined among the different thylakoid complexes (Fig. 8A), the majority was found as a monomer (band I). In particular, autotrophic samples showed a higher proportion (> 80% of total PSII) than mixotrophic cells (around 72% in both samples). On the contrary, PSII of band III (putative C_2S) was more abundant in mixotrophic cells, irrespective of dark-light acclimation (+ 60%, as compared to the corresponding autotrophic samples). In band IV, *LA* showed a negligible percentage of PSII, despite no significant differences were observed with *DA*, as well as between autotrophic and mixotrophic samples incubated in darkness. As seen in silver-stained gels, PSII did not characterize the region II and indeed its presence was not determined. Thus, it can be concluded that, irrespective of the light exposure before extraction, mixotrophic samples showed more abundant PSII in the dimeric, LHCII associated, forms as compared to the autotrophic samples. This tendency of PSII to organise more stably with LHCII was in line with the occurrence of megacomplexes.

Regarding the relative protein amount of PSI, the transition from dark to light did not induce a different distribution in the bands III and IV in autotrophic samples (Fig. 8B). Instead, in region II, PSI proportion decreased by 45% upon light exposure. On the contrary, PSI became more represented in the lighter form, co-migrating with PSII monomer in band I. In mixotrophic samples, the dark-to-light transition did not change PSI distribution among complexes. Interestingly, in those samples a lower proportion of PSI was found in complex III compared to autotrophic samples (about 65% less). As observed previously for PSII distribution, the presence of megacomplexes occurred only in mixotrophic samples (Fig. 8B).

433 The distribution of PSII and PSI in mixotrophic samples conveyed a picture of low dynamism of
434 thylakoid protein complexes, which was expected to have an impact on the thylakoid architecture.
435 In fact, TEM images showed in both autotrophic and mixotrophic cells a similar thylakoid system,
436 except for the very high degree of appression in the latter, even leading to a virtual absence of the
437 thylakoid lumen (Fig. 9).

438 *Detection of thylakoid phosphoproteins*

439 The determination of *in vivo* thylakoid phosphoproteins was important to understand the role of
440 band IV and megacomplexes detected in 2D/BN-SDS PAGE. In particular, the strength of LHCII-
441 PSII and LHCII-PSI association is usually linked to LHCII phosphorylation levels (Mekala *et al.*,
442 2015). The detection was obtained with anti-phosphothreonine (Fig. 10A). Coomassie-stained
443 SDS-PAGE of a replicate gel was performed to confirm the efficiency of the electrophoretic race
444 (Fig. 10B). In all the samples, the major phosphoproteins were identified as CP43, D2 and two
445 different proteins of LHCII (Fig. 10A), i.e. two less abundant subunits with high molecular mass
446 (Fig. 10B). LHCII phosphorylation was observed at basal levels when thylakoids were extracted
447 from dark-incubated autotrophic samples. As expected, a strong increase in the phosphorylation
448 level of LHCII proteins was very evident in *LA*. Intrinsic antenna CP43 and protein subunit D2 of
449 PSII core were not affected by the transition from dark to growth light and remained
450 phosphorylated at basal levels. When *DM* samples were considered, only CP43 appeared slightly
451 phosphorylated, whereas other phosphoproteins were barely detectable. Moreover, very
452 surprisingly, the extent of light-induced phosphorylation was very limited. The phosphorylation
453 levels were even lower than those observed in dark-acclimated autotrophic cells (Fig. 10A).

454

455

Discussion

In *N. oleoabundans*, only limited information concerning its photosynthetic metabolism is available. Recent works (Baldisserotto *et al.*, 2014; Giovanardi *et al.*, 2014; Sabia *et al.*, 2015, Baldisserotto *et al.*, 2016) have proved that the assimilation of organic carbon in this microalga interferes with the photosynthetic performance in a contrasting manner compared to other green microalgae, in which mixotrophy induces a down-regulation of photosynthesis (Oesterhelt *et al.*, 2007; Liu *et al.*, 2009). In order to explore the mechanisms involved during the mixotrophic growth, and understanding how the interaction between Chl-protein complexes are modified by the glucose assimilation and how light irradiance affects the photosynthetic apparatus, detailed analyses were performed on *N. oleoabundans* cultivated in the presence of 2.5 gL^{-1} of glucose, which promoted growth and F_V/F_M, consistent with previously published results (Supplementary Figure 1S; Giovanardi *et al.*, 2014).

Higher F_V/F_M in mixotrophic than in autotrophic cells is due to down-regulated chlororespiration

Measurements of Chl*a* fluorescence induction were performed on dark-adapted cells. This condition is meant to fully oxidise the PQ pool, leading to a complete opening of PSII. However, PQ reduction can partially occur in the dark in different organisms because of chlororespiratory pathways, which allow dissipating the excess of reducing power in the stroma by the ultimate reduction of O_2 (Bennoun, 1994; Feild *et al.*, 1998; Hoefnagel, 1998; Hill and Ralph, 2008; Cruz *et al.*, 2011). As a consequence of PQ reduction in darkness, the phosphorylation of LHCII and its migration to PSI is promoted (Krause and Weiss, 1984; Finazzi *et al.*, 1999; Houille-Vernes *et al.*, 2011), whereas when low actinic light is triggered, F_M' values gradually increase and exceed F_M (Cruz *et al.*, 2011; Houille-Vernes *et al.*, 2011). This is exactly observed in autotrophic *N. oleoabundans* cells (Fig. 1A). Very surprisingly, instead, mixotrophic cells did not appear much affected by chlororespiration in darkness, and, when samples were exposed to growth light

conditions, F_M' only slightly exceeded F_M values (Fig. 1B). It has been suggested that, if chlororespiration occurs, the maximum F_M' value measured under low actinic light (F_{Mtrue}) should be used instead of the dark-acclimated F_M (Serôdio et al, 2006). Then, if the F_V/F_{Mtrue} ratio was used instead of F_V/F_M, the same maximum photochemical activity was determined in autotrophic and mixotrophic cells (Table 1).

Further evidence for the fact that in autotrophic samples a dark incubation determines a partial association of LHCII with PSI was provided by illumination the cells with far red light (Fig. 2), which selectively excites PSI, promoting the maximum oxidation of the PQ pool and of the inter-system electron transport chain (Lokstein *et al.*, 1994; Schansker and Strasser, 2005; Hill and Ralph, 2008). In autotrophic cells, the gradual rise in F_M'/F_M during far red light treatment indicated a gradual increase in the LHCII proportion serving the PSII core. On the contrary, in mixotrophic cells the ratio soon reached a plateaux, suggesting that most LHCII was already linked to PSII in dark-acclimated samples.

In the light of above results, it emerges that the higher F_V/F_M ratio characterising mixotrophic *N. oleoabundans* actually occurred because the F_M levels of autotrophic samples were underestimated (Hill and Ralph, 2008; Giovanardi *et al.*, 2014). Therefore, the glucose-grown samples did not hold an improved maximum photosynthetic efficiency of PSII, but rather they might have experienced important effects on the reduction state of the photosynthetic electron transport chain (Baker, 2008; Roach *et al.*, 2013). On the other hand, the availability of oxidized PQ did not seem to be much influenced by the addition of glucose in the culture medium (Fig. 3), as previously shown also in *Chlamydomonas reinhardtii* (Roach *et al.*, 2013). However, it is noteworthy that in green microalgae, the fast reoxidation phase appears much more conspicuous compared to those measured in higher plants and cyanobacteria (Allahverdiyeva *et al.*, 2013; Volgusheva *et al.*, 2013; Deák *et al.*, 2014). This reflects a faster and more efficient forward electron transfer from Q_A^- to the Q_B present in the Q_B pocket of PSII as compared to other photosynthetic organisms, but, as a

side effect, it can also hide differences in the amplitudes and times of decay of the subsequent middle and slow phases of Chl fluorescence. The addition of DCMU, for instance, revealed a probable defect in the assembly of the oxygen evolving complex, despite incipient, in mixotrophic cells. A similar effect was also previously observed in mixotrophic *C. reinhardtii* (Roach *et al.*, 2013). This defect may be negligible in growth-light conditions, but could become relevant if cells were exposed to high light.

Mixotrophic cells are more sensitive to high-light exposure than autotrophic cells

Differences in properties of the electron transport pathways in mixotrophic and autotrophic growth conditions were not detectable under growth light conditions. This light regime, indeed, did not influence the F_tLL/F_{Mtrue} ratio (Table 1) and, thus, did not provoke an electron overloading of the thylakoid membrane. However, the capability to avoid photodamage under high light exposure was strongly affected in mixotrophic cells, as showed by the lower F_tHL/F_{Mtrue} ratio than in autotrophic samples. In the latter cells, according to Tikhonov (2015), when actinic high light was switched on, the gradual, sensible increase in F_t reflected the rapid reduction of the intermembrane PQ pool (Fig. 1). Subsequently, its decrease was linked to the activation of the Calvin-Benson cycle and concomitant acceleration of electron outflow from PSI, with the consequent PQH_2 pool reoxidation (Tikhonov, 2015). The mixotrophic samples reached in a very short time the maximum level of reduced PQ pool as compared to cells grown autotrophically. This led to the less evident peak of F_t observed in mixotrophic conditions. The subsequent decrease in the F_t values was likewise less evident. Accordingly, a slower electron flow in mixotrophy during high light exposure might be linked to a reduced activity of the Calvin-Benson cycle and a lower proportion of PSI in the thylakoid membrane (Tikhonov, 2015).

529 *PSII complexes become less dynamic in mixotrophic cells*

530 The redox state of the electron transport components influences not only the LHCII association to
531 PSII and PSI, but also the relative abundance of both photosystems (Kováks *et al.*, 2000). In this
532 work, mixotrophic samples were mainly characterised by a decrease in the amount of PSI and an
533 increase in the amount of PSII (Fig. 5A, B). Furthermore, Chl*a*/Chl*b* ratio was significantly higher
534 in cells grown with glucose. As Chl*b* is mostly located in LHCII complexes (Anderson *et al.*,
535 1995), and immunodetection did not reveal differences in the amount of LHCII between
536 autotrophic and mixotrophic cells (Fig. 5A), this result further supported a relative increase in PSII
537 reaction centres when cells were grown under mixotrophy. The analyses of supramolecular
538 organisation of thylakoid complexes allowed detection of a major difference in the amount of
539 trimeric LHCII, higher in cells grown autotrophically, in particular in *DA* samples, as compared
540 to mixotrophic samples. Free LHCII trimers are considered the only LHCII complexes involved
541 in state transition-like processes (Ünlü *et al.*, 2014). This confirms that autotrophic cells can rely
542 on a greater capability to modulate LHCII association with a better efficiency. More detailed
543 analyses of the supramolecular organisation of photosystems by 2D silver-stained SDS-PAGE and
544 corresponding quantitative distribution of PSI and PSII among the different major complexes
545 revealed the specificity of the pigment-protein complexes of each sample.

546 In all thylakoid samples, PSII was mostly monomeric. For many years, there has been a long-
547 standing discussion about the assembly of PSII components into functional multimeric protein
548 complexes in green algae and higher plants (Minagawa and Takahashi, 2004; Dekker and
549 Boekema, 2005). Currently, it is widely accepted that functional PSII is normally organised as a
550 dimer and concentrated in the stacked, appressed regions of thylakoids, whereas PSII monomer
551 units are usually found in the unstacked thylakoid membranes, where the PSII repair cycle occurs
552 (Kruse *et al.*, 2000; Minagawa and Takahashi, 2004; Dekker and Boekema, 2005; Daniellson *et*
553 *al.*, 2006). However, in some cases, PSII monomers were shown to be fully active and also located

554 both in grana cores and margins (Dekker and Boekema, 2005; Daniellson *et al.*, 2006; Takahashi
555 *et al.*, 2009). Moreover, Järvi *et al.* (2011) discovered that in the absence of an external charge in
556 BN/PAGE, PSII complexes were mainly found in the monomeric form. The debate is still open,
557 but what clearly emerged in *N. oleoabundans* was that PSII was more distributed in higher forms
558 of association in mixotrophic than in autotrophic samples, preferring the maintenance of PSII as a
559 dimer and even in megacomplexes together with PSI. In megacomplexes, there is a stable and
560 advantageous association between PSI and PSII that promotes photoprotective energy spillover
561 towards PSI (Grieco *et al.*, 2015; Yokono *et al.*, 2015; Ferroni et al., 2016). The strong interaction
562 between PSII and PSI limits also the necessity of D1 protein subunit of PSII to be replaced after
563 photodamage events. On the opposite, a fluent electron transfer through the thylakoid membranes,
564 as well as the maintenance of an excitation balance between PSII and PSI, is fundamental for an
565 efficient use of light for photochemistry (Mekala *et al.*, 2015).

566 On the whole, in autotrophic *N. oleoabundans*, then, the photosynthetic membrane is regulated as
567 expected. In darkness, chlororespiratory electron recycling is active and PQ pool is partially
568 reduced, as also demonstrated by the presence of phosphorylated LHCII and PSII subunits (Fig.
569 10). During the initial exposure to growth light conditions, the electron transfer components turn
570 at the oxidised state and maximum PSII quantum efficiency is reached. The role of LHCII
571 phosphorylation is mainly the balancing of energy excitation between PSII and PSI (Tikkanen and
572 Aro, 2012), and at low irradiances, maximal phosphorylation is induced in chloroplast *in vivo*
573 (Rintämaki *et al.*, 2000). Under a steady-state low-growth light conditions, maximum PSII core
574 and LHCII phosphorylation is then achieved in autotrophic cultures and ensures an even excitation
575 distribution between PSII and PSI (Tikkanen and Aro, 2012). This represents for the cells a highly
576 fluid condition of thylakoid complexes, which allows extensive, though labile, interactions
577 between photosystems and LHCII (Mekala *et al.*, 2015).

In dark-adapted mixotrophic *N. oleoabundans*, chlororespiration appears to be down-regulated and LHCII is mainly associated to PSII, sustained by the absence of phosphorylation of PSII core and LHCII (Fig. 10). Furthermore, the very weak phosphorylation even at growth light conditions, the poorness of free LHCII trimers, the very strong PSII-LHCII association of complexes and PSI-PSII-LHCII megacomplexes suggest a very low dynamicity of thylakoid protein complexes in mixotrophic cells. This is reflected also by a visibly higher appression degree of thylakoids in mixotrophic cells, presumably sustained by very low levels of protein phosphorylation (Fig. 9; Fristedt *et al.*, 2009). Some hypotheses might be advanced to explain this behaviour. The exogenous glucose - uptaken with such a high efficiency that results even in the accumulation of starch granules (Baldisserotto *et al.*, 2016) - might have contributed to an excess of available reducing power through respiration. This could have promoted the maintenance of plastid thioredoxins at the reduced state, leading to the inhibition of LHCII phosphorylation and thus to the promotion of PSII-LHCII association (Rintamäki *et al.*, 2000). Moreover, a higher respiration rate in mixotrophic cells can result in a high availability of ATP, with a consequent down-regulation of Calvin-Benson Cycle and of PSI. A lower PSI:PSII stoichiometry may depend also on incapability of proteolitic enzymes to degrade PSII subunits (Chow *et al.*, 1990). In fact, it was demonstrated that PSII is less accessible to degradation when associated in megacomplexes (Tikkanen and Aro, 2012). The low PSII core protein phosphorylation, as observed in mixotrophic microalgal thylakoids, limits the fluidity of the thylakoid membrane and cooperates in hindering the disassembly of PSII supercomplexes, affecting also the oligomerisation of PSII and the regulation of D1 protein degradation. This event impacts on the capability of mixotrophic samples to react to photodamage when cells are exposed to prolonged high-light conditions (Figure 1B; Tikkanen *et al.*, 2008; Tikkanen and Aro, 2012).

Conclusions

In conclusion, contrary to what previously hypothesised, the supply of glucose to *N. oleoabundans* cells does not induce an emphasised photosynthetic activity compared to autotrophic cultures, but rather provokes a decreased dynamicity of PSII assembly. Ultimately, the effect of such a low dynamicity is the preservation, or a delayed degradation, of PSII, in spite of the mixotrophic mode of growth.

Conflict of interest

The Authors declare no conflict of interest.

Author contribution

MG, LF, EMA and SP participated in the conception and design of the study; MG, MP, LF, ML, CB collected data and performed analyses; MG, LF and SP drafted the article; LF, EMA and SP assisted the results interpretation and critical reviewed the manuscript; all Authors read and approved the final manuscript.

Acknowledgments

This work was supported by ~~grants of~~ the University of Ferrara and the University Institute for Higher Studies, IUSS - Ferrara 1391, with a fellowship provided to MG, and by the Academy of Finland with grants no. 271832 and 273870 to EMA.

623 References

624 Allahverdiyeva Y, Mamedov F, Mäenpää P, Vass I, Aro EM. 2005. Modulation of photosynthetic
625 electron transport in the absence of terminal electron acceptors: Characterization of the *rbcL*
626 deletion mutant of tobacco. Biochimica and Biophysica Acta 1709, 69-83.

627 Allahverdiyeva Y, Mamedov F, Suorsa M, Styring S, Vass I, Aro EM. 2007. Insights into the
628 function of PsbR protein in *Arabidopsis thaliana*. Biochimica and Biophysica Acta 1767, 677-
629 685.

630 Allahverdiyeva Y, Mustila H, Ermakova M, Bersanini L, Richaud P, Ajlani G, Battchikova N,
631 Cournac L, Aro EM. 2013. Flavodiiron proteins Flv1 and Flv3 enable cyanobacterial growth and
632 photosynthesis under fluctuating light. Proceedings of the National Academy of Sciences of the
633 United States of America. 110, 4111-4116.

634 Anderson JM, Chow WS, Park YI. 1995. The grand design of photosynthesis: Acclimation of the
635 photosynthetic apparatus to environmental cues. Photosynthesis Research 46, 129-139.

636 Aro EM, Suorsa M, Rokka A, Allahverdiyeva Y, Paakkarinen V, Saleem A, Battchikova N,
637 Rintamäki E. 2005. Dynamics of photosystem II: a proteomic approach to thylakoid protein
638 complexes. Journal of Experimental Botany 56, 347-356.

639 Baker NR. 2008. Chlorophyll fluorescence. A probe of photosynthesis in vivo. Annual Review of
640 Plant Biology 59, 89-113.

641 Baldisserotto C, Ferroni L, Anfuso E, Pagnoni A, Fasulo MP, Pancaldi S. 2007. Responses of
642 *Trapa natans* L. floating laminae to high concentrations of manganese. Protoplasma. 231, 65-82.

643 Baldisserotto C, Ferroni L, Giovanardi M, Pantaleoni L, Boccaletti L, Pancaldi S. 2012. Salinity
644 promotes growth of freshwater *Neochloris oleoabindans* UTEX 1185 (Sphaeropleales,
645 Neochloridaceae): morpho-physiological aspects. Phycologia 51, 700-710.

646 Baldisserotto C, Giovanardi M, Ferroni L, Pancaldi S. 2014. Growth, morphology and
647 photosynthetic responses of *Neochloris oleoabundans* during cultivation in a mixotrophic brackish
648 medium and subsequent starvation. Acta Physiologiae Plantarum. 1, 461-72.

649 Baldisserotto C, Popovich C, Giovanardi M, Sabia A, Ferroni L, Constenla D, Leonardi P,
650 Pancaldi S. 2016. Photosynthetic aspects and lipid profiles in the mixotrophic alga *Neochloris*
651 *oleoabundans* as useful parameters for biodiesel production. Algal Research. 16, 255-65.

652 Barber J. 2002. Photosystem II: a multisubunit membrane protein that oxidises water. Current
653 Opinion in Structural Biology 12, 523-530.

654 Bennoun P. 1994. Chlororespiration revisited: mitochondrial-plastid interactions in
655 Chlamydomonas. Biochimica et Biophysica Acta-Bioenergetics. 1186, 59-66.

656 Borowitzka MA. 2013. High-value products from microalgae – their development and
657 commercialisation. Journal of Applied Phycology 25, 743-756.

658 Caffarri S, Kouřil R, Kereïche S, Boekema EJ, Croce R. 2009. Functional architecture of higher
659 plant photosystem II supercomplexes. The EMBO journal 28, 3052-63.

660 Chisti Y. 2007. Biodiesel from microalgae. Biotechnology Advances 25, 294-306.

661 Chow WS, Melis A, Anderson JM. 1990. Adjustments of photosystem stoichiometry in
662 chloroplasts improve the quantum efficiency of photosynthesis. Proceedings of the National
663 Academy of Science of the United States of America 87, 7502-7506.

664 Croce R, van Amerongen H. 2011. Light-harvesting and structural organization of photosystem
665 II: from individual complexes to thylakoid membrane. Journal of Photochemistry and
666 Photobiology B: Biology 104,142-53.

667 Cruz S, Goss R, Wilhelm C, Leegood R, Horton P, Jakob T. 2011. Impact of chlororespiration on
668 non-photochemical quenching of chlorophyll fluorescence and on the regulation of the
669 diadinoxanthin cycle in the diatom *Thalassiosira pseudonana*. Journal of Experimental Botany 62,
670 509-519.

671 Danielsson R, Suorsa M, Paakkarinen V, Alpertsson PÅ, Styring S, Aro EM, Mamedov F. 2006.
672 Dimeric and monomeric organisation of photosystem II. Journal of Biological Chemistry 281,
673 14241-14249.

674 DeáK Z, Lásló S, Kiss É, Vass I. 2014. Characterisation of wave phenomena in the relaxation of
675 flash-induced chlorophyll fluorescence yield in cyanobacteria. Biochimica et Biophysica Acta
676 1837, 1522-1532.

677 Dekker JP, Boekema EJ. 2005. Supramolecular organisation of thylakoid membranes proteins in
678 green plants. Biochimica and Biophysica Acta 1706, 12-39.

679 Falkowski PG, Raven JA. 2007. In: Falkowski PG, Raven JA, eds. Aquatic photosynthesis.
680 Princeton University Press, 1-43.

681 Feild TS, Nedbal L, Ort DR. 1998. Nonphotochemical reduction of the plastoquinone pool in
682 sunflower leaves originates from chlororespiration. Plant Physiology. 116, 1209-18.

683 Ferroni L, Baldisserotto C, Giovanardi M, Pantaleoni L, Morosinotto T, Pancaldi S. 2011. Revised
684 assignment of room-temperature chlorophyll fluorescence emission bands in single living cells of
685 *Chlamydomonas reinhardtii*. Journal of Bioenergy and Biomembranes 43, 163-173.

686 Ferroni L, Suorsa M, Aro EM, Baldisserotto C, Pancaldi S. (2016) Light acclimation in the
687 lycophyte *Selaginella martensii* depends on changes in the amount of photosystems and on the
688 flexibility of the light-harvesting complex II antenna association with both photosystems. New
689 Phytologist 211**,** 554-568.

690 Finazzi G, Furia A, Barbagallo RP, Forti G. 1999. State transitions, cyclic and linear electron
691 transport and photophosporylation in *Chlamydomonas reinhardtii*. Biochimica and Biophysica
692 Acta 1413, 117-129.

693 Fristedt R, Willig A, Granath P, Crèvecoeur M, Rochaix JD, Vener AV. 2009. Phosphorylation of
694 photosystem II controls functional macroscopic folding of photosynthetic membranes in
695 Arabidopsis. The Plant Cell 21, 3950-3964.

696 Geider RJ, MacIntyre HL. 2002. Physiology and Biochemistry of photosynthesis and algal carbon
697 acquisition. In: William PJleB, Thomas DR, Reynolds CS, eds. Phytoplankton productivity and
698 carbon assimilation in marine and freshwater ecosystems. London: Blackwell Science Ltd, 44-77.

699 Giovanardi M, Ferroni L, Baldisserotto C, Tedeschi P, Maietti A, Pantaleoni L, Pancaldi S. 2013.
700 Morpho-physiological analyses of *Neochloris oleoabundans* (Chlorophyta) grown
701 mixotrophically in a carbon-rich waste product. Protoplasma 250, 161-174.

702 Giovanardi M, Baldisserotto C, Ferroni L, Longoni P, Cella R, Pancaldi S. 2014. Growth and lipid
703 synthesis promotion in mixotrophic *Neochloris oleoabundans* (Chlorophyta) cultivated with
704 glucose. Protoplasma 251, 115-125.

705 Grieco M, Suorsa M, Jajoo A, Tikkanen M, Aro EM. 2015. Light-harvesting II antenna trimers
706 connect energetically the entire photosynthetic machinery – including both photosystems II and I.
707 Biochimica et Biophysica Acta – Bioenergetics 1847, 607-619.

708 Hill R, Ralph PJ. 2008. Dark-induced reduction of the plastoquinone pool in zooxanthellae of
709 scleractinian corals and implications for measurements of chlorophyll *a* fluorescence. Symbiosis
710 46, 45-56.

711 Hippler M, Klein J, Fink A, Allinger T, Hoerth P. 2001. Towards functional proteomics of
712 membrane protein complexes: analysis of thylakoid membranes from *Chlamydomonas*
713 *reinhardtii*. The Plant Journal 28, 595-606.

714 Hoefnagel MH, Atkin OK, Wiskich JT. 1998. Interdependence between chloroplasts and
715 mitochondria in the light and the dark. Biochimica et Biophysica Acta - Bioenergetics 1366, 235-
716 55.

717 Horton P, Ruban AV, Rees D, Pascal AA, Noctor G, Young AJ. 1991. Control of the light-
718 harvesting function of chloroplast membranes by aggregation of the LHCII chlorophyll-protein
719 complex. Journal of Federation of European Biochemical Societies 292, 1-4.

720 Horváth G, Melis A, Hideg É, Droppa M, Vigh L. 1987. Role of lipids in the organization and
721 function of photosystem II studied by homogeneous catalytic hydrogenation of thylakoid
722 membranes in situ. Biochimica et Biophysica Acta - Bioenergetics 891, 68-74.

723 Houille-Vernes L, Rappaport F, Wollman FA, Alric J, Johnson X. 2011. Plastid terminal oxidase
724 2 (PTOX2) is the major oxidase involved in chlororespiration in Chlamydomonas. Proceedings of
725 the National Academy of Sciences of the United States of America 108, 20820-20825.

726 Ivancich A, Horváth L, Droppa M, Horváth G, Farkas T. 1994. Spin label EPR study of lipid
727 solvation of supramolecular photosynthetic protein complexes in thylakoids. Biochimica et
728 Biophysica Acta - Biomembranes. 1196, 51-56.

729 Järvi S, Suorsa M, Paakkarinen V, Aro EM. 2011. Optimized native gel system for separation of
730 thylakoid protein complexes: novel super- and mega- complexes. Biochemical Journal 439, 207-
731 214.

732 Joliot A, Joliot P. 1964. Etude Cinétique de la reaction photochimique libérant l'oxigène au cours
733 de photosynhtèse. Comptes rendus de l'Académie des Sciences 258, 4622-4625.

734 Kirchhoff H, Mukherjee U, Galla HJ. 2002. Molecular architecture of the thylakoid membrane:
735 lipid diffusion space for plastoquinone. Biochemistry. 41, 4872-4882.

736 Kováks L, Wiessner W, Kis M, Nagy F, Mende D, Demeter S. 2000. Short- and long-term redox
737 regulation of photosynthetic light energy distribution and photosystem stoichiometry by acetate
738 metabolism in the green alga, *Chlamydobotrys stellata*. Photosynthesis Research 65, 231-247.

739 Krause GH, Weiss E. 1984. Chlorophyll fluorescence as a tool in plant physiology. II.
740 Interpretation of the fluorescence signals. Photosynthesis Research 5, 1139-157.

741 Kruse O, Hankamer B, Konczak C, Gerle C, Morris E, Radunz A, Schmid GH, Barber J. 2000.
742 Phosphatidylglycerol is involved in the dimerization of photosystem II. The Journal of Biological
743 Chemistry 275, 6509-6514.

744 Laemmli U. 1970. Cleavage of structural proteins during the assembly of the head of bacteriophage
745 T4. Nature 227, 680-685.

746 Lee Y. 2001. Microalgal mass culture systems and methods: their limitation and potential. Journal
747 of Applied Phycology 13, 307-315.

748 Lichtenthaler HK, Buschmann C, Knapp M. 2005. How to correctly determine the different
749 chlorophyll fluorescence parameters and the chlorophyll fluorescence decrease ratio RFd of leaves
750 with the PAM fluorometer. Photosynthetica 43, 379–393.

751 Liu X, Duan S, Li A, Xu N, Cai Z, Hu Z. 2009. Effects of organic carbon sources on growth,
752 photosynthesis, and respiration of *Phaeodactylum tricornutum*. Journal of Applied Phycology 21,
753 239-246.

754 Lokstein H, Härtel H, Hoffmann P, Woitke P, Renger G. 1994. The role of light-harvesting
755 complex II in excess excitation energy dissipation: an in-vivo fluorescence study on the origin of
756 high-energy quenching. Journal of Photochemistry and Photobiology B: Biology 26, 175-184.

757 Lowry OH, Rosebrough NJ, Farr AL, Randall RJ. 1951. Protein measurement with the Folin
758 phenol reagent. Journal of Biological Chemistry 193, 265-75.

759 Mekala NR, Suorsa M, Rantala M, Aro EM, Tikkanen M. 2015. Plants actively avoid state
760 transitions upon changes in light intensity: role of light-harvesting complex II protein
761 dephosphorylation in high light. Plant Physiology. 168, 721-34.

762 Minagawa J. 2009. Light-harvesting proteins. In: Stern D, Witman GB, Harris EH, eds.
763 *Chlamydomonas* sourcebook. Amsterdam: Elsevier, 503-540.

764 Minagawa J, Takahashi Y. 2004. Structure, function and assembly of Photosystem II and its light-
765 harvesting proteins. Photosynthesis Research 82, 241-263.

766 Nelson N, Ben-Shem A. 2004. The complex architecture of oxygenic photosynthesis. Nature
767 Reviews Molecular Cell Biology 5, 971-982.

768 Nelson N, Yocum CF. 2006. Structure and Function of Photosystems I and II. Annual Review of
769 Plant Biology 57, 521-565.

770 Nevo R, Charuvi D, Tsabari O, Reich Z. 2012. Composition, architecture and dynamics of the
771 photosynthetic apparatus in higher plants. The Plant Journal 70, 157-76.

772 Oesterhelt C, Schmalzlin E, Schmitt JM, Lokstein H. 2007. Regulation of photosynthesis in the
773 unicellular acidophilic red alga *Galdieria sulphuraria*. The Plant Journal 51, 500-511.

774 Porra RJ, Thompson WA, Kriedemann PE. 1989. Determination of accurate extinction coefficients
775 and simultaneous-equations for assaying chlorophyll-*a* and chlorophyll-*b* extracted with 4
776 different solvents: verification of the concentration of chlorophyll standards by atomic-absorption
777 spectroscopy. Biochimica and Biophysica Acta 975, 384-394.

778 Rintamäki E, Martinsuo P, Pursiheimo S, Aro EM. 2000. Cooperative regulation of light-
779 harvesting complex II phosphorylation via the plastoquinol and ferredoxin-thioredoxin system in
780 chloroplasts. Proceedings of the National Academy of Sciences of the United States of America
781 97, 11644-11649.

782 Roach T, Sedoud A, Krieger-Liszkay A. 2013. Acetate in mixotrophic growth medium affects
783 photosystem II in *Chlamydomonas reinhardtii* and protects against photoinhibition. Biochimica et
784 Biophysica Acta 1827, 1183-1190.

785 Rokka A, Suorsa M, Saleem A, Battchikova N, Aro EM. 2005. Synthesis and assembly of
786 thylakoid protein complexes: multiple assembly steps of photosystem II. Biochemical Journal 388,
787 159-168.

788 Sabia A, Baldisserotto C, Biondi S, Marchesini R, Tedeschi P, Maietti A, Giovanardi M, Ferroni
789 L, Pancaldi S. 2015. Re-cultivation of *Neochloris oleoabundans* in exhausted autotrophic and
790 mixotrophic media: the potential role of polyamines and free fatty acids. Applied Microbiology
791 and Biotechnology. 99, 10597-609.

792 Scott SA, Davey MP, Dennis JS, Horst I, Howe CJ, Lea-Smith DJ, Smith AG. 2010. Biodiesel
793 from algae: challenges and prospects. Current Opinion in Biotechnology 21, 277-286.

794 Serôdio J, Vieira S, Cruz S, Coelho H. 2006. Rapid light-response curves of chlorophyll
795 fluorescence in microalgae: relationship to steady-state light curves and non-photochemical
796 quenching in benthic diatom-dominated assemblages. Photosynthesis Research 90, 29-43.

797 Schansker G, Strasser RJ. 2005. Quantification of non-Q_B-reducing centers in leaves using a far-
798 red pre-illumination. Photosynthesis Research 84, 145-151.

799 Stephens E, Ross IL, Mussgnug JH, Wagner LD, Borowitzka MA, Posten C, Kruse O, Hankamer
800 B. 2010. Future prospects of microalgal biofuel production systems. Trends in Plant Science 15,
801 554-564.

802 Suorsa M, Rantala M, Mamedov F, Lespinasse M, Trotta M, Grieco M, Vuorio E, Tikkanen M,
803 Järvi S, Aro EM. 2015. Light acclimation involves dynamic re-organisation of the pigment-protein
804 megacomplexes in non-appressed thylakoid domains. The Plant Journal 84, 360-373.

805 Takahashi T, Inoue-Kashino N, Ozawa S, Takahashi Y, Kashino Y, Satoh K. 2009. Photosystem
806 II complex in vivo is a monomer. Journal of Biological Chemistry 284, 15598-15606.

807 Tikhonov AN. 2015. Induction events and short-term regulation of electron transport in
808 chloroplasts: an overview. Photosynthesis Research 125, 65-94.

809 Tikkanen M, Grieco M, Kangasjiärvi S, Aro EM. 2008. Thylakoid protein phosphorylation in
810 higher plant chloroplasts optimizes electron transfer under fluctuating light. Plant Physiology 152,
811 723-735.

812 Tikkanen M, Aro EM. 2012. Thylakoid protein phosphorylation in dynamic regulation of
813 photosystem II in higher plants. Biochimica et Biophysica Acta - Bioenergetics. 1817, 232-238.

814 Tornabene TG, Holzer G, Lien S, Burris N. 1983. Lipid composition of the nitrogen starved green
815 alga *Neochloris oleoabundans*. Enzyme Microbiology and Technology 5, 435-440.

816 Valverde F, Ortega JM, Losada M, Serrano A. 1995. Sugar-mediated transcriptional regulation of
817 the Gap gene system and concerted photosystem II functional modulation in the microalga
818 *Scenedesmus vacuolatus*. Planta 221, 937-952.

819 Vass I, Kirilovsky D, Etienne AL. 1999. UV-B radiation-induced donor- and acceptor-side
820 modifications of photosystem II in the cyanobacterium *Synechocystis* sp. PCC 6803, Biochemistry
821 39, 12786-12794.

822 Vass I, Turcsányi E, Touloupakis E, Ghanotakis D, Petrouleas V. 2002. The mechanism of UV-A
823 radiation-induced inhibition of photosystem II electron transport studied by EPR and Chlorophyll
824 Fluorescence. Biochemistry 41, 10200-10208.

825 Volgusheva A, Styring S, Mamedov F. 2013. Increased photosystem II stability promotes
826 H_2 production in sulfur-deprived *Chlamydomonas reinhardtii*. Proceedings of the National
827 Academy of Sciences of the United States of America 110, 7223-7228.

828 Ünlü C, Drop B, Croce R, van Amerongen H. 2014. State transitions in *Chlamydomonas*
829 *reinhardtii* strongly modulate the functional size of photosystem II but not of photosystem I.
830 Proceedings of the National Academy of Sciences of the United States of America 111, 3460-
831 3465.

832 Watanabe M, Iwai M, Narikawa R, Ikeuchi M. 2009. Is the photosystem II complex a monomer
833 or a dimer? Plant and cell physiology 50, 1674-1680.

834 Wellburn AR. 1994. The spectral determination of Chlorophylls *a* and *b*, as well as total
835 carotenoids, using various solvents with spectrophotometer of different resolution. Plant
836 Physiology 144, 307-313.

837 White S, Anandraj A, Bux F. 2011. PAM fluorometry as a tool to assess microalgal nutrient stress
838 and monitor cellular neutral lipids. Bioresource Technology 102, 1675-1682.

839 Xu H, Miao X, Wu Q. 2006. High-quality biodiesel production from a microalga *Chlorella*
840 *prototecoides* by heterotrophic growth in fermenters. Journal of Biotechnology 126, 499-507.

841 Yokono M, Takabayashi A, Akimoto S, Tanaka A. 2015. A megacomplex composed of both
842 photosystem reaction centres in higher plants. Nature Communications 6, 6675.

843

844 ## Figure captions

845 **Fig. 1. Representative curves of slow Chl*a* fluorescence kinetics in response to changing light**
846 **intensities in *N. oleoabundans* at the 6th day of cultivation.** A) cells grown with 0 gL^{-1} of
847 glucose. B) cells grown with 2.5 gL^{-1} of glucose. The measurements were started after 10 min of
848 incubation in darkness by turning on the actinic light, the fluorescence parameters F_M' and F_t were
849 monitored triggering the samples with different light intensities. F_{Mtrue} is maximum fluorescence
850 measured at the end of the exposure to 90 $\mu mol_{photons}\ m^{-2}s^{-1}$; F_tLL and F_tHL are steady-state
851 fluorescence values measured at the end of the exposure to 90 $\mu mol_{photons}\ m^{-2}s^{-1}$ and 1000
852 $\mu mol_{photons}\ m^{-2}s^{-1}$, respectively.

853 **Fig. 2. Representative curves of Chl*a* fluorescence kinetics during exposure to far red light.**
854 Excitation of autotrophic (filled circles) and mixotrophic (empty circles) *N. oleoabundans* cells
855 with far red light for 10 min (purple diagram) and subsequent dark relaxation (dark diagram). $n \geq 3$
856 ± standard error. $p < 0.05$ at times 1, 5-9. $p < 0.01$ at times 10, 11, 12, 15, 20, according with
857 Student's *t* test.

858 **Fig. 3. Relaxation of the flash-induced fluorescence in *N. oleoabundans* cells grown with 0**
859 **(filled circles) and 2.5 (empty circles) gL^{-1} of glucose**. In the insert, relaxation kinetics as
860 occurring in presence of 5 μM DCMU. Curves are average of at least 3 different biological
861 replicates and are normalised to the same amplitude. Arrows: saturating-light pulse.

Fig. 4. Coomassie-stained SDS-PAGE of thylakoids extracted from autotrophic and mixotrophic *N. oleoabundans*. On each lane, 2 µg of Chl (A) or 20 µg of proteins (B) were loaded. For comparison, three different amounts of thylakoids from autotrophic sample were loaded. Molecular weight marker is reported on the left side in each gel.

Fig. 5. ~~Western blot detection~~ Detection of thylakoid protein amount ~~of~~ in autotrophic and mixotrophic *N. oleoabundans* cells. A) Immunoblot detection of ATPβ (3 µg of Chl loaded in each lane), PsaB (0.5 µg of Chl loaded in each lane), D1-DE loop (0.5 µg of Chl loaded in each lane) and LHCII (0.25 µg of Chl loaded in each lane) in thylakoid membranes of *N. oleoabundans* grown with 0 (*A*), and 2.5 (*M*) gL^{-1} of glucose. For comparison, three different amounts of thylakoids from control sample were loaded. Molecular weight marker is reported on the left. B) 77K Fluorescence emission spectra recorded from autotrophic (black line) and mixotrophic (grey line) *N. oleoabundans* cells. For easier comparison, spectra were normalized to their maximum peak, corresponding to PSII emission region. Spectra are averages of at least 3 replicates for each biological sample.

Fig. 6. Representative BN-PAGE profiles of thylakoids from *N. oleoabundans*. *DA*: dark autotrophic cells; *LA*: light autotrophic cells; *DM*: dark mixotrophic cells; *LM*: light mixotrophic cells. For each lane, 8µg Chl were loaded. The position of major complexes is indicated by labels.

Fig. 7. 2D-BN/SDS-PAGE of protein complexes in thylakoid membranes from *N. oleoabundans*. A) comparison between autotrophic cells incubated in darkness (*DA*) or maintained in growth light (*LA*) before thylakoid extraction. B) comparison between mixotrophic cells incubated in darkness (*DM*) or in growth light (*LM*) before thylakoid extraction. The BN-PAGE strips were loaded horizontally on the SDS-PAGE. The highlighted silver-stained spots correspond to Psa A/B subunits of PSI, CP47, CP43, D1 and D2 subunits of PSII, and LHCII subunits. Two

885 different types of LHCII trimer are indicated by yellow arrows. Marker molecular weight of
886 proteins is reported on the left.

887 **Fig. 8. Relative amounts of PSII (A) and PSI (B) in thylakoids extracted from autotrophic**
888 **(*A*) and mixotrophic (*M*) *N. oleoabundans* cells incubated in darkness (*DA - DM*) or**
889 **maintained in growth light (*LA – LM*) before extraction.** Black: *DA;* line pattern: *LA*; diamond
890 pattern: *DM*; white: *LM*. Data are means of 4 replicates ± standard deviation and are obtained by
891 spot densitometry of 2D/BN-PAGE gels stained by SYPRO Ruby dye. Differences are not
892 significant (p>0.05) for groups with the same superscript using ANOVA comparison of means.

893 **Fig. 9. TEM images of autotrophic (A-B) and mixotrophic (C-D) *N. oleoabundans* cells after**
894 **6 days of cultivation.** Asterisks indicate starch granules, arrows highlight thighly-appressed
895 thylakoids in mixotrophic cells.

896 **Fig. 10. Detection of phosphorylated thylakoid proteins in autotrophic (*A*) and mixotrophic**
897 **(*M*) *N. oleoabundans* cells.** A) phosphorylation of thylakoid proteins of *N. oleoabundans* cells
898 incubated in darkness (*DA-DM*) or maintained in growth light (*LA-LM*) before extraction.
899 Phosphoproteins were detected by immunoblotting using an anti-phosphothreonine antibody.
900 LHCII, D2 and CP43 are indicated as major phosphoproteins. Molecular weights are expressed in
901 kDa. B) Coomassie-stained SDS-PAGE of thylakoids incubated in darkness (*DA-DM*) or
902 maintained in growth light (*LA-LM*) before extraction. Bands corresponding to LHCII subunits are
903 indicated. Dashed lines include phosphorylated subunits after immunoblotting.

Higher packing of thylakoid complexes ensures a preserved Photosystem II activity in mixotrophic *Neochloris oleoabundans*

Martina Giovanardi[1], Mariachiara Poggioli[1], Lorenzo Ferroni[1], Maija Lespinasse[2], Costanza Baldisserotto[1], Eva-Mari Aro[2], Simonetta Pancaldi[1*]

[1]University of Ferrara, Department of Life Science and Biotechnology, C.so Ercole I d'Este 32, 44121 Ferrara, Italy.

[2] University of Turku, Molecular Plant Biology, Department of Biochemistry, FI-20014, Turku, Finland.

*Corresponding Author. E-mail address: simonetta.pancaldi@unife.it (S. Pancaldi)

Abbreviations:

2D: second dimension; ATPase: ATP synthase; BN-PAGE: Blue-Native polyacrylamide gel electrophoresis; BSA: bovin serum albumin; Chl: chlorophyll; Cyt: cytochrome; DCMU: 3-(3,4-dichlorophenyl)-1,1-dimethylurea; F_0: basal fluorescence level excited by a very low measuring light after dark incubation; F_M: maximum fluorescence level obtained by a saturating light pulse after dark incubation; F_M': maximum fluorescence level during a light-adapted state; F_t: basal fluorescence level during a light-adapted state; F_V: variable fluorescence level obtained by the difference of F_M and F_0; F_V/F_M: maximum photochemical quantum yield of Photosystem II; LHC: Light-harvesting pigment-protein complexes; PAM: pulse amplitude modulation; PQ: plastoquinone; PQH_2: plastohydroquinone; PSI: Photosystem I; PSII: Photosystem II; Q_A: quinone A; Q_B: quinone B; SDS-PAGE: Sodium Dodecyl Sulphate polyacrylamide gel electrophoresis; TEM: transmission electron microscopy.

Abstract

A better understanding of the microalgal basic biology is still required to improve the feasibility of algal bio-products. The photosynthetic capability is one of the parameters that need further progress in research. A superior PSII activity was previously described in the green alga *Neochloris oleoabundan*s. In this study, *N. oleoabundans* was grown in a glucose-supplied culture medium, in order to provide new information on the organisation and interaction of thylakoid protein complexes under mixotrophy. Fluorescence measurements suggested a strong association of light harvesting complex II (LHCII) to PSII in mixotrophic samples, confirmed by the lack of LHCII phosphorylation under growth light and the presence of PSI-PSII-LHCII megacomplexes in Blue-Native gel profile. The chloroplast ultrastructure was accordingly characterised by a higher degree of thylakoid appression compared to autotrophic microalgae. This also affected the capability of mixotrophic microalgae to avoid photodamage when exposed to high-light conditions. On the whole, it emerged that the presence of glucose affected the photosynthetic performance of mixotrophic samples, apparently limiting the dynamicity of thylakoid protein complexes. As a consequence, PSII is preserved against degradation and the PSI:PSII is lowered upon mixotrophic growth. Apparent increase in PSII photochemical activity was attributed to a down-regulated chlororespiratory electron recycling.

Key words: *Neochloris oleoabundans*, mixotrophy, Photosystem II, thylakoid protein complexes, photosynthetic performance, Blue-Native PAGE, fluorescence measurements.

Introduction

Photosynthesis supports almost all life on Earth and involves several light-dependent reactions, which start with the absorption of light energy for the synthesis of NADPH and ATP (Geider and MacIntyre, 2002), used during the Calvin-Benson cycle for CO_2 fixation (Falkowski and Raven, 2007). Important features of the light reactions of photosynthesis are: collection of photons by light-harvesting antennae, migration of excitation energy to the reaction centers, electron transfer from H_2O to $NADP^+$, and ATP generation (Geider and MacIntyre, 2002). Light-harvesting pigment-protein complexes (LHC) deliver the absorbed light energy to the reaction centers of Photosystem II (PSII) and Photosystem I (PSI) (Minagawa and Takahashi, 2004). The major LHC of PSII, LHCII, is also essential for maintaining thylakoid membranes stacked and promoting distribution of absorbed light energy between photosystems (Tikkanen *et al.*, 2008; Nevo *et al.*, 2012). PSII transfers electrons from water to plastoquinone (PQ) using light energy as a driving force (Chow *et al.*, 1990; Minagawa and Takahashi, 2004; Daniellson *et al.*, 2006). The electrons from plastohydroquinone reach PSI via Cytochrome (Cyt) b_6f complex and plastocyanin. PSI is involved in a light-dependent electron transport to ferredoxin and to $NADP^+$ (Chow *et al.*, 1990). ATP synthase (ATPase) is the highly-conserved complex that catalyses ATP synthesis using the trans-membrane proton gradient created during the electron flow (Nelson and Ben-Shem, 2004).

Important for understanding the molecular basis of the photosynthetic process is a detailed knowledge of the structure of its components (Barber, 2002; Dekker and Boekema, 2005; Nelson and Yocum, 2006). All protein complexes are composed of several protein subunits coordinating a large number of cofactors, which show a tendency to form higher-order associations, the so-called supercomplexes (Dekker and Boekema, 2005; Caffarri, 2009; Minagawa, 2009; Croce and van Amerongen, 2011; Suorsa *et al.*, 2015). The dynamic organisation of the pigment-protein complexes in the thylakoid membrane plays important roles in maintaining an optimal photosynthetic efficiency under several conditions, including different light regimes, temperature

and nutrient supply (Chow et al., 1990; Anderson *et al.*, 1995). In green microalgae, whose cell volume is mainly occupied by the chloroplast, the photosynthetic efficiency is an indicator of their wellness conditions (White *et al.*, 2011). This is an important factor to be taken into account, considering the importance of green microalgae for biotechnological purposes (Chisti, 2007; Borowitzka, 2013). In this scenario, mixotrophic microalgae have been largely investigated for their capability to highly increase their biomass content, benefitting from the exogenous organic carbon source assimilation together with light harvesting and CO_2 fixation for growth (Lee, 2001; Xu *et al.*, 2006; Scott *et al.*, 2010; Stephens *et al.*, 2010). However, there are few works concerning the interaction between photosynthetic complexes in thylakoid membranes during the assimilation of organic carbon by microalgae; in general, a specific reduction in PSII photochemistry was observed (Valverde *et al.*, 2005; Oesterhelt *et al.*, 2007; Liu *et al.*, 2009). Very differently, mixotrophy promoted a very high PSII maximum quantum efficiency in the Chlorophyta *Neochloris oleoabundans* (Baldisserotto *et al.*, 2014; Giovanardi *et al.*, 2014). In this work, the effects of glucose supplied in the culture media of *N. oleoabundans* were assessed in order to provide new information on the photosynthetic metabolism and to understand the interaction of the different pigment-protein complexes during the organic carbon source assimilation. Immunodetection of different subunits of thylakoid multi-protein complexes was employed to identify differences in their relative abundance between autotrophic and mixotrophic samples, whereas Blue-Native polyacrylamide gel electrophoresis (BN-PAGE) was employed to obtain information on native interactions of photosynthetic protein complexes in thylakoids (Hippler *et al.*, 2001; Rokka *et al.*, 2005). In parallel, chlorophyll (Chl) fluorescence measurements were performed *in vivo* on freshly-collected samples to identify differences in photosynthetic electron transport in autotrophic and mixotrophic cells.

Materials and methods

Algal strain and culture condition

The Chlorophyta *Neochloris oleoabundans* UTEX 1185 (syn. *Ettlia oleoabundans*, *Sphaeropleales, Neochloridaceae*) was obtained from the Culture collection of the University of Texas (UTEX, USA; www.utex.org). Cells were grown and maintained in axenic liquid BM medium (Baldisserotto *et al.*, 2012) in a growth chamber (24 ± 1 °C temperature, 80 $\mu mol_{photons}$ m^{-2} s^{-1} PAR and 16:8 h of light-darkness photoperiod), without shaking and external CO_2 supply. For experiments, cells were inoculated at least in triplicate at a density of 0.6 ± 0.1 x 10^6 cells mL^{-1} in BM medium containing 0 (autotrophic cells) or 2.5 gL^{-1} of glucose and grown in 500 mL Erlenmeyer flasks (300 mL of total volume) in the growth chamber described above, with continuous shaking at 80 rpm. The glucose concentration of 2.5 gL^{-1} was selected in previous experiments in which the microalga was grown in the presence of increasing concentrations of glucose from 0 to 30 gL^{-1}, comparing among them growth rates, cell morphology, glucose consumption and lipid accumulation inside cells, as reported in Giovanardi et al. (2014). Growth was estimated measuring the optical density at 750 nm with a Pharmacia Biotech Ultrospec®2000 UV–vis spectrophotometer (1 nm bandwidth; Amersham Biosciences, Piscataway, NJ, USA) and counting cells with a Thoma's haemocytometer under the light microscope (Zeiss, Axiophot, Jena, DE), on 1 mL of culture samples at days 0, 2, 3, 4, 7, 9, 11.

Fluorescence measurements

Modulated chlorophyll fluorescence: slow kinetics.

In vivo Chl*a* fluorescence was determined from liquid cultures at the late exponential phase of growth, i.e. at the 6th day from the inoculum, harvested by centrifugation to contain 15 μg mL^{-1} Chl. Chlorophyll quantification was performed according to Wellburn (1994). Cell suspensions

were pre-incubated in darkness for 10 min and samples were subsequently exposed to actinic blue light. The following program was triggered: 90 $\mu mol_{photons}\ m^{-2}s^{-1}$, 11 min; dark, 11 min; 1000 $\mu mol_{photons}\ m^{-2}s^{-1}$, 15 min; dark, 5 min. Light saturating pulses (0.6 s) were given every 40 s. Initial fluorescence F_0 and maximum fluorescence F_M after dark incubation were used to calculate the maximum quantum yield of PSII (F_V/F_M ratio), according to Lichtenthaler *et al.* (2005). Time course of Chl fluorescence parameters F_M', i.e. the maximum fluorescence in the light-adapted state measured applying the pulse, and F_t, i.e. the steady-state fluorescence yield, were determined with a DUAL-PAM-100 (Walz, Germany).

The effects of far red light on PSII fluorescence were determined using an ODC OS1-FL portable fluorimeter (ADC Bioscientific Ltd, Hoddesdon, Hertfordshire, UK) on cell pellets prepared as described in Ferroni *et al.* (2011). Measurements were performed on 10 min dark-adapted samples. Cells were excited with far red light (740 nm) for 10 min. After that, recovery was followed for 10 min in darkness. During the experiment, light saturating pulses were given every minute during the far red light exposure and at times 1, 2, 5 and 10 min during dark relaxation. The F_M'/F_M ratio was calculated and used to determine variations of PSII fluorescence.

Fast chlorophyll fluorescence.

Q_A^- reoxidation kinetics was determined by flash-induced Chl fluorescence relaxation kinetics. The single turnover flash-induced increase in Chl*a* fluorescence yield and its subsequent relaxation in darkness (FF-relaxation) were measured with a double-modulation fluorimeter (Photon System Instruments, Brno, Czech Republic). For analyses, 1 mL of samples containing 8 $\mu g\ mL^{-1}$ Chl was incubated in darkness for 10 min and then Q_A^- reoxidation kinetics was recorded, after a single-saturating flash (10 μs) provided by red LED, in the 150 μs - 100 s time range. Analyses were carried out either in the presence or absence of 5 μM 3-(3,4-dichlorophenyl)-1,1-dimethylurea (DCMU) (Allahverdiyeva *et al.*, 2007). For easier comparison, the fluorescence relaxation curves

were averaged and normalised to the same amplitude. The relative Q_A^- concentration was estimated according to the model of Joliot (Joliot and Joliot, 1964). Multicomponent deconvolution of the relaxation curves was performed according to Vass and colleagues (1999).

77K fluorescence emission spectra

Fluorescence emission spectra measured *in vivo* from samples containing 8 μg mL^{-1} Chl were recorded at 77 K using a diode array spectrophotometer (S2000; Ocean Optics, Dunedin, FL, USA) equipped with a reflectance probe as described in Keranen et al. (1999). The spectra were obtained by excitation with light at 440 nm, defined using LS500S and LS700S filters (Corion, Holliston, MA, USA) placed in front of a slide projector, whereas the emission between 600 and 800 nm was recorded. For each biological replicate, at least 3 measurements were recorded.

Thylakoid isolation

Thylakoid membranes were isolated according to Järvi *et al.* (2011), with modifications. For extraction, 300 mL of cultures in late-exponential phase of growth were harvested by centrifugation at 600 *g* for 10 min. Pellets were transferred to an ice-cold mortar containing sand quartz. The extraction was performed grinding cells with liquid N_2, then the lysate was resuspended in a grinding buffer (330 mM sorbitol, 50 mM Tricine-NaOH pH 7.5, 2 mM Na_2EDTA, 1 mM $MgCl_2$, 5 mM ascorbate, 0.05% bovine serum albumin, 10 mM NaF) and transferred to 15 mL tubes. Samples were centrifuged at 300 *g* for 5 min at 4°C and then at 700 *g* for 5 min at 4°C, to remove sand quartz and cell debries. Pellets were discarded and the thylakoids present in the supernatant were collected by centrifugation at 7000 *g* for 10 min at 4°C. The supernatant was discarded and thylakoids were resuspended in 1 mL of shock buffer (5 mM sorbitol, 50 mM Tricine-NaOH pH 7.5, 2 mM Na_2EDTA, 5 mM $MgCl_2$, 10 mM NaF) and centrifuged at 7000 *g* for 10 min at 4°C. After that, the supernatant was removed and around 100 μL of storage buffer (100 mM sorbitol, 50 mM Tricine1-NaOH pH 7.5, 2 mM Na_2EDTA, 5 mM

$MgCl_2$, 10 mM NaF) were added to the pellet. Thylakoid samples were rapidly frozen in liquid nitrogen and stored at -80°C until further analyses. Manipulation was always performed on ice and in very dim safe light. Quantification of Chl and proteins in thylakoid samples was performed according to Porra *et al.* (1989) and Lowry (1951), respectively. Before extraction, autotrophic and mixotrophic cultures were incubated in darkness for 1 h or maintained in growth light (80 $\mu mol_{photons}\ m^{-2}\ s^{-1}$) inside the growth chamber.

SDS-PAGE and immunoblotting

Thylakoid proteins were separated by SDS-PAGE according to Laemmli (1970) on a 15% acrylamide resolving gel containing 6 M urea. After electrophoresis, proteins were visualised by Coomassie staining overnight, followed by destaining for 5 h, or blotted onto a polyvinylidene difluoride membrane (Millipore, Watford, Hertforshire, U.K.). Western blotting was performed with standard techniques using protein-specific antibodies. For the detection of D1-DE loop of D1 protein, PsaB subunit of PSI and ATP-β subunit of ATPase, the antibodies were obtained from Agrisera (www.agrisera.com), whereas for the detection of the entire LHCII complex the antibody was kindly provided by L. Zhang. Before immunodetection, membranes were blocked with 5% milk (www.bio-rad.com) in TBS buffer (Tris-HCl 10 mM pH 7.4 and NaCl 1.5 M). For the detection of phosphoproteins, a polyclonal anti-phosphothreonin antibody was used (Zymed, www-invitrogen.com) and membranes were blocked with 1% BSA in TBS buffer. Horseradish peroxidase-linked secondary antibody in conjunction with chemiluminescent agent (GE heathcare, www.gehealthcare.com) was used for protein detection. Protein band intensity was quantified with Image J freeware (National Institutes of Health, Bethesda, MD, USA).

BN-PAGE and second dimension (2D) electrophoresis

BN-PAGE was performed according to Järvi *et al.* (2011) with minor modifications. Thylakoids (8 µg Chl) were solubilised on ice for 15 min with dodecyl β-D-maltoside (Sigma) at a final

concentration of 1.5% (w/v), followed by centrifugation at 18000 *g* at 4°C for 15 min. Electrophoresis was performed with a Hoefer Mighty Small system (Amersham Biosciences) at 0°C for 3.5 h by gradually increasing the voltage from 75 to 200 V. For comparison, thylakoids from *Arabidopsis thaliana* were included in the analyses. Quantification of band volume was performed with Image J software. After BN-PAGE, the lanes were cut out and incubated in 10% SDS Laemmli buffer (Laemmli, 1970) containing 5% (v/v) β-mercaptoethanol for 1.5 h, followed by separation of the protein subunits of the complexes in the 2D with SDS-PAGE (12% polyacrylamide and 6 M urea). After electrophoresis, proteins were visualised by silver or SYPRO Ruby staining, according to the manufacturer's instructions (www.invitrogen.com). The intensity of every spot in SYPRO- stained gels was determined with ProFinder 2D, version 2005 (Nonlinear Dynamics).

Transmission electron microscopy (TEM)

For transmission electron microscopy, autotrophic and mixotrophic cells were harvested after 6 days of growth and prepared as previously reported (Baldisserotto *et al.*, 2007; Baldisserotto *et al.*, 2016).

Statistical analyses

For each analysis, at least three biological replicates for each sample were set up. Elaboration of data was carried out with Origin Pro 2015 software (OriginLab, Northampton, MA, USA). To compare autotrophic and mixotrophic samples, Student's *t* test was used. For statistical comparison of data obtained by SYPRO Ruby staining, one-way analysis of variance (ANOVA) was used.

Results

Growth kinetics of autotrophic and mixotrophic *N. oleoabundans* cells

Cell density of autotrophic and mixotrophic cultures during the experiment is reported in Supplementary Figure S1. As expected, cell densities were comparable with those observed in previous works (Giovanardi *et al.*, 2014; Baldisserotto *et al.,* 2016). Autotrophic and mixotrophic cells grew with no differences during the first 2 days, after that a significant cell density enhancement was observed in cells grown in presence of glucose starting from the 3rd day (p<0.01 at day 3, p<0.001 at the following times). At the 7th day, both autotrophic and mixotrophic samples entered the stationary phase. Between day 2 and 7, an increase in PSII maximum quantum yield F_V/F_M occurred in mixotrophic cells. Analyses were subsequently performed on cells sampled at the 6th day of growth, period in which mixotrophic cells, still having high F_V/F_M values, also showed the maximum cell density value before entering the stationary phase of growth.

In vivo fluorimetric analyses of autotrophic and mixotrophic *N. oleoabundans*

*Slow kinetics of Chl*a *fluorescence*

In order to clarify the effects of glucose on the dynamics of photosynthetic electron transfer in *N. oleoabundans*, Pulse Amplitude Modulated (PAM) fluorescence trace was monitored in freshly-collected samples of autotrophic and mixotrophic cultures, measuring the time-course of Chl fluorescence parameters F_M' and F_t. Samples were pre-incubated in darkness for 10 min for determination of the initial F_0 and F_M values before triggering the measuring routine. A 90 $\mu mol_{photons}\ m^{-2}s^{-1}$ irradiance was meant to reproduce a growth light condition, while a 1000 $\mu mol_{photons}\ m^{-2}s^{-1}$ represented a condition of high light stress. In Fig. 1 representative Chl*a* fluorescence kinetics are shown for autotrophic (Fig. 1A) and mixotrophic (Fig. 1B) cells. On the whole: i) no differences in the minimal level of fluorescence F_0 were observed before turning on the actinic light; ii) during the 90 $\mu mol_{photons}\ m^{-2}s^{-1}$ - darkness sequence of the triggered program,

F_M' increased over the initial F_M in autotrophic cells (Fig. 1A). On the other hand, the F_M' increase effect in the light was not always observed in mixotrophic samples and, when it occurred, the fluorescence increase was not as marked as in cells grown in the absence of glucose (Fig. 1B). In the light of these results, maximum quantum yield of PSII was re-calculated for both samples considering the real maximum F_M value, i.e. F_M' at the end of 90 $\mu mol_{photons}\ m^{-2}s^{-1}$ irradiance, hereafter named F_{Mtrue}. The obtained F_V/F_{Mtrue} ratio revealed no differences between autotrophic and mixotrophic cells in the maximum photochemistry quantum yield (Table 1). Same result was obtained calculating the F_tLL/F_{Mtrue} ratio, where F_tLL was the basal fluorescence at the end of the 90 $\mu mol_{photons}\ m^{-2}s^{-1}$ exposure period (Table 1); iii) when cells were exposed to 1000 $\mu mol_{photons}\ m^{-2}s^{-1}$, an initial rise in the basal fluorescence F_t was observed in autotrophic cells, followed by a strong decrease. These two phases were less evident in mixotrophic samples because of a less marked fluorescence rise as compared to autotrophic cells at the beginning of the high-light exposure period. Interestingly, the calculated F_tHL/F_{Mtrue} ratio, where F_tHL was the basal fluorescence at the end of the 1000 $\mu mol_{photons}\ m^{-2}s^{-1}$ exposure period, was significantly lower in autotrophic (-41%, $p<0.01$) than in mixotrophic cells (Table 1), suggesting a more reduced state of plastoquinone in mixotrophic cells after a prolonged exposure to high-light conditions; iv) when cells were finally exposed to darkness, maximum fluorescence F_M' gradually increased with no differences between samples.

	Autotrophic *N. oleoabundans*	Mixotrophic *N. oleoabundans*
F_V/F_{Mtrue}	0.708 ± 0.018	0.704 ± 0.044
F_tLL/F_{Mtrue}	0.409 ± 0.076	0.374 ± 0.042
F_tHL/F_{Mtrue}	0.303 ± 0.046	0.510 ± 0.125**

Table 1. PSII fluorescence ratios in autotrophic and mixotrophic *N. oleoabundans*. Values were obtained from Chl*a* fluorescence kinetics traces reported in Fig. 1. Values are means of n≥3 ± standard deviation. **: $p < 0.01$ according with Student's *t* test.

Effect of far red exposure on PSII photochemistry

In order to investigate the reason for the increase in F_M' beyond F_M during the exposure of autotrophic cells to growth light conditions, dark-adapted samples were exposed to far red light (740 nm), which selectively excites PSI and promotes the association of LHCII to PSII. Chl*a* fluorescence, recorded as F_M' and normalised on the initial fluorescence F_M, gradually and significantly increased in autotrophic samples to a maximum value of 1.78 after 9 min of far red exposure ($p<0.05$ at times 1, 5-9 min; $p<0.01$ from the 10th min) (Fig. 2). Conversely, in mixotrophic samples Chl*a* fluorescence increased during the first 3 min, but subsequently stabilized at values of about 1.3 during far red exposure, indicating that LHCII relocation to PSII

in mixotrophic cells was less inducible by far red treatment. During the subsequent dark relaxation, Chl*a* fluorescence rapidly decreased in both samples, even though the autotrophic cells maintained values higher (around 1.1) than initial fluorescence value, whereas mixotrophic samples showed values around 0.9 (p<0.01).

Effects of mixotrophy on reoxidation kinetics of Q_A

The effects of mixotrophy on the activity of both quinone components of the quinone-iron acceptor complex, Q_A and Q_B, can be studied by measuring flash-induced changes in the yield of Chl fluorescence (Vass *et al.*, 2002). The reduction of Q_A upon flash excitation results in a prompt increase in Chl fluorescence yield, which is followed by a dark decay in the range of 100 μs – 100 s, a time range allowing the reoxidation of Q_A through various pathways (Vass *et al.*, 2002). The fluorescence relaxation is dominated by a fast component (few-hundred μs), arising from Q_A^- to Q_B electron transfer in the RCII that had an oxidised or semi-reduced PQ molecule in the Q_B pocket at the time of flashing. The middle phase (few ms) arises from Q_A^- reoxidation in centers in which Q_B site in darkness is empty and PQ has to be bound from the pool. Finally, the slow phase of flash-induced fluorescence relaxation curve (few s) shows the recombination of the S2 state of the water oxidising complex with Q_B^- via the $Q_A^-Q_B \leftrightarrow Q_AQ_B^-$ equilibrium (Vass *et al.*, 1999; Vass *et al.*, 2002; Allahverdiyeva *et al.*, 2005). Analyses of the kinetics of the flash-induced fluorescence relaxation showed no differences between autotrophic and mixotrophic samples, suggesting that the presence of glucose in the cultivation medium did not affect the forward electron transfer through the PQ pool (Fig. 3; Table 2). The kinetics was dominated by the fast phase of decay (around 560 μs; 85%), followed by a middle phase of around 10 ms time of decay with 7.7% amplitude and a slow phase of around 2 s with 7% amplitude. Despite mixotrophic samples showed a tendency to accelerated time of decay during the middle phase (around 30% less), the results were not statistically significant compared to autotrophic samples (p=0.42). In the presence of DCMU, which blocks the reoxidation of Q_A^- by forward electron transfer, the fluorescence

relaxation indicates the status of the PSII donor side as revealed by recombination of Q_A^- with donor side components. In a functional PSII complex, the recombination partner of Q_A^- is the S2 state of the water oxidising complex (Allahverdiyeva *et al.*, 2005). As is shown in Fig. 3 (insert), Q_A^- reoxidation kinetics in the presence of DCMU appeared slowed-down in mixotrophic samples. This might reflect a defect in the assembly of the oxygen evolving complex (Allahverdiyeva *et al.*, 2013).

Sample	Total Amp (%)	Fast phase T/Amp (ms/%)	Middle phase T/Amp (ms/%)	Slow phase T/Amp (s/%)
A	100	0.568 ± 0.081 / 85.825 ± 2.597	13.500 ± 4.759 / 7.694 ± 1.300	2.066 ± 0.665 / 6.480 ± 1.369
M	100	0.553 ± 0.116 / 84.835 ± 4.471	9.414 ± 1.960 / 7.891 ± 2.187	1.806 ± 0.577 / 7.275 ± 2.335

Table 2. Characteristics of flash-induced Chl fluorescence relaxation in autotrophic (A) and mixotrophic (M) *N. oleoabundans* cells. Values are time of decay (T) and relative amplitudes (Amp) in percent of total variable fluorescence obtained after the fired flash. Values are means of $n \geq 3$ ± standard deviation.

Chl-protein complexes in thylakoid membranes of autotrophic and mixotrophic *N. oleoabundans* exposed to different light

Chl and protein quantification

Quantification of Chl and protein amounts in thylakoids of autotrophic and mixotrophic *N. oleoabundans* are reported in Table 3. Total Chl quantified in thylakoids was compared with the protein amount, to obtain Chl/protein ratios. Interestingly, in the mixotrophic cultures, Chl/protein was halved as compared to autotrophic samples, because of a halved concentration of pigments upon an unchanged amount of proteins. This result was clearly visible also observing Coomassie-stained SDS-PAGE (Fig. 4). About the Chl*a*/Chl*b* molar ratio, instead, higher values were calculated in mixotrophic samples than in the autotrophic, suggesting a different distribution in the proportion of Chl*a* and Chl*b* between samples (Table 3). Some of the key proteins which belong to major thylakoid complexes were detected and quantified by immunoblot analyses (Fig. 5A). Interestingly, lower amounts of PsaA (Supplementary Figure S2) and PsaB were detected in mixotrophic samples (-42.4% as compared to autotrophic cells). A slight decrease in the amount of ATP-β and LHCII protein was also observed with the addition of glucose upon growth, but it was not significant. Conversely, D1 protein was detected in higher amounts in 2.5 gL^{-1} of glucose-grown cells (+47% as compared to autotrophic samples).

To support the belief that autotrophic and mixotrophic cells had a different PSI:PSII stoichiometry, 77K spectra were recorded *in vivo* from aliquots of samples containing 8 $\mu g\ mL^{-1}$ Chl, frozen and maintained in liquid N_2 before analyses (Fig. 5B). As clearly visible in mixotrophic samples, the peak at around 684 nm was attributed to PSII, while the peak at 714 nm was attributed to PSI-LHCI (Ferroni et al., 2011). Moreover, a broad shoulder between 692 and 703 nm was observed. Emission around 700 nm can be attributed to LHCII aggregates (Horton et al., 1991). When mixotrophic were compared to autotrophic samples, spectra, normalized at the PSII emission

region, appeared very different (Fig. 5B). In fact, peaks were slightly shifted in control, at 683 nm for PSII and 713 nm for PSI-LHCI. Moreover, the shoulder at 692-703 nm was not observed between PSII and PSI emission regions. It is possible that this emission was not evident because of the higher emission from PSI-LHCI in autotrophic samples, confirming, then, the decrease in the PSI amount over PSII in mixotrophic *vs* autotrophic cells observed by immunoblot reactions.

Sample	Chlorophylls (µg µL^{-1})	Proteins (µg µL^{-1})	Chl/proteins	Chl*a*/Chl*b*
A	3.38 ± 0.19	24.30 ± 1.53	0.139 ± 0.014	3.47 ± 0.10
M	1.65 ± 0.23 ***	25.77 ± 1.79	0.064 ± 0.011 **	4.09 ± 0.03***

Table 3. Chl amounts, protein amounts and corresponding ratios in thylakoids extracted from *N. oleoabundans* grown with 0 (*A*) and 2.5 gL^{-1} (*M*) of glucose. n≥3 ± standard deviation. **: $p < 0.01$; ***: $p < 0.001$, according with Student's *t* test.

Organisation of thylakoid complexes

In order to obtain the separation of the thylakoid membrane complexes from autotrophic and mixotrophic *N. oleoabundans*, a BN-PAGE system was optimised. In a first analysis, the pattern of protein complexes in autotrophic *N. oleoabundans* was compared to that of *A. thaliana*.

(Supplementary Figure S3), whose BN-PAGE profile was structured as previously described (Aro *et al.*, 2005; Caffarri, 2009; Croce and van Amerongen, 2011). In the BN-PAGE of autotrophic *N. oleoabundans*, only some protein complexes corresponded to those separated in *A. thaliana*. Autotrophic *N. oleoabundans* lacked the LHCII assembly complex. Moreover, LHCII monomers were extremely abundant as compared to LHCII trimers. The following bands with higher molecular mass were identified: band I, apparently corresponding to PSII monomer; region II, which comprised all the smearing profile between band I and the following more intense band; band III and band IV, which had a mass similar to C_2S supercomplexes of *A. thaliana*.

In a subsequent step, membrane protein complexes from autotrophic and mixotrophic *N. oleoabundans* were solubilized with dodecyl β-D-maltoside and separated by BN-PAGE with the same procedure (Fig. 6). Before thylakoid extraction, autotrophic and mixotrophic cells were exposed in parallel to darkness (dark autotrophic-*DA* and mixotrophic-*DM* samples) or maintained in growth light for 1 h (light autotrophic-*LA* and mixotrophic-*LM* samples), in order to detect differences in the protein-complexes organisation of photosynthetic membranes between samples and after a dark-light transition. BN-PAGE of the thylakoid protein complexes demonstrated a less abundant band of LHCII trimers in mixotrophic samples compared to the autotrophic ones (Fig. 6), but the light-dark differences were not evident in BN-PAGE in the first dimension.

Subsequently, each stripe from the BN-PAGE was analysed by SDS-PAGE in the 2D, enabling the separation of different protein complexes into constituting subunits (Fig. 7). In 2D silver-stained gel of dark and light autotrophic cells (Fig. 7A), the first conspicuous band from right to left was identified as the LHCII monomers. The subsequent band corresponded to LHCII trimers. Two different series of LHCII protein spots were resolved, indicating the co-existence of two types of LHCII trimers with slightly different molecular mass. The more evident BN-PAGE band above LHCII trimers, the above-mentioned complex I, comprised a small amount of Psa A/B subunits co-migrating with all the subunits of PSII monomer. Just below band I, a very faint band, indicated

as I', was shown to contain PSII monomer subunits, except CP47. Interestingly, different spots corresponding to Psa A/B subunits characterized the series of complexes having increasing molecular mass in the so-called region II. Band III, fainter than band I, comprised Psa A/B subunits of PSI co-migrating with CP43, CP47, D1 and D2 subunits of dimeric PSII. In this complex, small amounts of LHCII were also observed. Based on the comparison with *A. thaliana* profile (Supplementary Figure S3), band III was interpreted as the result of the co-migration of two independent complexes, PSII-LHCII (C_2S) and PSI-LHCII (state-transition-like complex). Finally, in band IV Psa A/B subunits of PSI were observed associated to noticeable amounts of LHCI and LHCII complexes, but only negligible amount of PSII. Interestingly, despite silver-stained gels are not precisely quantitative, two aspects were noteworthy in autotrophic samples: 1) the amount of LHC associated with PSI in band IV decreased during the dark-light transition of the microalga, suggesting a stronger affinity of the subunits which compose this complex in darkness; 2) PSI subunits of thylakoids extracted from samples maintained in growth light were more evenly distributed from lower to higher molecular mass complexes as compared to thylakoids extracted from cells incubated in the dark. About the 2D BN/SDS-PAGE silver-stained image of mixotrophic samples (Fig. 7B), no major differences were observed in the general thylakoid protein pattern by comparison with autotrophic samples, except for the presence of a region above band IV, indicated as "megacomplexes", which was resolved in the 2D gel in subunits belonging to PSII and PSI. In dark-acclimated mixotrophic samples, only Psa A/B subunits were clearly detectable in the band, whereas in light-acclimated mixotrophic samples CP47, CP43, D2, D1 and LHC proteins were also resolved. As compared to the autotrophic samples, in the mixotrophic cells: 1) PSI was mainly concentrated in band IV independent of the dark/light incubation; 2) band IV was shown to also contain PSII, i.e. presumably a C_2S LHCII-PSII supercomplex with higher molecular mass than the C_2S PSII complex in band III; 3) PSI and PSII tended to associate into stable large megacomplexes with LHCII, especially in light conditions.

Quantification of spot density of thylakoid proteins was performed staining the 2D BN/SDS-PAGE gels with SYPRO® Ruby dye. Psa A/B and CP43 were used to quantify the relative amounts of PSI and PSII, respectively. LHC proteins generated too intense signal to give reliable results in a gel-stained protein quantification. PSI and PSII distribution in thylakoid complexes was compared between light and dark autotrophic and mixotrophic samples (Fig. 8). When PSII distribution was examined among the different thylakoid complexes (Fig. 8A), the majority was found as a monomer (band I). In particular, autotrophic samples showed a higher proportion (> 80% of total PSII) than mixotrophic cells (around 72% in both samples). On the contrary, PSII of band III (putative C_2S) was more abundant in mixotrophic cells, irrespective of dark-light acclimation (+ 60%, as compared to the corresponding autotrophic samples). In band IV, *LA* showed a negligible percentage of PSII, despite no significant differences were observed with *DA*, as well as between autotrophic and mixotrophic samples incubated in darkness. As seen in silver-stained gels, PSII did not characterize the region II and indeed its presence was not determined. Thus, it can be concluded that, irrespective of the light exposure before extraction, mixotrophic samples showed more abundant PSII in the dimeric, LHCII associated, forms as compared to the autotrophic samples. This tendency of PSII to organise more stably with LHCII was in line with the occurrence of megacomplexes.

Regarding the relative protein amount of PSI, the transition from dark to light did not induce a different distribution in the bands III and IV in autotrophic samples (Fig. 8B). Instead, in region II, PSI proportion decreased by 45% upon light exposure. On the contrary, PSI became more represented in the lighter form, co-migrating with PSII monomer in band I. In mixotrophic samples, the dark-to-light transition did not change PSI distribution among complexes. Interestingly, in those samples a lower proportion of PSI was found in complex III compared to autotrophic samples (about 65% less). As observed previously for PSII distribution, the presence of megacomplexes occurred only in mixotrophic samples (Fig. 8B).

The distribution of PSII and PSI in mixotrophic samples conveyed a picture of low dynamism of thylakoid protein complexes, which was expected to have an impact on the thylakoid architecture. In fact, TEM images showed in both autotrophic and mixotrophic cells a similar thylakoid system, except for the very high degree of appression in the latter, even leading to a virtual absence of the thylakoid lumen (Fig. 9).

Detection of thylakoid phosphoproteins

The determination of *in vivo* thylakoid phosphoproteins was important to understand the role of band IV and megacomplexes detected in 2D/BN-SDS PAGE. In particular, the strength of LHCII-PSII and LHCII-PSI association is usually linked to LHCII phosphorylation levels (Mekala *et al.*, 2015). The detection was obtained with anti-phosphothreonine (Fig. 10A). Coomassie-stained SDS-PAGE of a replicate gel was performed to confirm the efficiency of the electrophoretic race (Fig. 10B). In all the samples, the major phosphoproteins were identified as CP43, D2 and two different proteins of LHCII (Fig. 10A), i.e. two less abundant subunits with high molecular mass (Fig. 10B). LHCII phosphorylation was observed at basal levels when thylakoids were extracted from dark-incubated autotrophic samples. As expected, a strong increase in the phosphorylation level of LHCII proteins was very evident in *LA*. Intrinsic antenna CP43 and protein subunit D2 of PSII core were not affected by the transition from dark to growth light and remained phosphorylated at basal levels. When *DM* samples were considered, only CP43 appeared slightly phosphorylated, whereas other phosphoproteins were barely detectable. Moreover, very surprisingly, the extent of light-induced phosphorylation was very limited. The phosphorylation levels were even lower than those observed in dark-acclimated autotrophic cells (Fig. 10A).

Discussion

In *N. oleoabundans*, only limited information concerning its photosynthetic metabolism is available. Recent works (Baldisserotto *et al.*, 2014; Giovanardi *et al.*, 2014; Sabia *et al.*, 2015, Baldisserotto *et al.*, 2016) have proved that the assimilation of organic carbon in this microalga interferes with the photosynthetic performance in a contrasting manner compared to other green microalgae, in which mixotrophy induces a down-regulation of photosynthesis (Oesterhelt *et al.*, 2007; Liu *et al.*, 2009). In order to explore the mechanisms involved during the mixotrophic growth, and understanding how the interaction between Chl-protein complexes are modified by the glucose assimilation and how light irradiance affects the photosynthetic apparatus, detailed analyses were performed on *N. oleoabundans* cultivated in the presence of 2.5 gL^{-1} of glucose, which promoted growth and F_V/F_M, consistent with previously published results (Supplementary Figure 1S; Giovanardi *et al.*, 2014).

Higher F_V/F_M in mixotrophic than in autotrophic cells is due to down-regulated chlororespiration

Measurements of Chl*a* fluorescence induction were performed on dark-adapted cells. This condition is meant to fully oxidise the PQ pool, leading to a complete opening of PSII. However, PQ reduction can partially occur in the dark in different organisms because of chlororespiratory pathways, which allow dissipating the excess of reducing power in the stroma by the ultimate reduction of O_2 (Bennoun, 1994; Feild *et al.*, 1998; Hoefnagel, 1998; Hill and Ralph, 2008; Cruz *et al.*, 2011). As a consequence of PQ reduction in darkness, the phosphorylation of LHCII and its migration to PSI is promoted (Krause and Weiss, 1984; Finazzi *et al.*, 1999; Houille-Vernes *et al.*, 2011), whereas when low actinic light is triggered, F_M' values gradually increase and exceed F_M (Cruz *et al.*, 2011; Houille-Vernes *et al.*, 2011). This is exactly observed in autotrophic *N. oleoabundans* cells (Fig. 1A). Very surprisingly, instead, mixotrophic cells did not appear much affected by chlororespiration in darkness, and, when samples were exposed to growth light

conditions, F_M' only slightly exceeded F_M values (Fig. 1B). It has been suggested that, if chlororespiration occurs, the maximum F_M' value measured under low actinic light (F_{Mtrue}) should be used instead of the dark-acclimated F_M (Serôdio et al, 2006). Then, if the F_V/F_{Mtrue} ratio was used instead of F_V/F_M, the same maximum photochemical activity was determined in autotrophic and mixotrophic cells (Table 1).

Further evidence for the fact that in autotrophic samples a dark incubation determines a partial association of LHCII with PSI was provided by illumination the cells with far red light (Fig. 2), which selectively excites PSI, promoting the maximum oxidation of the PQ pool and of the inter-system electron transport chain (Lokstein *et al.*, 1994; Schansker and Strasser, 2005; Hill and Ralph, 2008). In autotrophic cells, the gradual rise in F_M'/F_M during far red light treatment indicated a gradual increase in the LHCII proportion serving the PSII core. On the contrary, in mixotrophic cells the ratio soon reached a plateaux, suggesting that most LHCII was already linked to PSII in dark-acclimated samples.

In the light of above results, it emerges that the higher F_V/F_M ratio characterising mixotrophic *N. oleoabundans* actually occurred because the F_M levels of autotrophic samples were underestimated (Hill and Ralph, 2008; Giovanardi *et al.*, 2014). Therefore, the glucose-grown samples did not hold an improved maximum photosynthetic efficiency of PSII, but rather they might have experienced important effects on the reduction state of the photosynthetic electron transport chain (Baker, 2008; Roach *et al.*, 2013). On the other hand, the availability of oxidized PQ did not seem to be much influenced by the addition of glucose in the culture medium (Fig. 3), as previously shown also in *Chlamydomonas reinhardtii* (Roach *et al.*, 2013). However, it is noteworthy that in green microalgae, the fast reoxidation phase appears much more conspicuous compared to those measured in higher plants and cyanobacteria (Allahverdiyeva *et al.*, 2013; Volgusheva *et al.*, 2013; Deák *et al.*, 2014). This reflects a faster and more efficient forward electron transfer from Q_A^- to the Q_B present in the Q_B pocket of PSII as compared to other photosynthetic organisms, but, as a

side effect, it can also hide differences in the amplitudes and times of decay of the subsequent middle and slow phases of Chl fluorescence. The addition of DCMU, for instance, revealed a probable defect in the assembly of the oxygen evolving complex, despite incipient, in mixotrophic cells. A similar effect was also previously observed in mixotrophic *C. reinhardtii* (Roach *et al.*, 2013). This defect may be negligible in growth-light conditions, but could become relevant if cells were exposed to high light.

Mixotrophic cells are more sensitive to high-light exposure than autotrophic cells

Differences in properties of the electron transport pathways in mixotrophic and autotrophic growth conditions were not detectable under growth light conditions. This light regime, indeed, did not influence the F_tLL/F_{Mtrue} ratio (Table 1) and, thus, did not provoke an electron overloading of the thylakoid membrane. However, the capability to avoid photodamage under high light exposure was strongly affected in mixotrophic cells, as showed by the lower F_tHL/F_{Mtrue} ratio than in autotrophic samples. In the latter cells, according to Tikhonov (2015), when actinic high light was switched on, the gradual, sensible increase in F_t reflected the rapid reduction of the intermembrane PQ pool (Fig. 1). Subsequently, its decrease was linked to the activation of the Calvin-Benson cycle and concomitant acceleration of electron outflow from PSI, with the consequent PQH_2 pool reoxidation (Tikhonov, 2015). The mixotrophic samples reached in a very short time the maximum level of reduced PQ pool as compared to cells grown autotrophically. This led to the less evident peak of F_t observed in mixotrophic conditions. The subsequent decrease in the F_t values was likewise less evident. Accordingly, a slower electron flow in mixotrophy during high light exposure might be linked to a reduced activity of the Calvin-Benson cycle and a lower proportion of PSI in the thylakoid membrane (Tikhonov, 2015).

PSII complexes become less dynamic in mixotrophic cells

The redox state of the electron transport components influences not only the LHCII association to PSII and PSI, but also the relative abundance of both photosystems (Kováks *et al.*, 2000). In this work, mixotrophic samples were mainly characterised by a decrease in the amount of PSI and an increase in the amount of PSII (Fig. 5A, B). Furthermore, Chl*a*/Chl*b* ratio was significantly higher in cells grown with glucose. As Chl*b* is mostly located in LHCII complexes (Anderson *et al.*, 1995), and immunodetection did not reveal differences in the amount of LHCII between autotrophic and mixotrophic cells (Fig. 5A), this result further supported a relative increase in PSII reaction centres when cells were grown under mixotrophy. The analyses of supramolecular organisation of thylakoid complexes allowed detection of a major difference in the amount of trimeric LHCII, higher in cells grown autotrophically, in particular in *DA* samples, as compared to mixotrophic samples. Free LHCII trimers are considered the only LHCII complexes involved in state transition-like processes (Ünlü *et al.*, 2014). This confirms that autotrophic cells can rely on a greater capability to modulate LHCII association with a better efficiency. More detailed analyses of the supramolecular organisation of photosystems by 2D silver-stained SDS-PAGE and corresponding quantitative distribution of PSI and PSII among the different major complexes revealed the specificity of the pigment-protein complexes of each sample.

In all thylakoid samples, PSII was mostly monomeric. For many years, there has been a long-standing discussion about the assembly of PSII components into functional multimeric protein complexes in green algae and higher plants (Minagawa and Takahashi, 2004; Dekker and Boekema, 2005). Currently, it is widely accepted that functional PSII is normally organised as a dimer and concentrated in the stacked, appressed regions of thylakoids, whereas PSII monomer units are usually found in the unstacked thylakoid membranes, where the PSII repair cycle occurs (Kruse *et al.*, 2000; Minagawa and Takahashi, 2004; Dekker and Boekema, 2005; Daniellson *et al.*, 2006). However, in some cases, PSII monomers were shown to be fully active and also located

both in grana cores and margins (Dekker and Boekema, 2005; Daniellson *et al.*, 2006; Takahashi *et al.*, 2009). Moreover, Järvi *et al.* (2011) discovered that in the absence of an external charge in BN/PAGE, PSII complexes were mainly found in the monomeric form. The debate is still open, but what clearly emerged in *N. oleoabundans* was that PSII was more distributed in higher forms of association in mixotrophic than in autotrophic samples, preferring the maintenance of PSII as a dimer and even in megacomplexes together with PSI. In megacomplexes, there is a stable and advantageous association between PSI and PSII that promotes photoprotective energy spillover towards PSI (Grieco *et al.*, 2015; Yokono *et al.*, 2015; Ferroni et al., 2016). The strong interaction between PSII and PSI limits also the necessity of D1 protein subunit of PSII to be replaced after photodamage events. On the opposite, a fluent electron transfer through the thylakoid membranes, as well as the maintenance of an excitation balance between PSII and PSI, is fundamental for an efficient use of light for photochemistry (Mekala *et al.*, 2015).

On the whole, in autotrophic *N. oleoabundans*, then, the photosynthetic membrane is regulated as expected. In darkness, chlororespiratory electron recycling is active and PQ pool is partially reduced, as also demonstrated by the presence of phosphorylated LHCII and PSII subunits (Fig. 10). During the initial exposure to growth light conditions, the electron transfer components turn at the oxidised state and maximum PSII quantum efficiency is reached. The role of LHCII phosphorylation is mainly the balancing of energy excitation between PSII and PSI (Tikkanen and Aro, 2012), and at low irradiances, maximal phosphorylation is induced in chloroplast *in vivo* (Rintämaki *et al.*, 2000). Under a steady-state low-growth light conditions, maximum PSII core and LHCII phosphorylation is then achieved in autotrophic cultures and ensures an even excitation distribution between PSII and PSI (Tikkanen and Aro, 2012). This represents for the cells a highly fluid condition of thylakoid complexes, which allows extensive, though labile, interactions between photosystems and LHCII (Mekala *et al.*, 2015).

In dark-adapted mixotrophic *N. oleoabundans*, chlororespiration appears to be down-regulated and LHCII is mainly associated to PSII, sustained by the absence of phosphorylation of PSII core and LHCII (Fig. 10). Furthermore, the very weak phosphorylation even at growth light conditions, the poorness of free LHCII trimers, the very strong PSII-LHCII association of complexes and PSI-PSII-LHCII megacomplexes suggest a very low dynamicity of thylakoid protein complexes in mixotrophic cells. This is reflected also by a visibly higher appression degree of thylakoids in mixotrophic cells, presumably sustained by very low levels of protein phosphorylation (Fig. 9; Fristedt *et al.*, 2009). Some hypotheses might be advanced to explain this behaviour. The exogenous glucose - uptaken with such a high efficiency that results even in the accumulation of starch granules (Baldisserotto *et al.*, 2016) - might have contributed to an excess of available reducing power through respiration. This could have promoted the maintenance of plastid thioredoxins at the reduced state, leading to the inhibition of LHCII phosphorylation and thus to the promotion of PSII-LHCII association (Rintamäki *et al.*, 2000). Moreover, a higher respiration rate in mixotrophic cells can result in a high availability of ATP, with a consequent down-regulation of Calvin-Benson Cycle and of PSI. A lower PSI:PSII stoichiometry may depend also on incapability of proteolitic enzymes to degrade PSII subunits (Chow *et al.*, 1990). In fact, it was demonstrated that PSII is less accessible to degradation when associated in megacomplexes (Tikkanen and Aro, 2012). The low PSII core protein phosphorylation, as observed in mixotrophic microalgal thylakoids, limits the fluidity of the thylakoid membrane and cooperates in hindering the disassembly of PSII supercomplexes, affecting also the oligomerisation of PSII and the regulation of D1 protein degradation. This event impacts on the capability of mixotrophic samples to react to photodamage when cells are exposed to prolonged high-light conditions (Figure 1B; Tikkanen *et al.*, 2008; Tikkanen and Aro, 2012).

Conclusions

In conclusion, contrary to what previously hypothesised, the supply of glucose to *N. oleoabundans* cells does not induce an emphasised photosynthetic activity compared to autotrophic cultures, but rather provokes a decreased dynamicity of PSII assembly. Ultimately, the effect of such a low dynamicity is the preservation, or a delayed degradation, of PSII, in spite of the mixotrophic mode of growth.

Conflict of interest

The Authors declare no conflict of interest.

Author contribution

MG, LF, EMA and SP participated in the conception and design of the study; MG, MP, LF, ML, CB collected data and performed analyses; MG, LF and SP drafted the article; LF, EMA and SP assisted the results interpretation and critical reviewed the manuscript; all Authors read and approved the final manuscript.

Acknowledgments

This work was supported by the University of Ferrara and the University Institute for Higher Studies, IUSS - Ferrara 1391, with a fellowship provided to MG, and by the Academy of Finland with grants no. 271832 and 273870 to EMA.

References

Allahverdiyeva Y, Mamedov F, Mäenpää P, Vass I, Aro EM. 2005. Modulation of photosynthetic electron transport in the absence of terminal electron acceptors: Characterization of the *rbcL* deletion mutant of tobacco. Biochimica and Biophysica Acta 1709, 69-83.

Allahverdiyeva Y, Mamedov F, Suorsa M, Styring S, Vass I, Aro EM. 2007. Insights into the function of PsbR protein in *Arabidopsis thaliana*. Biochimica and Biophysica Acta 1767, 677-685.

Allahverdiyeva Y, Mustila H, Ermakova M, Bersanini L, Richaud P, Ajlani G, Battchikova N, Cournac L, Aro EM. 2013. Flavodiiron proteins Flv1 and Flv3 enable cyanobacterial growth and photosynthesis under fluctuating light. Proceedings of the National Academy of Sciences of the United States of America. 110, 4111-4116.

Anderson JM, Chow WS, Park YI. 1995. The grand design of photosynthesis: Acclimation of the photosynthetic apparatus to environmental cues. Photosynthesis Research 46, 129-139.

Aro EM, Suorsa M, Rokka A, Allahverdiyeva Y, Paakkarinen V, Saleem A, Battchikova N, Rintamäki E. 2005. Dynamics of photosystem II: a proteomic approach to thylakoid protein complexes. Journal of Experimental Botany 56, 347-356.

Baker NR. 2008. Chlorophyll fluorescence. A probe of photosynthesis in vivo. Annual Review of Plant Biology 59, 89-113.

Baldisserotto C, Ferroni L, Anfuso E, Pagnoni A, Fasulo MP, Pancaldi S. 2007. Responses of *Trapa natans* L. floating laminae to high concentrations of manganese. Protoplasma. 231, 65-82.

Baldisserotto C, Ferroni L, Giovanardi M, Pantaleoni L, Boccaletti L, Pancaldi S. 2012. Salinity promotes growth of freshwater *Neochloris oleoabindans* UTEX 1185 (Sphaeropleales, Neochloridaceae): morpho-physiological aspects. Phycologia 51, 700-710.

Baldisserotto C, Giovanardi M, Ferroni L, Pancaldi S. 2014. Growth, morphology and photosynthetic responses of *Neochloris oleoabundans* during cultivation in a mixotrophic brackish medium and subsequent starvation. Acta Physiologiae Plantarum. 1, 461-72.

Baldisserotto C, Popovich C, Giovanardi M, Sabia A, Ferroni L, Constenla D, Leonardi P, Pancaldi S. 2016. Photosynthetic aspects and lipid profiles in the mixotrophic alga *Neochloris oleoabundans* as useful parameters for biodiesel production. Algal Research. 16, 255-65.

Barber J. 2002. Photosystem II: a multisubunit membrane protein that oxidises water. Current Opinion in Structural Biology 12, 523-530.

Bennoun P. 1994. Chlororespiration revisited: mitochondrial-plastid interactions in Chlamydomonas. Biochimica et Biophysica Acta-Bioenergetics. 1186, 59-66.

Borowitzka MA. 2013. High-value products from microalgae – their development and commercialisation. Journal of Applied Phycology 25, 743-756.

Caffarri S, Kouřil R, Kereïche S, Boekema EJ, Croce R. 2009. Functional architecture of higher plant photosystem II supercomplexes. The EMBO journal 28, 3052-63.

Chisti Y. 2007. Biodiesel from microalgae. Biotechnology Advances 25, 294-306.

Chow WS, Melis A, Anderson JM. 1990. Adjustments of photosystem stoichiometry in chloroplasts improve the quantum efficiency of photosynthesis. Proceedings of the National Academy of Science of the United States of America 87, 7502-7506.

Croce R, van Amerongen H. 2011. Light-harvesting and structural organization of photosystem II: from individual complexes to thylakoid membrane. Journal of Photochemistry and Photobiology B: Biology 104,142-53.

Cruz S, Goss R, Wilhelm C, Leegood R, Horton P, Jakob T. 2011. Impact of chlororespiration on non-photochemical quenching of chlorophyll fluorescence and on the regulation of the diadinoxanthin cycle in the diatom *Thalassiosira pseudonana*. Journal of Experimental Botany 62, 509-519.

Danielsson R, Suorsa M, Paakkarinen V, Alpertsson PÅ, Styring S, Aro EM, Mamedov F. 2006. Dimeric and monomeric organisation of photosystem II. Journal of Biological Chemistry 281, 14241-14249.

DeáK Z, Lásló S, Kiss É, Vass I. 2014. Characterisation of wave phenomena in the relaxation of flash-induced chlorophyll fluorescence yield in cyanobacteria. Biochimica et Biophysica Acta 1837, 1522-1532.

Dekker JP, Boekema EJ. 2005. Supramolecular organisation of thylakoid membranes proteins in green plants. Biochimica and Biophysica Acta 1706, 12-39.

Falkowski PG, Raven JA. 2007. In: Falkowski PG, Raven JA, eds. Aquatic photosynthesis. Princeton University Press, 1-43.

Feild TS, Nedbal L, Ort DR. 1998. Nonphotochemical reduction of the plastoquinone pool in sunflower leaves originates from chlororespiration. Plant Physiology. 116, 1209-18.

Ferroni L, Baldisserotto C, Giovanardi M, Pantaleoni L, Morosinotto T, Pancaldi S. 2011. Revised assignment of room-temperature chlorophyll fluorescence emission bands in single living cells of *Chlamydomonas reinhardtii*. Journal of Bioenergy and Biomembranes 43, 163-173.

Ferroni L, Suorsa M, Aro EM, Baldisserotto C, Pancaldi S. (2016) Light acclimation in the lycophyte *Selaginella martensii* depends on changes in the amount of photosystems and on the flexibility of the light-harvesting complex II antenna association with both photosystems. New Phytologist 211**,** 554-568.

Finazzi G, Furia A, Barbagallo RP, Forti G. 1999. State transitions, cyclic and linear electron transport and photophosporylation in *Chlamydomonas reinhardtii*. Biochimica and Biophysica Acta 1413, 117-129.

Fristedt R, Willig A, Granath P, Crèvecoeur M, Rochaix JD, Vener AV. 2009. Phosphorylation of photosystem II controls functional macroscopic folding of photosynthetic membranes in Arabidopsis. The Plant Cell 21, 3950-3964.

Geider RJ, MacIntyre HL. 2002. Physiology and Biochemistry of photosynthesis and algal carbon acquisition. In: William PJleB, Thomas DR, Reynolds CS, eds. Phytoplankton productivity and carbon assimilation in marine and freshwater ecosystems. London: Blackwell Science Ltd, 44-77.

Giovanardi M, Ferroni L, Baldisserotto C, Tedeschi P, Maietti A, Pantaleoni L, Pancaldi S. 2013. Morpho-physiological analyses of *Neochloris oleoabundans* (Chlorophyta) grown mixotrophically in a carbon-rich waste product. Protoplasma 250, 161-174.

Giovanardi M, Baldisserotto C, Ferroni L, Longoni P, Cella R, Pancaldi S. 2014. Growth and lipid synthesis promotion in mixotrophic *Neochloris oleoabundans* (Chlorophyta) cultivated with glucose. Protoplasma 251, 115-125.

Grieco M, Suorsa M, Jajoo A, Tikkanen M, Aro EM. 2015. Light-harvesting II antenna trimers connect energetically the entire photosynthetic machinery – including both photosystems II and I. Biochimica et Biophysica Acta – Bioenergetics 1847, 607-619.

Hill R, Ralph PJ. 2008. Dark-induced reduction of the plastoquinone pool in zooxanthellae of scleractinian corals and implications for measurements of chlorophyll *a* fluorescence. Symbiosis 46, 45-56.

Hippler M, Klein J, Fink A, Allinger T, Hoerth P. 2001. Towards functional proteomics of membrane protein complexes: analysis of thylakoid membranes from *Chlamydomonas reinhardtii*. The Plant Journal 28, 595-606.

Hoefnagel MH, Atkin OK, Wiskich JT. 1998. Interdependence between chloroplasts and mitochondria in the light and the dark. Biochimica et Biophysica Acta - Bioenergetics 1366, 235-55.

Horton P, Ruban AV, Rees D, Pascal AA, Noctor G, Young AJ. 1991. Control of the light-harvesting function of chloroplast membranes by aggregation of the LHCII chlorophyll-protein complex. Journal of Federation of European Biochemical Societies 292, 1-4.

Horváth G, Melis A, Hideg É, Droppa M, Vigh L. 1987. Role of lipids in the organization and function of photosystem II studied by homogeneous catalytic hydrogenation of thylakoid membranes in situ. Biochimica et Biophysica Acta - Bioenergetics 891, 68-74.

Houille-Vernes L, Rappaport F, Wollman FA, Alric J, Johnson X. 2011. Plastid terminal oxidase 2 (PTOX2) is the major oxidase involved in chlororespiration in Chlamydomonas. Proceedings of the National Academy of Sciences of the United States of America 108, 20820-20825.

Ivancich A, Horváth L, Droppa M, Horváth G, Farkas T. 1994. Spin label EPR study of lipid solvation of supramolecular photosynthetic protein complexes in thylakoids. Biochimica et Biophysica Acta - Biomembranes. 1196, 51-56.

Järvi S, Suorsa M, Paakkarinen V, Aro EM. 2011. Optimized native gel system for separation of thylakoid protein complexes: novel super- and mega- complexes. Biochemical Journal 439, 207-214.

Joliot A, Joliot P. 1964. Etude Cinétique de la reaction photochimique libérant l'oxigène au cours de photosynhtèse. Comptes rendus de l'Académie des Sciences 258, 4622-4625.

Kirchhoff H, Mukherjee U, Galla HJ. 2002. Molecular architecture of the thylakoid membrane: lipid diffusion space for plastoquinone. Biochemistry. 41, 4872-4882.

Kováks L, Wiessner W, Kis M, Nagy F, Mende D, Demeter S. 2000. Short- and long-term redox regulation of photosynthetic light energy distribution and photosystem stoichiometry by acetate metabolism in the green alga, *Chlamydobotrys stellata*. Photosynthesis Research 65, 231-247.

Krause GH, Weiss E. 1984. Chlorophyll fluorescence as a tool in plant physiology. II. Interpretation of the fluorescence signals. Photosynthesis Research 5, 1139-157.

Kruse O, Hankamer B, Konczak C, Gerle C, Morris E, Radunz A, Schmid GH, Barber J. 2000. Phosphatidylglycerol is involved in the dimerization of photosystem II. The Journal of Biological Chemistry 275, 6509-6514.

Laemmli U. 1970. Cleavage of structural proteins during the assembly of the head of bacteriophage T4. Nature 227, 680-685.

Lee Y. 2001. Microalgal mass culture systems and methods: their limitation and potential. Journal of Applied Phycology 13, 307-315.

Lichtenthaler HK, Buschmann C, Knapp M. 2005. How to correctly determine the different chlorophyll fluorescence parameters and the chlorophyll fluorescence decrease ratio RFd of leaves with the PAM fluorometer. Photosynthetica 43, 379–393.

Liu X, Duan S, Li A, Xu N, Cai Z, Hu Z. 2009. Effects of organic carbon sources on growth, photosynthesis, and respiration of *Phaeodactylum tricornutum*. Journal of Applied Phycology 21, 239-246.

Lokstein H, Härtel H, Hoffmann P, Woitke P, Renger G. 1994. The role of light-harvesting complex II in excess excitation energy dissipation: an in-vivo fluorescence study on the origin of high-energy quenching. Journal of Photochemistry and Photobiology B: Biology 26, 175-184.

Lowry OH, Rosebrough NJ, Farr AL, Randall RJ. 1951. Protein measurement with the Folin phenol reagent. Journal of Biological Chemistry 193, 265-75.

Mekala NR, Suorsa M, Rantala M, Aro EM, Tikkanen M. 2015. Plants actively avoid state transitions upon changes in light intensity: role of light-harvesting complex II protein dephosphorylation in high light. Plant Physiology. 168, 721-34.

Minagawa J. 2009. Light-harvesting proteins. In: Stern D, Witman GB, Harris EH, eds. *Chlamydomonas* sourcebook. Amsterdam: Elsevier, 503-540.

Minagawa J, Takahashi Y. 2004. Structure, function and assembly of Photosystem II and its light-harvesting proteins. Photosynthesis Research 82, 241-263.

Nelson N, Ben-Shem A. 2004. The complex architecture of oxygenic photosynthesis. Nature Reviews Molecular Cell Biology 5, 971-982.

Nelson N, Yocum CF. 2006. Structure and Function of Photosystems I and II. Annual Review of Plant Biology 57, 521-565.

Nevo R, Charuvi D, Tsabari O, Reich Z. 2012. Composition, architecture and dynamics of the photosynthetic apparatus in higher plants. The Plant Journal 70, 157-76.

Oesterhelt C, Schmalzlin E, Schmitt JM, Lokstein H. 2007. Regulation of photosynthesis in the unicellular acidophilic red alga *Galdieria sulphuraria*. The Plant Journal 51, 500-511.

Porra RJ, Thompson WA, Kriedemann PE. 1989. Determination of accurate extinction coefficients and simultaneous-equations for assaying chlorophyll-*a* and chlorophyll-*b* extracted with 4 different solvents: verification of the concentration of chlorophyll standards by atomic-absorption spectroscopy. Biochimica and Biophysica Acta 975, 384-394.

Rintamäki E, Martinsuo P, Pursiheimo S, Aro EM. 2000. Cooperative regulation of light-harvesting complex II phosphorylation via the plastoquinol and ferredoxin-thioredoxin system in chloroplasts. Proceedings of the National Academy of Sciences of the United States of America 97, 11644-11649.

Roach T, Sedoud A, Krieger-Liszkay A. 2013. Acetate in mixotrophic growth medium affects photosystem II in *Chlamydomonas reinhardtii* and protects against photoinhibition. Biochimica et Biophysica Acta 1827, 1183-1190.

Rokka A, Suorsa M, Saleem A, Battchikova N, Aro EM. 2005. Synthesis and assembly of thylakoid protein complexes: multiple assembly steps of photosystem II. Biochemical Journal 388, 159-168.

Sabia A, Baldisserotto C, Biondi S, Marchesini R, Tedeschi P, Maietti A, Giovanardi M, Ferroni L, Pancaldi S. 2015. Re-cultivation of *Neochloris oleoabundans* in exhausted autotrophic and mixotrophic media: the potential role of polyamines and free fatty acids. Applied Microbiology and Biotechnology. 99, 10597-609.

Scott SA, Davey MP, Dennis JS, Horst I, Howe CJ, Lea-Smith DJ, Smith AG. 2010. Biodiesel from algae: challenges and prospects. Current Opinion in Biotechnology 21, 277-286.

Serôdio J, Vieira S, Cruz S, Coelho H. 2006. Rapid light-response curves of chlorophyll fluorescence in microalgae: relationship to steady-state light curves and non-photochemical quenching in benthic diatom-dominated assemblages. Photosynthesis Research 90, 29-43.

Schansker G, Strasser RJ. 2005. Quantification of non-Q_B-reducing centers in leaves using a far-red pre-illumination. Photosynthesis Research 84, 145-151.

Stephens E, Ross IL, Mussgnug JH, Wagner LD, Borowitzka MA, Posten C, Kruse O, Hankamer B. 2010. Future prospects of microalgal biofuel production systems. Trends in Plant Science 15, 554-564.

Suorsa M, Rantala M, Mamedov F, Lespinasse M, Trotta M, Grieco M, Vuorio E, Tikkanen M, Järvi S, Aro EM. 2015. Light acclimation involves dynamic re-organisation of the pigment-protein megacomplexes in non-appressed thylakoid domains. The Plant Journal 84, 360-373.

Takahashi T, Inoue-Kashino N, Ozawa S, Takahashi Y, Kashino Y, Satoh K. 2009. Photosystem II complex in vivo is a monomer. Journal of Biological Chemistry 284, 15598-15606.

Tikhonov AN. 2015. Induction events and short-term regulation of electron transport in chloroplasts: an overview. Photosynthesis Research 125, 65-94.

Tikkanen M, Grieco M, Kangasjiärvi S, Aro EM. 2008. Thylakoid protein phosphorylation in higher plant chloroplasts optimizes electron transfer under fluctuating light. Plant Physiology 152, 723-735.

Tikkanen M, Aro EM. 2012. Thylakoid protein phosphorylation in dynamic regulation of photosystem II in higher plants. Biochimica et Biophysica Acta - Bioenergetics. 1817, 232-238.

Tornabene TG, Holzer G, Lien S, Burris N. 1983. Lipid composition of the nitrogen starved green alga *Neochloris oleoabundans*. Enzyme Microbiology and Technology 5, 435-440.

Valverde F, Ortega JM, Losada M, Serrano A. 1995. Sugar-mediated transcriptional regulation of the Gap gene system and concerted photosystem II functional modulation in the microalga *Scenedesmus vacuolatus*. Planta 221, 937-952.

Vass I, Kirilovsky D, Etienne AL. 1999. UV-B radiation-induced donor- and acceptor-side modifications of photosystem II in the cyanobacterium *Synechocystis* sp. PCC 6803, Biochemistry 39, 12786-12794.

Vass I, Turcsányi E, Touloupakis E, Ghanotakis D, Petrouleas V. 2002. The mechanism of UV-A radiation-induced inhibition of photosystem II electron transport studied by EPR and Chlorophyll Fluorescence. Biochemistry 41, 10200-10208.

Volgusheva A, Styring S, Mamedov F. 2013. Increased photosystem II stability promotes H_2 production in sulfur-deprived *Chlamydomonas reinhardtii*. Proceedings of the National Academy of Sciences of the United States of America 110, 7223-7228.

Ünlü C, Drop B, Croce R, van Amerongen H. 2014. State transitions in *Chlamydomonas reinhardtii* strongly modulate the functional size of photosystem II but not of photosystem I. Proceedings of the National Academy of Sciences of the United States of America 111, 3460-3465.

Watanabe M, Iwai M, Narikawa R, Ikeuchi M. 2009. Is the photosystem II complex a monomer or a dimer? Plant and cell physiology 50, 1674-1680.

Wellburn AR. 1994. The spectral determination of Chlorophylls *a* and *b*, as well as total carotenoids, using various solvents with spectrophotometer of different resolution. Plant Physiology 144, 307-313.

White S, Anandraj A, Bux F. 2011. PAM fluorometry as a tool to assess microalgal nutrient stress and monitor cellular neutral lipids. Bioresource Technology 102, 1675-1682.

Xu H, Miao X, Wu Q. 2006. High-quality biodiesel production from a microalga *Chlorella prototecoides* by heterotrophic growth in fermenters. Journal of Biotechnology 126, 499-507.

Yokono M, Takabayashi A, Akimoto S, Tanaka A. 2015. A megacomplex composed of both photosystem reaction centres in higher plants. Nature Communications 6, 6675.

Figure captions

Fig. 1. Representative curves of slow Chl*a* fluorescence kinetics in response to changing light intensities in *N. oleoabundans* at the 6th day of cultivation. A) cells grown with 0 gL^{-1} of glucose. B) cells grown with 2.5 gL^{-1} of glucose. The measurements were started after 10 min of incubation in darkness by turning on the actinic light, the fluorescence parameters F_M' and F_t were monitored triggering the samples with different light intensities. F_{Mtrue} is maximum fluorescence measured at the end of the exposure to 90 $\mu mol_{photons}\ m^{-2}s^{-1}$; F_tLL and F_tHL are steady-state fluorescence values measured at the end of the exposure to 90 $\mu mol_{photons}\ m^{-2}s^{-1}$ and 1000 $\mu mol_{photons}\ m^{-2}s^{-1}$, respectively.

Fig. 2. Representative curves of Chl*a* fluorescence kinetics during exposure to far red light. Excitation of autotrophic (filled circles) and mixotrophic (empty circles) *N. oleoabundans* cells with far red light for 10 min (purple diagram) and subsequent dark relaxation (dark diagram). $n \geq 3$ ± standard error. $p < 0.05$ at times 1, 5-9. $p < 0.01$ at times 10, 11, 12, 15, 20, according with Student's *t* test.

Fig. 3. Relaxation of the flash-induced fluorescence in *N. oleoabundans* cells grown with 0 (filled circles) and 2.5 (empty circles) gL^{-1} of glucose. In the insert, relaxation kinetics as occurring in presence of 5 μM DCMU. Curves are average of at least 3 different biological replicates and are normalised to the same amplitude. Arrows: saturating-light pulse.

Fig. 4. Coomassie-stained SDS-PAGE of thylakoids extracted from autotrophic and mixotrophic *N. oleoabundans*. On each lane, 2 μg of Chl (A) or 20 μg of proteins (B) were loaded. For comparison, three different amounts of thylakoids from autotrophic sample were loaded. Molecular weight marker is reported on the left side in each gel.

Fig. 5. Detection of thylakoid protein amount in autotrophic and mixotrophic *N. oleoabundans* cells. A) Immunoblot detection of ATPβ (3 μg of Chl loaded in each lane), PsaB (0.5 μg of Chl loaded in each lane), D1-DE loop (0.5 μg of Chl loaded in each lane) and LHCII (0.25 μg of Chl loaded in each lane) in thylakoid membranes of *N. oleoabundans* grown with 0 (*A*), and 2.5 (*M*) gL^{-1} of glucose. For comparison, three different amounts of thylakoids from control sample were loaded. Molecular weight marker is reported on the left. B) 77K Fluorescence emission spectra recorded from autotrophic (black line) and mixotrophic (grey line) *N. oleoabundans* cells. For easier comparison, spectra were normalized to their maximum peak, corresponding to PSII emission region. Spectra are averages of at least 3 replicates for each biological sample.

Fig. 6. Representative BN-PAGE profiles of thylakoids from *N. oleoabundans*. *DA*: dark autotrophic cells; *LA*: light autotrophic cells; *DM*: dark mixotrophic cells; *LM*: light mixotrophic cells. For each lane, 8μg Chl were loaded. The position of major complexes is indicated by labels.

Fig. 7. 2D-BN/SDS-PAGE of protein complexes in thylakoid membranes from *N. oleoabundans*. A) comparison between autotrophic cells incubated in darkness (*DA*) or maintained in growth light (*LA*) before thylakoid extraction. B) comparison between mixotrophic cells incubated in darkness (*DM*) or in growth light (*LM*) before thylakoid extraction. The BN-PAGE strips were loaded horizontally on the SDS-PAGE. The highlighted silver-stained spots correspond to Psa A/B subunits of PSI, CP47, CP43, D1 and D2 subunits of PSII, and LHCII subunits. Two

different types of LHCII trimer are indicated by yellow arrows. Marker molecular weight of proteins is reported on the left.

Fig. 8. Relative amounts of PSII (A) and PSI (B) in thylakoids extracted from autotrophic (*A*) and mixotrophic (*M*) *N. oleoabundans* cells incubated in darkness (*DA - DM*) or maintained in growth light (*LA – LM*) before extraction. Black: *DA;* line pattern: *LA*; diamond pattern: *DM*; white: *LM*. Data are means of 4 replicates ± standard deviation and are obtained by spot densitometry of 2D/BN-PAGE gels stained by SYPRO Ruby dye. Differences are not significant (p>0.05) for groups with the same superscript using ANOVA comparison of means.

Fig. 9. TEM images of autotrophic (A-B) and mixotrophic (C-D) *N. oleoabundans* cells after 6 days of cultivation. Asterisks indicate starch granules, arrows highlight thighly-appressed thylakoids in mixotrophic cells.

Fig. 10. Detection of phosphorylated thylakoid proteins in autotrophic (*A*) and mixotrophic (*M*) *N. oleoabundans* cells. A) phosphorylation of thylakoid proteins of *N. oleoabundans* cells incubated in darkness (*DA-DM*) or maintained in growth light (*LA-LM*) before extraction. Phosphoproteins were detected by immunoblotting using an anti-phosphothreonine antibody. LHCII, D2 and CP43 are indicated as major phosphoproteins. Molecular weights are expressed in kDa. B) Coomassie-stained SDS-PAGE of thylakoids incubated in darkness (*DA-DM*) or maintained in growth light (*LA-LM*) before extraction. Bands corresponding to LHCII subunits are indicated. Dashed lines include phosphorylated subunits after immunoblotting.

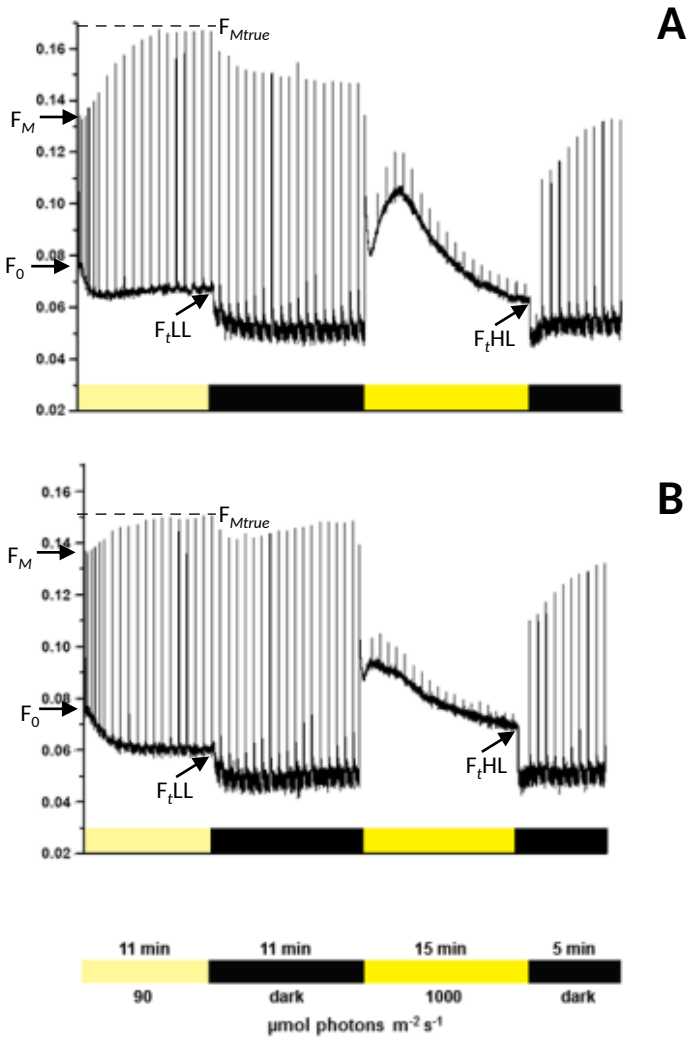
A
B
F_Mtrue
F_M
F_0
F_tLL
F_tHL
0.16
0.14
0.12
0.10
0.08
0.06
0.04
0.02
11 min
11 min
15 min
5 min
90
dark
1000
dark
µmol photons m-2 s-1

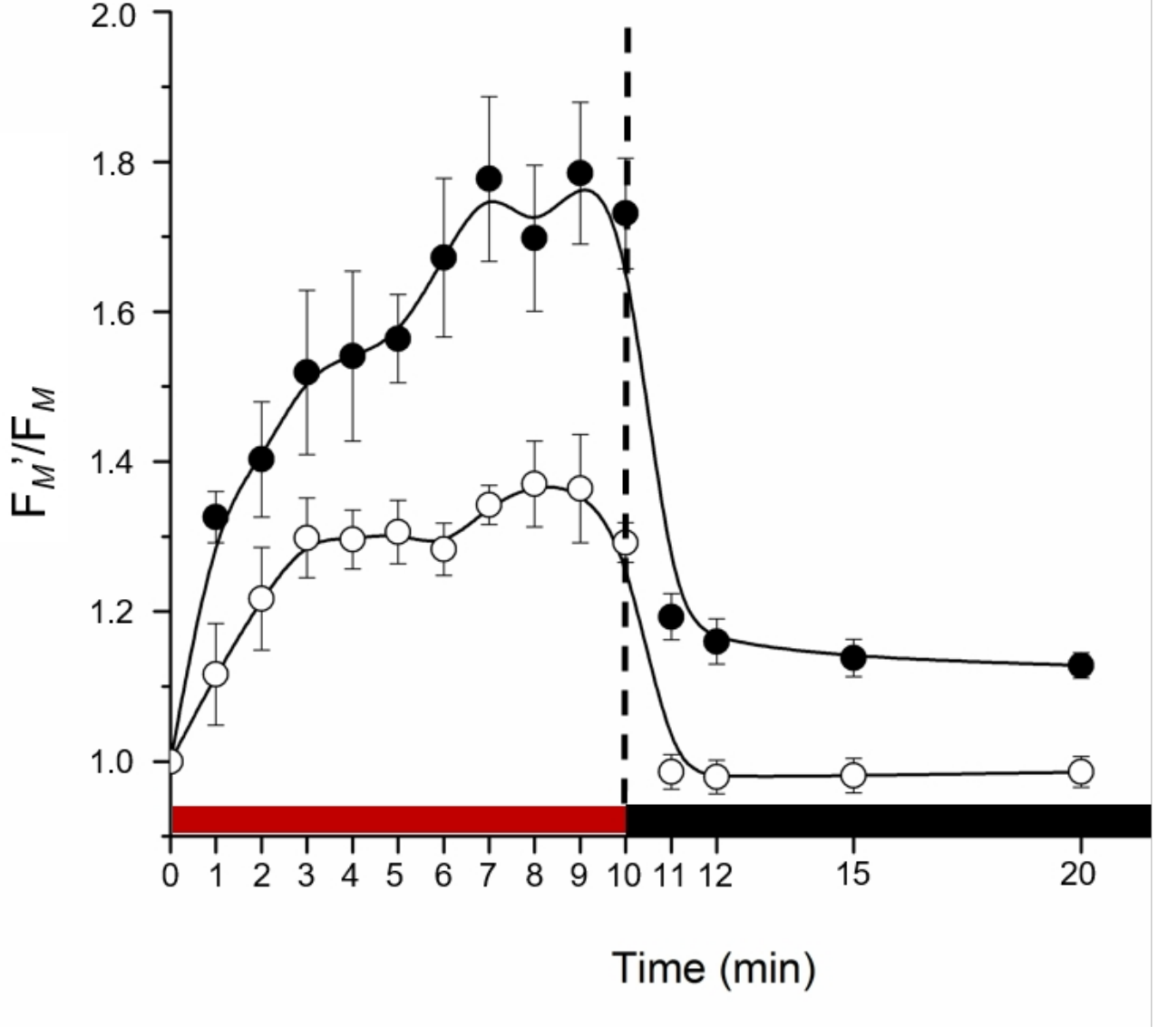
2.0
1.8
1.6
1.4
1.2
1.0
F_M'/F_M
0 1 2 3 4 5 6 7 8 9 10 11 12 15 20
Time (min)

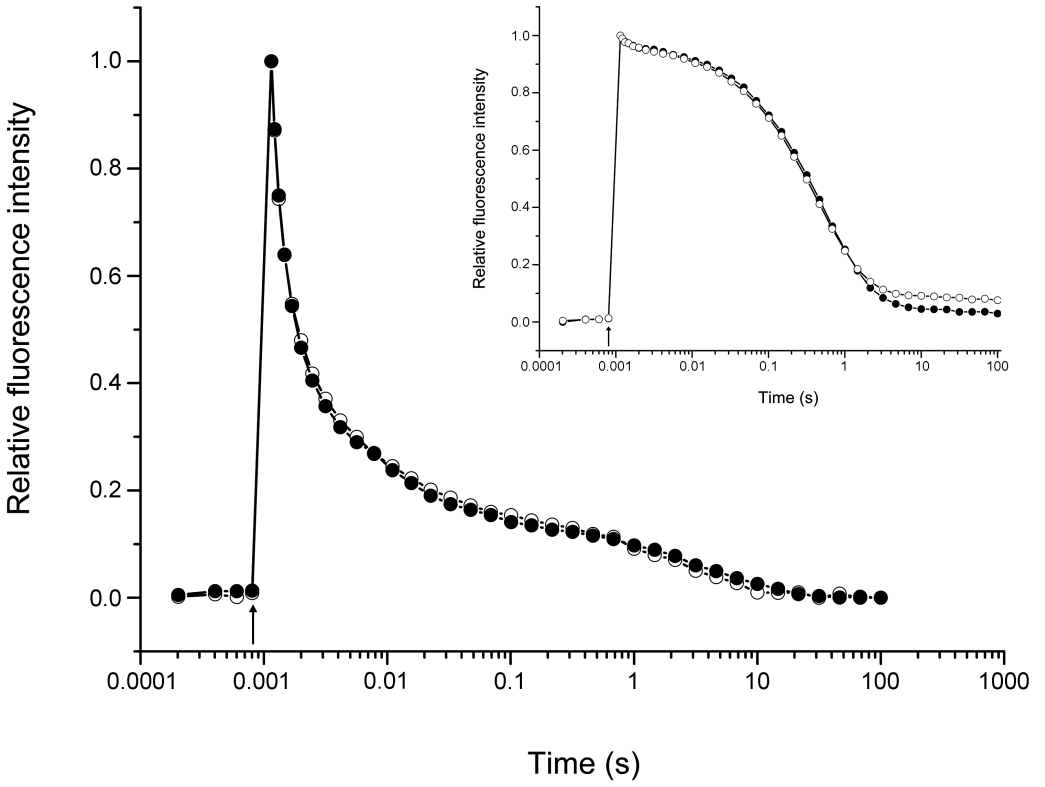
Relative fluorescence intensity
1.0
0.8
0.6
0.4
0.2
0.0
0.0001
0.001
0.01
0.1
1
10
100
1000
Time (s)
Relative fluorescence intensity
1.0
0.8
0.6
0.4
0.2
0.0
0.0001
0.001
0.01
0.1
1
10
100
Time (s)

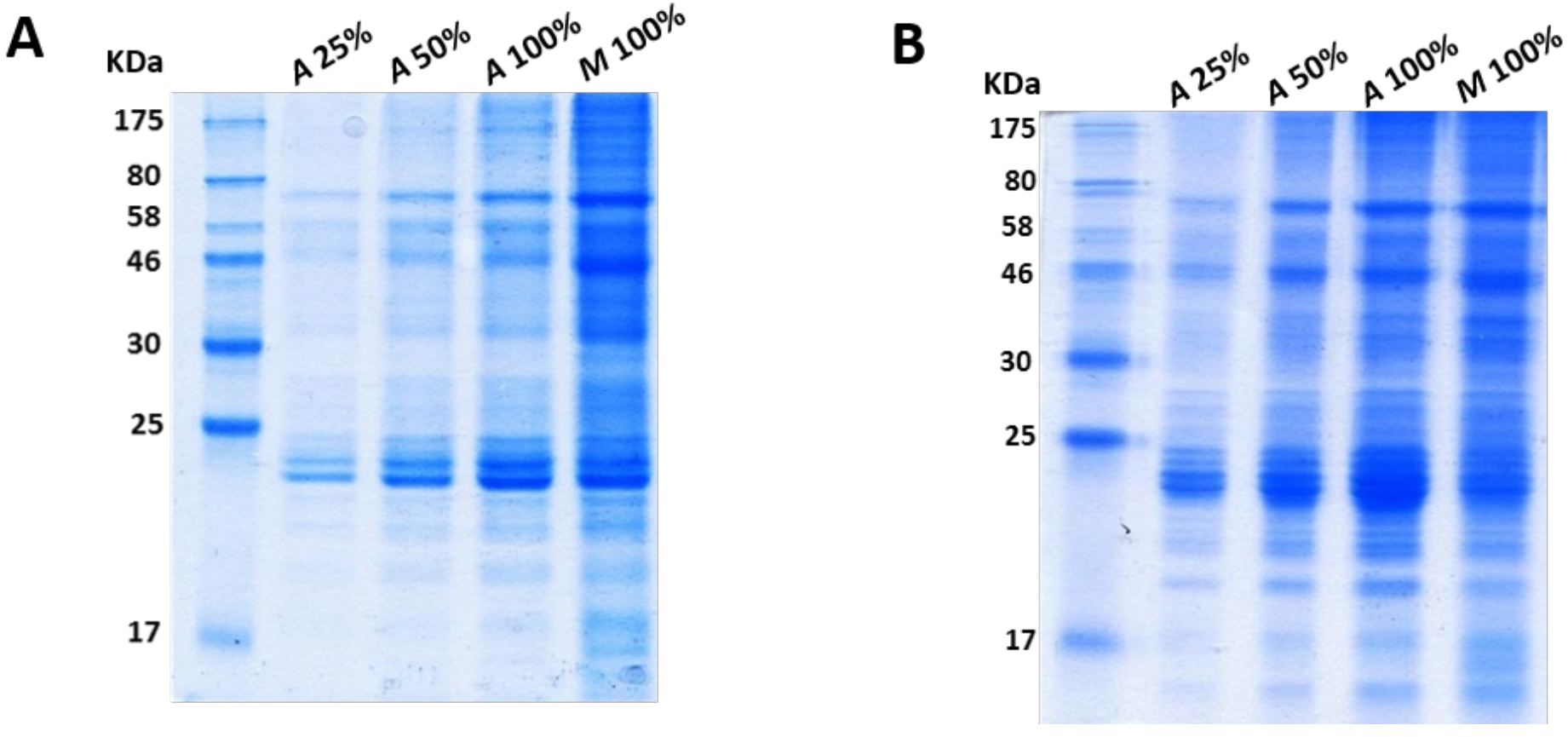
A
KDa
A 25%
A 50%
A 100%
M 100%
175
80
58
46
30
25
17
B
KDa
A 25%
A 50%
A 100%
M 100%
175
80
58
46
30
25
17

A

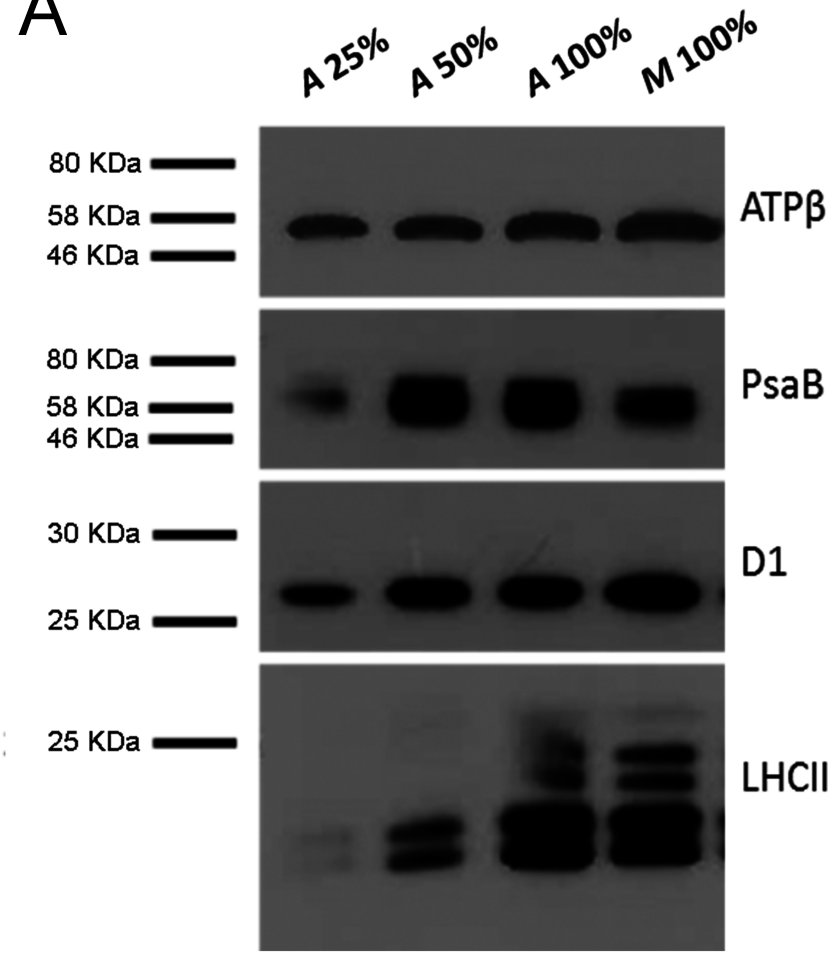
A 25%
A 50%
A 100%
M 100%
80 KDa
58 KDa
46 KDa
ATPβ
80 KDa
58 KDa
46 KDa
PsaB
30 KDa
25 KDa
D1
25 KDa
LHCII

B

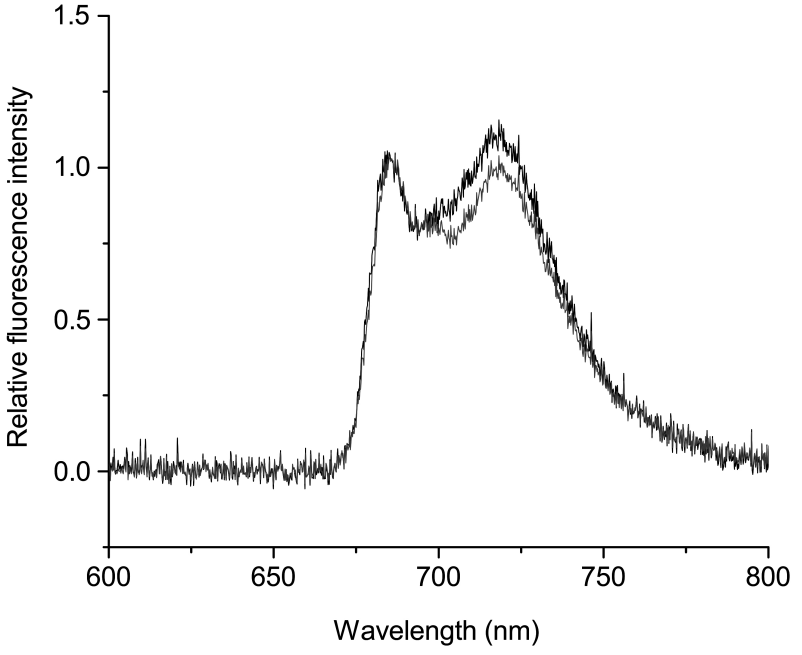
1.5
1.0
0.5
0.0
Relative fluorescence intensity
600
650
700
750
800
Wavelength (nm)

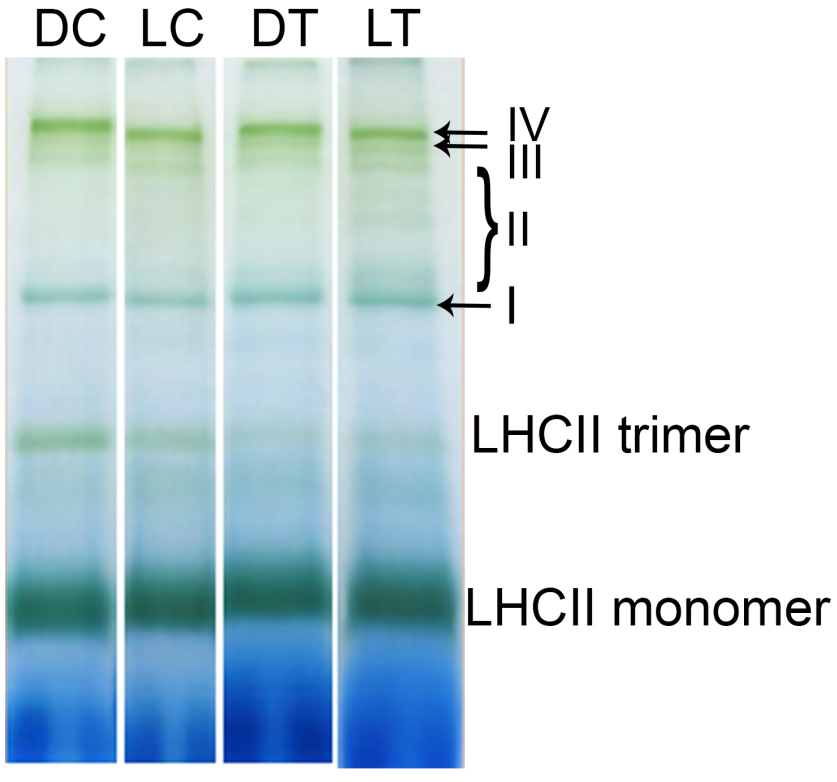
DC
LC
DT
LT
IV
III
II
I
LHCII trimer
LHCII monomer

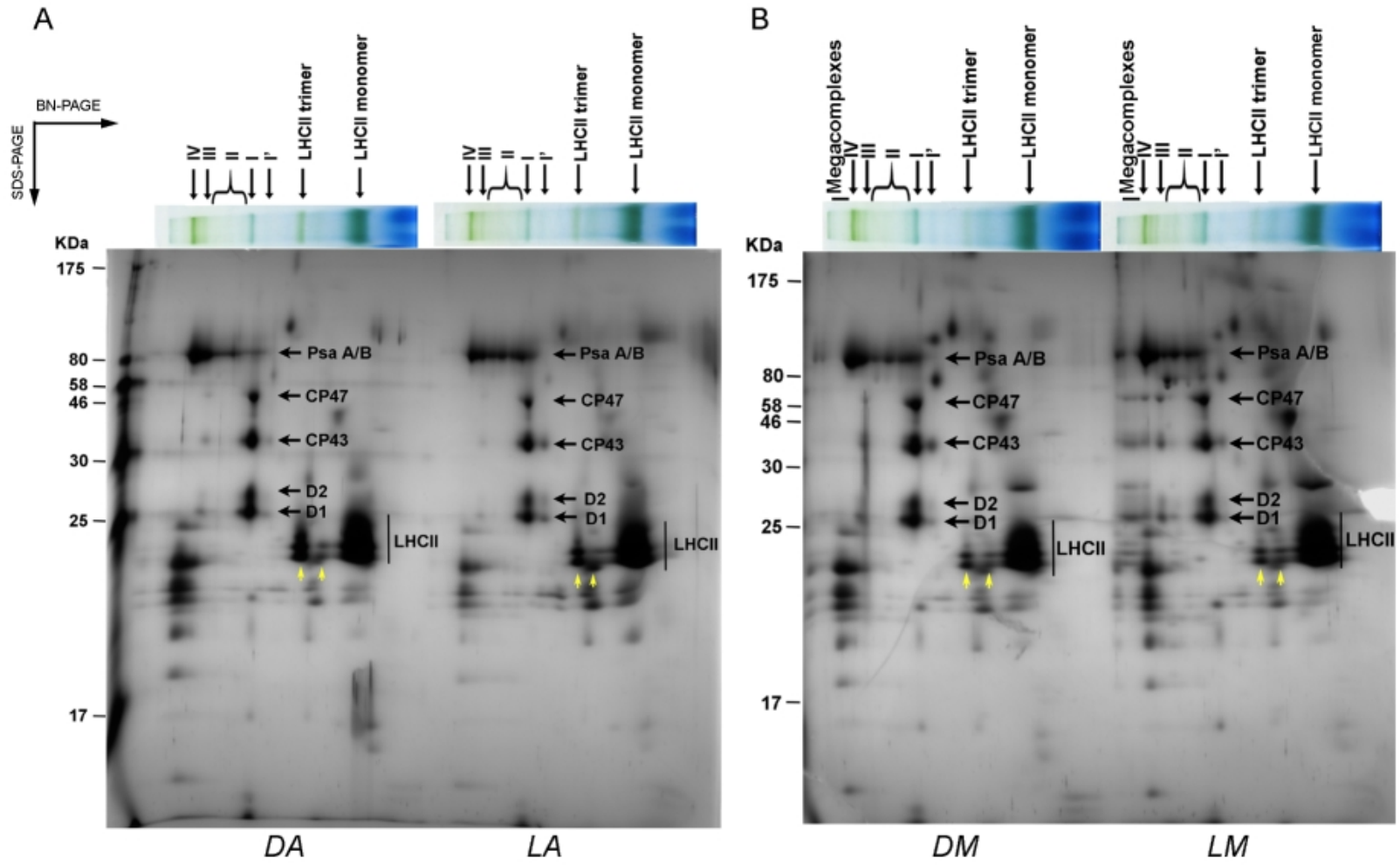
A
BN-PAGE
SDS-PAGE
IV
III
II
I
I'
LHCII trimer
LHCII monomer
KDa
175
80
58
46
30
25
17
Psa A/B
CP47
CP43
D2
D1
LHCII
DA
LA
B
Megacomplexes
DM
LM

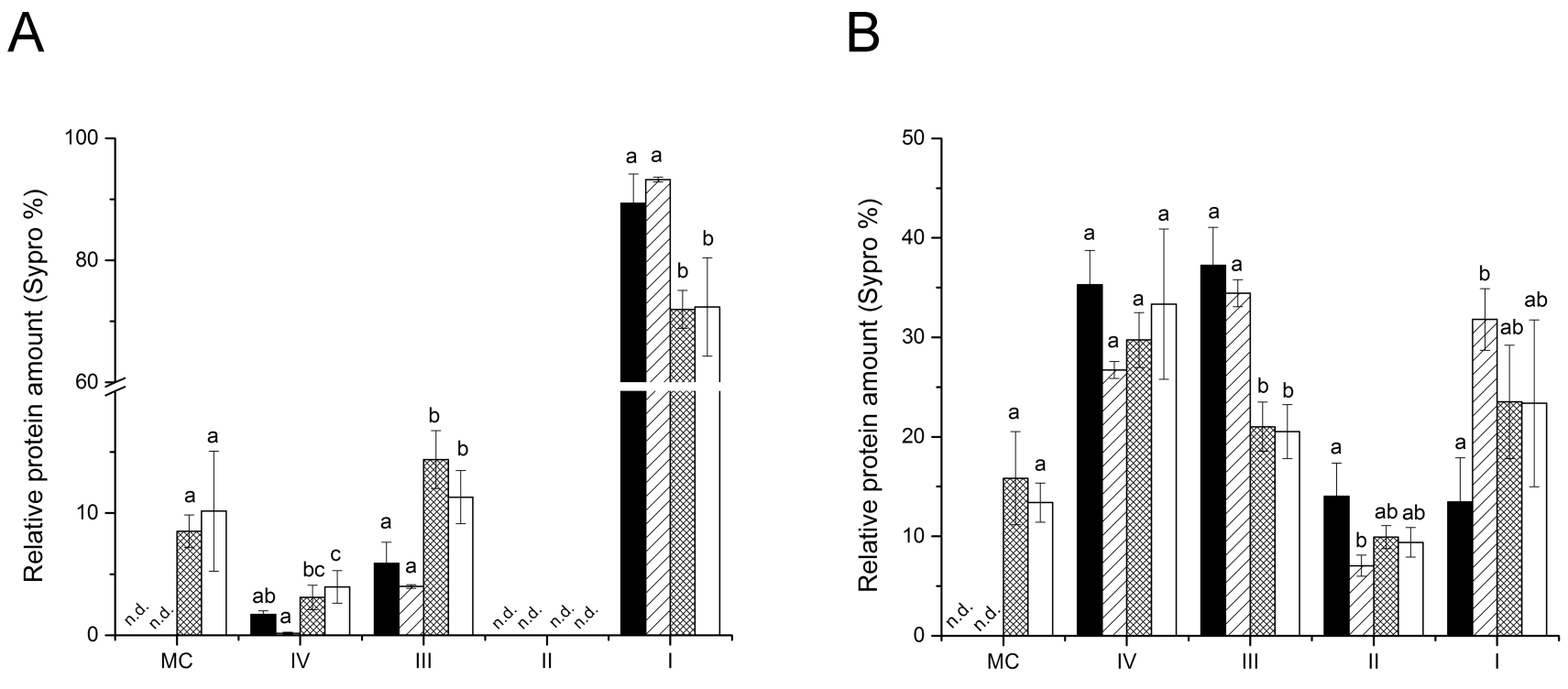
A
B
Relative protein amount (Sypro %)
100
80
60
10
0
50
40
30
20
n.d.
MC
IV
III
II
I
a
ab
bc
c
b
ab

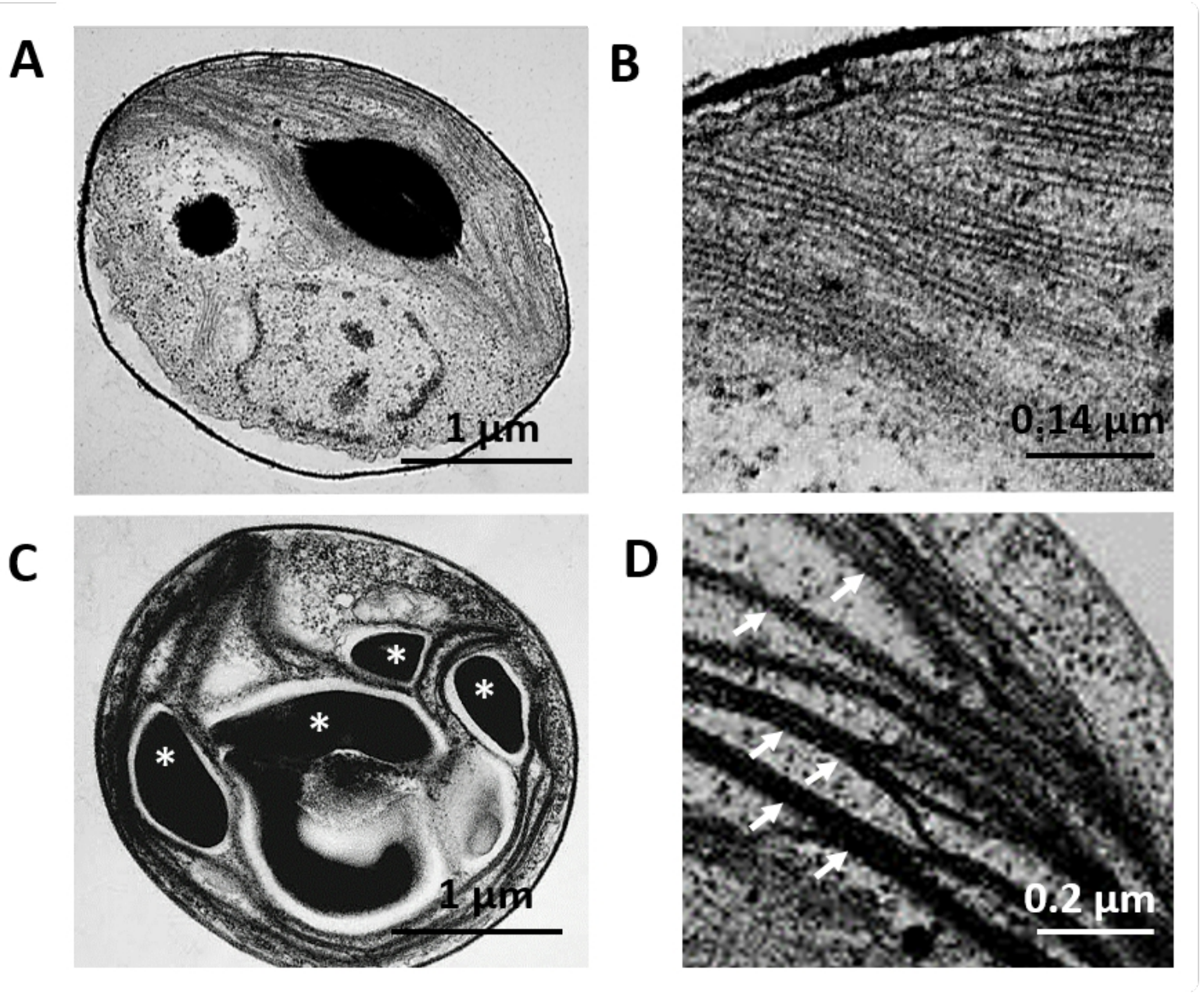
A
1 µm
B
0.14 µm
C
1 µm
D
0.2 µm

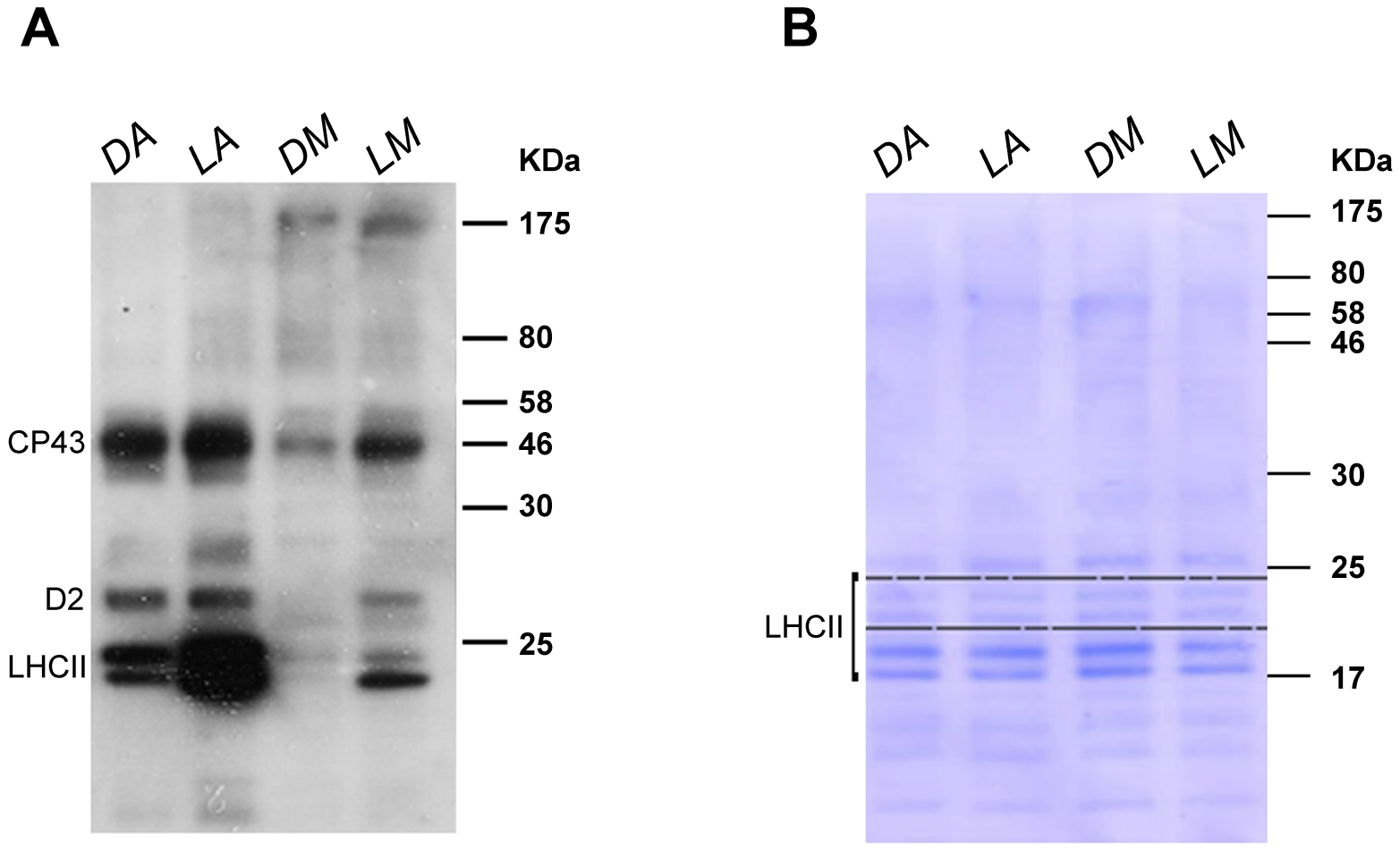
A
DA
LA
DM
LM
KDa
175
80
58
46
30
25
CP43
D2
LHCII
B
DA
LA
DM
LM
KDa
175
80
58
46
30
25
17
LHCII

Highlights:

- Mixotrophy influences the photosynthetic performance of *Neochloris oleoabundans*
- High F_V/F_M values are linked to a down-regulated chlororespiration under mixotrophy
- A stronger association of thylakoid complexes is promoted in mixotrophic cells
- Lower dynamicity of complexes allows PSII preservation under growth light

Acknowledgments

This work was supported by the University of Ferrara and the University Institute for Higher Studies, IUSS - Ferrara 1391, with a fellowship provided to MG, and by the Academy of Finland with grants no. 271832 and 273870 to EMA.

Supplementary Figures

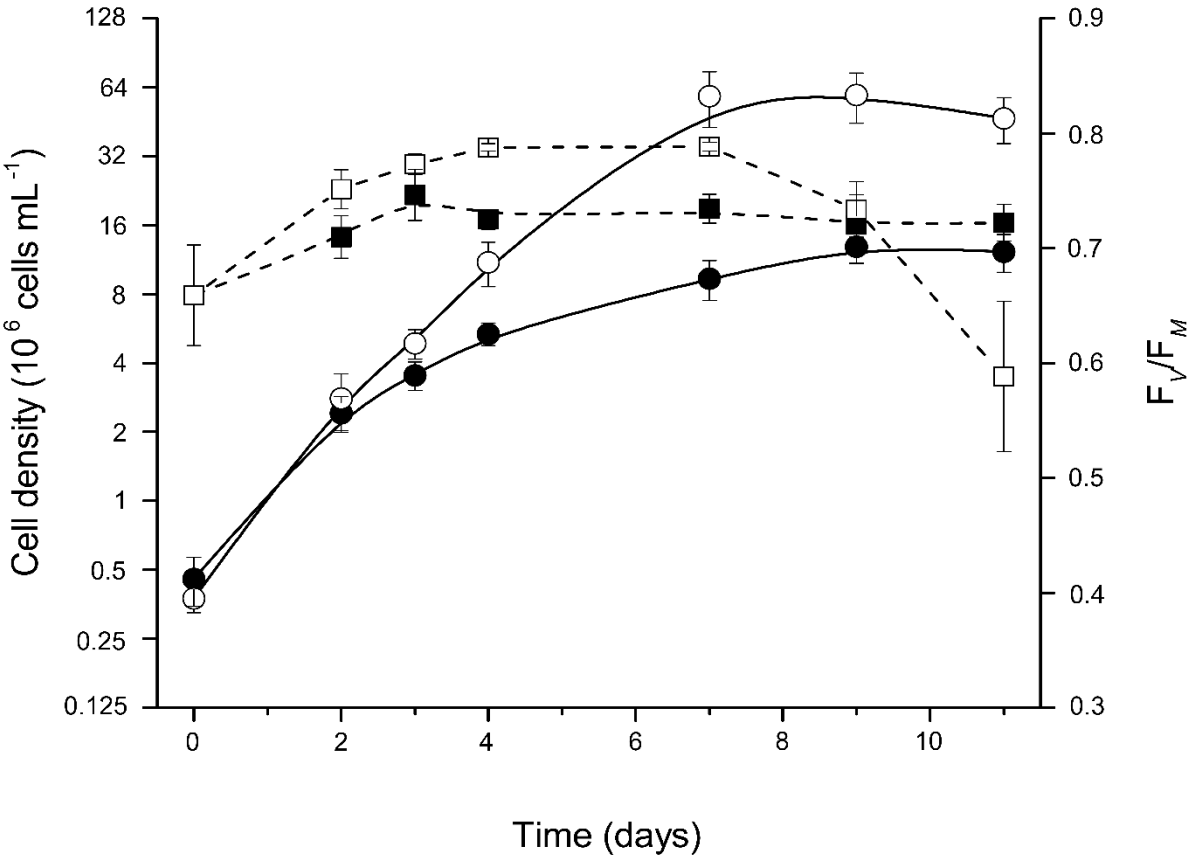

Figure S1. Cell density (solid line-circles) and PSII maximum quantum yield F_V/F_M (dashed line-squares) of *N. oleoabundans* grown in autotrophic (filled symbols) and mixotrophic (2.5 gL^{-1} of glucose; empty symbols) media. For statistical comparison of data on cell density, $p < 0.01$ at day 3, $p < 0.001$ at the following times; for statistical comparison of data on F_V/F_M ratio, $p < 0.05$ at day 2, $p < 0.01$ at day 7, $p < 0.001$ at day 4, according with Student's *t* test. Data are averages of at least 3 biological replicates ± standard deviation.

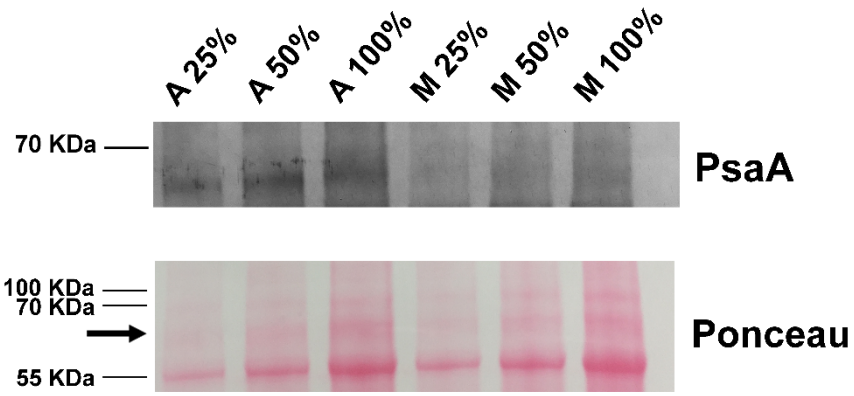

Figure S2. Immunoblot detection of PsaA subunit of PSI in thylakoid membranes of *N. oleoabundans* grown with 0 (A), and 2.5 (M) gL^{-1} of glucose. All samples were loaded on a Chl basis and at the following concentrations: 1.5 (25%), 3 (50%) and 6 (100%) µg Chl per lane. Thylakoid proteins were separated by SDS-PAGE and electroblotted on a nitrocellulose membrane as described in "Material and Methods" section. PsaA was provided from Agrisera (www.agrisera.com). After Western Blot, membranes were blocked with 0.5% BSA in TBS buffer. The alkaline phosphatase conjugate method was used for protein detection using a goat anti-Rabbit IgG secondary antibody also provided from Agrisera. To confirm the reliability of the protein detection and verify that thylakoid proteins were properly electroblotted, Ponceau-stained nitrocellulose membrane is also reported. The black arrow indicates the band related to PSI. Molecular weight marker is reported on the left.

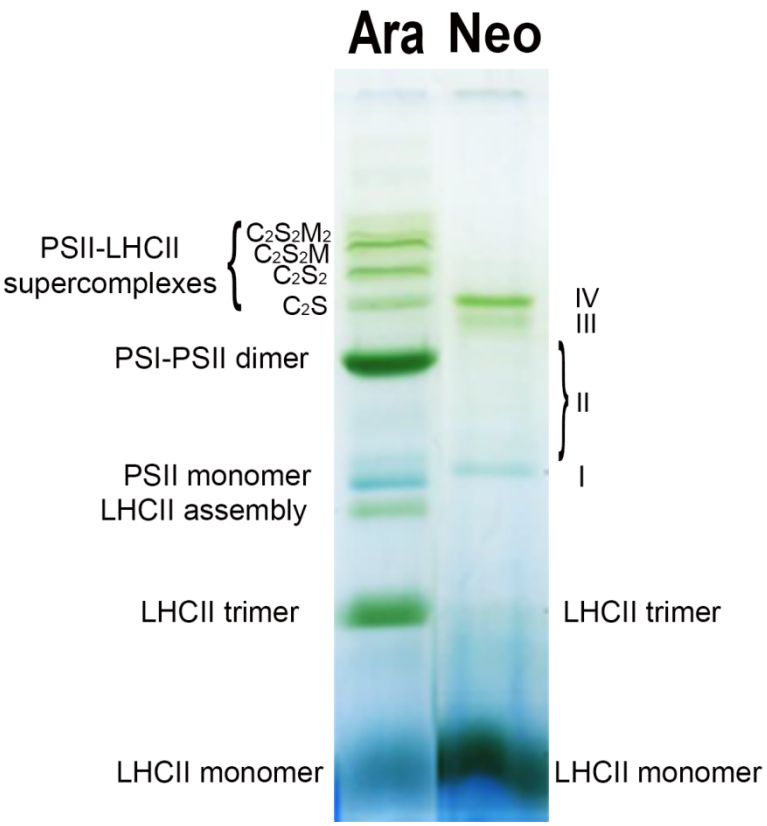

Figure S3. Blue Native (BN) - SDS PAGE profile of thylakoids membranes (see Material and Methods section) from *Arabidopsis thaliana* (Ara) and autotrophic *N. oleoabundans* (Neo). The position of major complexes is indicated by labels. For Arabidopsis, the position of major complexes reflects that reported in previous works: one band corresponding to free LHCII monomer; a more intense band of the free LHCII trimer; an LHCII assembly complex (LHCII trimer-CP24-CP29, Aro et al., 2005) close to the band corresponding to PSII in the momomeric form; a very intense band corresponding to PSI co-migrating with PSII in the dimeric form; and, finally, four bands of PSII-LHCII supercomplexes, structured as the so-called C_2S, C_2S_2, C_2S_2M and $C_2S_2M_2$ complexes (Caffarri, 2009; Croce and van Amerongen, 2011).